

Geological Modelling and Reservoir Simulation

Chris L. Farmer^{1,2}

¹ Schlumberger, Abingdon Technology Centre, Abingdon, UK

² University of Oxford, Oxford Centre for Industrial and Applied Mathematics

Summary. The main mathematical techniques used in building geological models for input to fluid flow simulation are reviewed. The subject matter concerns the entire geological and reservoir simulation modelling workflow relating to the subsurface. To provide a realistic illustration of a complete fluid flow model, a short outline of two-phase incompressible flow through porous media is given. The mathematics of model building is discussed in a context of seismic acquisition, processing and interpretation, well logging and geology. Grid generation, geometric modelling and spatial statistics are covered in considerable detail. A few new results in the area of geostatistics are proved. In particular the equivalence of radial basis functions, general forms of kriging and minimum curvature methods is shown. A Bayesian formulation of uncertainty assessment is outlined. The theory of inverse problems is discussed in a general way, from both deterministic and statistical points of view. There is a brief discussion of upscaling. A case for multiscale geological modelling is made and the outstanding research problems to be solved in building multiscale models from many types of data are discussed.

1 Introduction

1.1 Model Based Decision Making under Uncertainty

Hydrocarbons are found in rocks at depths of up to five or more kilometers below the surface of the Earth. Temperatures can be higher than 130 °C and pressures can reach the order of 1000 atmospheres. The rocks may be more than 100 million years old.

Finding and recovering hydrocarbons uses knowledge from most of the geosciences, physics and engineering. The focus of this article is upon the contribution of mathematics to these disciplines in building, analysing and applying models of fluid flow in the subsurface.

Hydrocarbon recovery involves drilling wells into the rock. Usually these wells are cased with metal tubing. The tubing is perforated at various places, called completions, to allow flow in and out of the well. Some wells are injectors in which fluid, usually water and sometimes gas, is pushed into the rocks to force other fluid toward the producing wells. Designing and operating the system of wells, and the associated surface facilities is an expensive and risky activity.

Reservoir engineers, who decide where to drill, how to complete and how to operate the wells, work in conditions of considerable uncertainty. Although the dominating uncertainty is the price of oil, uncertainties concerning subsurface structure and properties are under some control. This control involves assimilating various measurements into models. Sometimes only one model will be constructed, but usually several models, all incorporating the available data, are made. Some models will be optimistic, some pessimistic, but all are designed to characterise the reservoir and the uncertainty about the reservoir. There is a definite trend toward ensemble reservoir forecasting, where a wide range of models are developed that sample probability distributions of reservoir parameters. Such stochastic models represent, in some sense, an infinite number of deterministic models.

The models may be simple conceptual models in the mind of an engineer, sophisticated but relatively simple mathematical models that can be understood with analytical methods or more complicated models that involve numerical approximations and computer simulation. The idea is that an optimal decision over the models will be optimal in the real world.

The following explains how geological and flow simulation model building takes place.

1.2 About this Chapter

The following chapter is mainly a review. However, there are a few new mathematical results in Section 4, and some personal opinions of the author, about the current state of the art and possible ways to progress, are expressed throughout.

At the centre of the decision making workflow is the fluid flow model. This model is normally solved using numerical methods. The review describes a simplified version of such an approach so that the focus - building the flow model input - makes sense to a general reader.

Fluid flow models require quantitative description of all input parameters. These include functions of spatial position such as porosity and permeability. Techniques for building quantitative descriptions are reviewed in the following.

The following material is a mixture of general background, mathematical detail and a guide to the literature. It is hoped the review adds some extra ingredients helping relate the referenced articles and books to one another to develop a coherent story.

Structure of the Chapter: This chapter is written with a view to helping engineers, mathematicians, geoscientists and others, gain an appreciation of the more mathematical parts of an interdisciplinary subject.

The main stages in the workflow are to gather seismic observations, take cores from wells, to log wells, to study outcrops chosen via examination of

cores, to perform well tests, and to incorporate production history into the models. All stages involve direct interaction with data. To use the data there are intermediate stages involving geometric modelling, property interpolation and assimilation of measurements into the models.

It is impossible to devise a structure, following the workflow used in oil companies and oil service companies, that is comprehensible to all readers without excessive use of footnotes and digressions. The structure of the following is thus designed to enable a linear development of the subject.

The structure follows an order where, at the beginning, essentially isolated subjects are reviewed. In the later sections these are brought together in a description of geological and simulation modelling. The first major topic, in Section 2, is flow through porous media and reservoir simulation. Then, in Section 3 the topic of grid generation is covered. Following this, in Section 4, the subject of spatial statistics, also known as geostatistics, scattered data interpolation or property modelling is reviewed in some depth. Section 4 is at the centre of the chapter and places the most demands upon the reader. This section contains some new results that link different methods together.

In Section 5 a general discussion of approaches to inverse problems is provided. The geoscience aspects of the chapter start in Section 6 where the various types of field measurements are described. With all the main concepts in place, Section 7 describes how geological models are constructed. This section on geological modelling also contains additional material on grid generation and spatial statistics that is special to geological modelling. Section 8 covers the topics of upscaling and upgridding - the theory of approximating detailed models with less detailed models. Upscaling and upgridding are currently necessary, in general, if a flow simulation is to be performed with the geological model as input. Of course, upscaling is always needed when it is necessary to relate data on one scale to data on a different scale.

The topic of history matching, where the inverse problem for reservoir simulation is tackled is the subject of Section 9. This builds on the general discussion of inverse problems given in Section 5. In Section 10 an outline analysis of possible workflows is given. The concluding discussion, Section 11, lists some of the suggested open problems and fruitful areas for further research and finishes with a summary of the main conclusion.

This structure, it is hoped, will help readers, depending on their backgrounds and their objectives, to read this chapter in a selective and perhaps nonlinear manner.

Summary of the Argument: With a view to building models suitable for flow simulation, the current approach is explained and criticised. The current approach involves building as detailed model as possible of the *whole* system. The detailed model is then *coarsened* by averaging out detail that cannot be resolved in flow models.

The difficulties with this approach are that (i) the initial level of detail is insufficient to resolve all that is important and (ii) the averaging process

leads to inaccurate coarse models even if the fine model is, itself, accurate. This is a dilemma; on the one hand the model is not fine enough and on the other hand it is too fine.

A way around this dilemma, at least for stable flow processes, is suggested in which exceptionally detailed models, but only in the vicinity of the wells are subjected to careful analysis of their scaling behaviour. It is suggested that the coarse model is then constructed by interpolation (stochastic or deterministic) of the scaled local models.

2 Flow Through Porous Media and Reservoir Simulation

This section, after some general remarks, outlines the theory of two-phase flow through porous media. The intention is to introduce readers to a concrete example for later discussion on inverse modelling, scale dependence and heterogeneity. This example also motivates ideas and activities involved in geological and reservoir simulation modelling. Detailed reviews of fluid flow can be found in [11, 37, 50, 128]. For information on reservoir engineering in general and more about reservoir simulation see [9].

Some Remarks about Continuum Mechanics: Continuum mechanics studies deformation and flow of material bodies defined as continua of material points. This idealisation is analogous to idealisations in geometry where properties of shapes and surfaces, defined by simple rules or equations, are analysed. Indeed some scientists view continuum mechanics as a body of theoretical knowledge of the same status as other branches of mathematics such as differential geometry. If one takes this view, then it is necessary that the axioms of the theory are not regarded as *a priori* truths but rather as assumptions characterising a *possible* material that might be found to approximate the behaviour of some physically real material.

Continuum theories characterise the state of a physical system using scalar, vector and tensor valued functions of position x , a three dimensional point, and time t , a real number. These functions sometimes correspond to observable characteristics, such as velocity or position, and other times to more indirectly observable characteristics such as stress. Indirectly observable fields are theoretical constructs of a theory, and need the theory to determine their values. Note that in the following, the symbol x is used to represent a 3D point, an N -D point or the x -component of a 3D vector, $x = (x, y, z)$ or a 2D vector, $x = (x, y)$; the particular meaning of the symbol is always clear from the context.

The principles of continuum theory fall into two classes: balance laws, pertaining to wide classes of materials, and constitutive laws defining particular

materials. Wide classes of system are subject to balances of energy, momentum, angular momentum, and mass, but only special systems are subject to constitutive laws such as Fourier's law (heat conduction) or Darcy's law (flow through porous media). The use of the word *law* does not imply a universal truth; it merely distinguishes an important component of a mathematical model.

The Balance Laws of Porous Medium Flow: Porous medium flow theories only use balance laws of mass and energy. This introduction will only define objects using a *mass balance*.

The following considers flow of a fluid with two phases in which there is no mass transfer between the phases. The phases are called phase-A and phase-B. One might picture them, for example, as water and oil. The fluids are characterised by pressures $p_A = p_A(x, t)$ and $p_B = p_B(x, t)$, two scalar functions of position and time. The phase densities, ρ_A and ρ_B are generally functions of the phase pressures, so that $\rho_A = \rho_A(p_A)$ and $\rho_B = \rho_B(p_B)$. The rock is characterised by the *porosity* $\phi = \phi(x)$, a function of position such that the integral

$$V_f = \int_V \phi(x) d^3x$$

is interpreted as the volume of space within the volume V accessible to fluid flow. In practice one must use sufficiently large volumes V , so that the granularity of the porous medium does not significantly influence volume values obtained in measurements. A more general model might make the porosity a function of the *average pressure* $p = \frac{1}{2}(p_A + p_B)$. Yet more general theories use a complete elastic model.

Introducing the function $S = S(x, t)$, called the *saturation of phase-A*, the integral

$$M_A(t) = \int_V \rho_A \phi(x) S(x, t) d^3x$$

is interpreted as the mass of phase-A in the volume V in the pore space V_f .

By definition the phase-B saturation is $1 - S(x, t)$.

Volumetric flux vectors, u_A and u_B , are defined so that the surface integrals, over the surface ∂V of V , where n is the outward pointing unit normal vector,

$$\int_{\partial V} \rho_A u_A \cdot n ds$$

and

$$\int_{\partial V} \rho_B u_B \cdot n ds$$

are interpreted as net mass rates of flow through the surface of the volume V . Finally introducing the *source terms* q_A and q_B , the *mass balance* laws are,

$$\begin{aligned}\frac{d}{dt} \int_V \rho_A \phi(x) S(x, t) d^3x + \int_{\partial V} \rho_A u_A \cdot n ds &= \int_V q_A d^3x, \\ \frac{d}{dt} \int_V \rho_B \phi(x) (1 - S(x, t)) d^3x + \int_{\partial V} \rho_B u_B \cdot n ds &= \int_V q_B d^3x.\end{aligned}$$

Darcy's Law and Generalisations: Balance laws provide a framework requiring further assumptions before interesting or useful mathematical structures, to be used as models of real systems, can be finalised.

Now assume, for each phase, the generalised Darcy's law, due to Muskat and his associates (see the book by Bear [16] for the Muskat and other references of historical interest),

$$u_A = -\frac{k k_A}{\mu_A} (\nabla p_A - \rho_A g \nabla h),$$

and

$$u_B = -\frac{k k_B}{\mu_B} (\nabla p_B - \rho_B g \nabla h).$$

In these equations k is a tensor valued function of position called the *permeability*, $k_A = k_A(S, x)$ is the scalar valued *relative permeability* of phase-A and μ_A its *viscosity*. Similar definitions apply to phase-B. The function $h = h(x)$ is the *depth* of the point x below some horizontal datum plane and g is the gravitational acceleration. In general k is a second order symmetric tensor. However, it is very convenient when writing simulators or upscaling packages, to approximate k as diagonal in the selected coordinate system. This assumption is made here, as the use of tensors is not central to our topic. (Note, however, that the wider use of tensors by geologists when building geological models, could reduce the eventual resolution requirements.) The relative permeability of phase-A is a monotonic increasing function of S with values in $[0, 1]$ that must include zero. The relative permeability of phase-B is a monotonic decreasing function of S with values in $[0, 1]$ that must also include zero.

Capillary Pressure: The system of equations is closed by the capillary pressure function $p_c = p_c(S, x)$ such that

$$p_B - p_A = p_c(S, x).$$

The capillary pressure function is a monotonic function of S , often with regions of near zero or near infinite gradient with respect to S . Capillary pressure differences have their origin in surface tension effects, and in some explicit forms of the capillary pressure function the surface tension appears as a parameter. In most applications of continuum theory to porous medium flow there is no need to consider a microscopic explanation and the capillary function is measured in the laboratory or inferred from field data.

Phase Behaviour: In more general models there can be three or even more phases with mass transfer between phases. For example the *black oil model* is a three component system of oil, gas and water components separating into three phases; oleic, gaseous and aqueous. Gas can move between the oleic, gaseous and aqueous phases. The oleic phase is a mixture of oil and gas, the aqueous phase a mixture of water and gas, and the gaseous phase is just gas.

Compressible Single Phase Flow: Single phase flow is of theoretical and practical importance. In this simpler model there is only one phase so that a single balance law, for phase-A say, and a single constitutive equation, the classical Darcy's law

$$u_A = -\frac{k}{\mu_A}(\nabla p_A - \rho_A g \nabla h)$$

are used. Note that the relative permeability is not required in this model. The single phase compressible flow model forms the basis of much of the theory of well and flow-based formation testing.

Incompressible Single Phase Flow: In an incompressible flow without sources, and with constant permeability the pressure is a solution of Laplace's equation.

Formulations: The equations of flow through porous media are generally too complicated to have exact solutions in analytical form and numerical methods must be used. There are special cases, however, of great theoretical interest that are valuable for benchmarking numerical methods and validating computer implementations. As part of the process of deriving a numerical method it is sometimes useful to reformulate the differential equations to clarify the mathematical structure. It is also useful to relate the theory to diffusion, convection or wave propagation, for which there are models with canonical interpretations. To illustrate this idea, and to derive results needed in a later section, the reformulation of *incompressible*, two-phase flow will be developed. For simplicity, the case without sources is studied.

For reference, the equations as they arise naturally from the balance law and constitutive equations, are called the *natural formulation*. The derived formulation will be called the *pressure-saturation formulation*.

In terms of the average pressure, p , define

$$p_A = p - \frac{p_c}{2}$$

and

$$p_B = p + \frac{p_c}{2}.$$

Then the phase fluxes are given by

$$u_A = -\lambda_A k (\nabla p - \frac{1}{2} \nabla p_c - \rho_A g \nabla h)$$

and

$$u_B = -\lambda_B k (\nabla p + \frac{1}{2} \nabla p_c - \rho_B g \nabla h),$$

where the notation $\lambda_A = \frac{k_A}{\mu_A}$ and $\lambda_B = \frac{k_B}{\mu_B}$ has been introduced. λ_A and λ_B are known as *mobilities*.

Multiplying the expression for u_A by λ_B and the expression for u_B by λ_A , subtracting one equation from the other and substituting $u_B = u - u_A$ where the total flux, u , is defined by $u = u_A + u_B$, it follows that

$$u_A = f_A u + f_A \lambda_B k \nabla p_c + f_A \lambda_B k (\rho_A - \rho_B) g \nabla h,$$

where the *fractional flow* of phase-A,

$$f_A = \frac{\lambda_A}{\lambda_A + \lambda_B},$$

has been introduced.

By adding the mass balance equations, and substituting Darcy's law, one finds that

$$\nabla \cdot u = 0$$

and

$$u = -k(\lambda_A + \lambda_B) \nabla p + k(\lambda_A - \lambda_B) \frac{1}{2} \nabla p_c + k(\lambda_A \rho_A + \lambda_B \rho_B) g \nabla h.$$

Substitution of the last equation for the total flux into the zero divergence condition provides an elliptic equation for the total pressure, p .

Substitution of the equation for the flux of phase-A into the phase-A mass balance gives the equation

$$\phi \frac{\partial S}{\partial t} + \nabla \cdot (f_A u) + \nabla \cdot (f_A \lambda_B k (\rho_A - \rho_B) g \nabla h) = -\nabla \cdot (f_A \lambda_B k \nabla p_c).$$

This last equation, for a given flux u , is a parabolic equation for the saturation, S . In the limit of high flow rates, the flux term on the left dominates the capillary diffusion term on the right, and so the diffusion term is often neglected. There are, however, subtleties involving boundaries and discontinuities that merit further investigation regarding the neglect of capillary effects at high flow rates.

In the yet further specialisation of neglecting gravity effects one arrives at the celebrated Buckley-Leverett equation, [28],

$$\phi \frac{\partial S}{\partial t} + \nabla \cdot (f_A u) = 0.$$

There is not enough space to describe the properties of this equation. Suffice it to say that the Buckley-Leverett equation has shock-like solutions, where the saturation *front* is a wave propagating through the reservoir. This combination of an elliptic equation for the total pressure and a parabolic, but nearly hyperbolic equation for the saturation, gives rise to great mathematical interest in two-phase flow through porous media.

For further discussion of the pressure-saturation formulation see [128].

Notes on Dual Porosity and Dual Permeability Models: Systems with two or more distinct types of flow path such as (i) fractures and matrix blocks or (ii) high porosity, low permeability inclusions in a moderate porosity and permeability background, can be modelled as a single spatially rapidly varying, heterogeneous continuum or as two interpenetrating slowly varying continua. In *dual porosity* models, all flow takes place in one of the continua and the other acts as a spatially distributed source or sink. In a *dual permeability* model, flow can take place in both continua with mass transfer between them. Such models are a practical way for predicting behaviour in systems that have small length scale heterogeneities possessing different characteristic *time* scales from their surroundings. The idea was introduced in the classical paper [14]. Dual porosity and dual permeability models are usually used for fractured reservoirs, but they could have application in a more general way [23] to reservoirs displaying two or more local time scales.

Numerical Methods for Fluid Flow Simulation: The main classes of traditional numerical methods are: finite difference methods, finite element methods, finite volume methods, spectral methods and pseudo-spectral methods. When applied to the saturation equation in the pressure-saturation formulation, the important device of a moving coordinate system has sometimes been tried.

Most numerical methods work by introducing a grid of points or cells in the 3D space occupied by the reservoir model, and a discrete series of time steps, t^n .

It is assumed that the reader has at least a basic knowledge of numerical methods. The next paragraphs give an overview of the properties of the different methods.

The finite difference technique replaces the differential operators in the partial differential equation formulations with difference operators. For porous media flow studies, this is almost never done, except possibly in situations where the properties are constant. As there exists no variational principle for the full two-phase flow equations, the finite element method must be used

in the Galerkin approach. In its simpler forms, this uses a piecewise linear trial function and orthogonalises the residuals against localised basis functions. Finite element methods can be made to work, but there are suspicions regarding the robustness of a pure finite element method when applied to a hyperbolic equation. Spurious wiggles appear near shock fronts and produce non-physical values which, in turn, cause problems when passed as arguments to relative permeability or capillary pressure functions.

The finite volume method, which returns to the balance equation form of the equations, where one level of spatial derivatives are removed is the method of choice; always for the pressure equation and nearly always for the saturation equation. Commercial reservoir simulators are, with the exception of streamline simulators, entirely based on the finite volume method. See [11] for some background on the finite volume method, and [26] for an introduction to the streamline method. The robustness of the finite volume method, as used in oil reservoir simulation, is partly due to the diffusive nature of the numerical error, known as *numerical diffusion*, that arises from upwind difference methods. An interesting research problem would be to analyse the *essential* role that numerical diffusion might play in the actual physical modelling process; particularly in situations with unstable flow. In the natural formulation, where the character of the problem is not clear, and special methods applicable to hyperbolic, or near hyperbolic problems are not applicable, the finite volume method, in the opinion of the author, is the most trustworthy approach.

Finally there are spectral and pseudo-spectral methods [75] which use a global basis related to Fourier or Chebyshev expansions. The order of accuracy is $O(N)$ in the number of nodes. In simple geometries the method is of great power, at least for the hyperbolic equation. It has not to our knowledge been tried on the pressure equation of reservoir modelling. One might expect difficulties relating to the discontinuous nature of permeability, but these might be surmountable. The pseudo-spectral method mixes working in Fourier space and real space. In this way it is possible to apply spectral-like methods to problems with non-polynomial nonlinearity. The pseudo-spectral method, which uses spectral interpolation on a grid, is slightly less accurate than a spectral method although it is of the same order of accuracy. However, the pseudo-spectral method is more efficient and also simpler than the spectral method [24].

Classification of Simulation Methods by Time Stepping Scheme: Commercial flow simulators generally discretise time derivatives using a first order finite difference formula (Euler's method). The time derivative thus involves the difference of functions at the end and at the start of each time step. All other terms in the equations are discretised to involve functions evaluated at the start and the end of each time step. The pressure *always* appears at the end of the time step and one says that the pressure is *implicit*. Saturations appear at the end of the time step in the *fully implicit* approach. The saturation

only appears at the start of the time step in the *implicit in pressure, explicit in saturation* method (IMPES). When some regions of the flow domain are IMPES and some are fully implicit, and the regions are modified during the simulation, then the time stepping is said to be the *adaptive implicit* method (AIM).

Generally speaking, the more implicit is the simulation method, the more stable is the scheme. The more stable schemes can take longer time steps without spurious, growing, transients. However, stability is usually accompanied by loss of accuracy.

There are many variants on these ideas. For example, one can form a scheme in the pressure-saturation formulation where the pressure is implicit, as usual, but in the pressure equation the saturation is evaluated at the start of the time step, and in the saturation equation the scheme is fully implicit in all variables. This gives improved stability compared to the IMPES scheme, but it is not as stable as the fully implicit method.

Finite Volume Methods: The finite volume method, when the permeability tensor is diagonal in the selected coordinate system, approximates the pressure and saturation functions as piecewise constant in each grid block. The flux components are assumed constant in their related half-cells. Thus when two cells are joined by a face, the related component of flux is assumed to be the same each side of the face. The balance laws are invoked separately on each grid block, and are discretised in time either by an explicit or fully implicit first order Euler scheme or other variant as discussed in the previous subsection.

The final expression for the numerical flux uses the central difference approximation to $\nabla p_A - \rho_{Ag} \nabla h$. When the permeability tensor is diagonal, for the x -component say, Darcy's law can be arranged to read

$$\frac{u_A^x}{k^x} = -\lambda_A \left(\frac{\partial p_A}{\partial x} - \rho_{Ag} \frac{\partial h}{\partial x} \right),$$

where a superscript notation is used to denote the x -components of flux and the tensor. In the central difference approximation λ_A is assumed constant over the two half-cells adjoining a face with a value equal to that in the cell which is *upstream* of the face. The upstream direction is determined from the sign of $\frac{\partial p_A}{\partial x} - \rho_{Ag} \frac{\partial h}{\partial x}$. The device of using the upstream mobility is necessary for numerical stability. However, it does not take into account any vector attributes of the information flow direction. For this reason the numerical scheme can exhibit grid orientation effects, where results are sensitive to the grid used, and may not converge under grid refinement. This is particularly so when the flow is physically unstable. Some further detail about the finite volume scheme is given in [58], and for a full description, [11] is recommended.

Streamline Methods: For some years, originating with [69] there has been interest in applying the method of characteristics to the solution of the hyperbolic equation. Such methods do not possess a local mass conservation

property, as is the case with the finite volume method, but, nevertheless, when applicable they are spectacularly more accurate than finite volume techniques. This is particularly the case for miscible displacement, which is analogous to using *straight line* relative permeabilities. Here the characteristics are the streamlines of the velocity field, and so points distributed in the volume of interest move in the direction of the local total velocity, and carry a constant, or perhaps slowly changing, saturation value. For a detailed review of these moving point methods see [54].

The paper [130] describes a method of characteristics accounting for shock waves. In one dimension the two-phase flow problem can be solved using characteristics even with capillary pressure effects. In two dimensions the situation is more difficult as a result of diffraction of characteristics at permeability discontinuities. Other than [130] there was no progress in applying methods using characteristics on the full two-phase flow case, with general relative permeability curves. However in the paper of [26], the idea of simply solving the Buckley-Leverett equation along pre-calculated streamlines was introduced. This has led to a whole new class of numerical methods, the *streamline methods*. There has not been much rigorous analysis of the convergence of these schemes, and some people are of the view that they are not *proper* numerical methods. However, their simpler and older cousins the moving point methods can be brought into the fold of rigorous approaches (even when diffusive effects are included) and so it may not be long before the streamline method is also rigorously analysed. (For a proof that variants of the moving point method do converge see [53].)

Streamline methods are very fast compared to fully implicit and IMPES methods. This, however, has little to do with their streamline character but more to do with their close similarity to implicit-in-pressure, implicit-in-saturation methods, with the additional feature of very large time steps between updates of the pressure, and many small time steps that update the saturation between the pressure updates.

Instability and Viscous Fingering: The main method of secondary oil recovery injects water into oil reservoirs to push oil towards the producing wells. When the viscosity of the water is less than that of the oil, any small perturbation in the shape of the oil-water front is unstable. Indeed, the shorter wavelength disturbances can grow faster than longer wavelengths, until damped by nonlinear effects. This phenomenon, known as *viscous fingering*, makes the prediction of the fluid flow even more difficult. The viscous fingering instability is closely related to the famous *Hele-Shaw* problem upon which there is a large mathematical literature [86].

The Effects of Heterogeneity: Natural rocks are generally very heterogeneous in the spatial distribution of their properties. There are usually at least three length scales in the variations of permeability. At the lamination scale of centimeters, at the layer scale of meters, and on areal scales of 10's of meters.

It is impossible to resolve all of these scales in detail, and so it is necessary to choose a *cut-off* length scale in any particular modelling exercise, and all phenomena on a scale below the cut-off must be modelled by the appropriate assignment of the properties that appear in the equations.

Different values of the cut-off imply, in general, different values of the properties in the equations. Sometimes, even the form of the equations must be modified for different values of the cut-off length scale.

Sometimes there might be actual or interpreted data that provides a description on some small scale. Then it becomes essential to find a model that only predicts the larger, tractable, scales by a process of upscaling.

The Structure of a Reservoir Simulator: A reservoir simulator is software for solving the porous medium flow equations with detailed models of the spatial distribution of rock properties, detailed models of the thermodynamics of phase behaviour, of the wells and how the wells connect with each other through surface networks. Further, a reservoir simulator will have built-in support for optimisation software in that derivatives of specified flow diagnostics, such as well rates, or masses of chemical components in specified volumes, with respect to a variety of parameters can be computed.

Thus a simulator is a complicated item of software. The simulation of fluid flow through rocks is just a small part.

The Assembly Stage: The simulator starts from the discrete nonlinear equations relating the state of the reservoir at one time step to the values at a previous step. These equations are linearised using Newton's method for nonlinear equations. Experience shows that simulators are more robust when linearisation derivatives are found analytically, rather than numerically. The derivatives have to be chained through the thermodynamics in the reservoir, up the wells and into the separators.

The result of linearisation is a large, mainly sparse, system of linear equations which are generally non-symmetric. Any significant departure from sparsity arises from coupling of geometrically distant parts of the reservoir along wells or large, explicitly modelled, fractures [98].

Linear Solvers: Although general purpose solvers exist, major improvements in efficiency can be gained by exploiting structural features of the linear equations that are particular to reservoir simulation. The key parts of any linear solver are (i) a method of pre-conditioning, essentially an approximation to the system of equations that can be solved directly, but without storage or speed problems (ii) an iteration scheme.

For many years the standard preconditioner has been the method of nested factorisation due to [8]. The iteration scheme of choice, based on well known approaches to nonlinear optimisation, has been the orthomin method of [153]. Only recently have there been challenges to nested factorisation from multigrid methods and domain decomposition methods. Deeper analysis may lead to improvements on basic orthomin. (See [134] for a complete overview and [150] for a review of multigrid.)

Multiscale Simulation Techniques: Recent developments in geological modelling have led to a need for simulations on models so large that linear solvers cannot operate without virtual memory. One approach to this problem is upscaling, another is the use of multiscale simulation. Upscaling is essentially an averaging method that can be performed separately from simulation. Thus upscaling is usually done in another application, the model generator itself or a special purpose model translator. Multiscale simulation is more drastic, at least in its most promising forms. Here instead of assuming in each grid cell that the pressures and fluxes are constant, or possibly linear plus a constant, the variables are complicated functions of position, calculated from small-scale simulations. This technique, introduced by [91] is the current focus of world-wide research efforts [94].

Monte Carlo Simulation: Under most circumstances, models that are implied by data are non-unique. Many different models integrate the same data. Hence a probabilistic description is appropriate. This is reviewed in detail later. However, it requires the results from multiple simulations to assess the implied statistics of the diagnostic functions.

As of now, the only practical approach when dealing with nonlinear systems with stochastic input, is to sample the input and then run the simulator to gather a sample of the diagnostics. In practice people use rather small samples, but numerical experiments show that many samples are needed if the mean and the standard deviations of the output are to be estimated with any accuracy.

One answer is to use smaller, less detailed models, so that many samples can be obtained. More research is needed to establish optimal workflows regarding this problem.

The Bayesian Analysis of the Output from Large, Complex, Computer Codes: In practice one is faced with having to *guess* the answers to difficult technical problems. This is formalised in the Bayesian approach to statistics. Some background knowledge is needed to enable results to be guessed to some reasonable level of accuracy. For example, this knowledge might be based on large numbers of coarse grid simulations. Then one can form a rational view of the statistics of the output. A few detailed simulations can then be performed, that through the application of Bayes' rule can be used to update our prior probability assessment. This is a new, exciting approach, to the analysis of simulation output and has been explored in [38, 99, 100]. Note that this application of Bayesian statistics is quite distinct from the application to the evaluation of uncertainty arising from measurement error and under-determination.

3 Grid Generation

A grid is a decomposition of some volume, Ω , into a finite set of subvolumes, Ω_b such that (i) the union of the subvolumes is approximately equal to the parent volume and (ii) most of the intersection of the surfaces of any pair of subvolumes is included in the intersection of their respective volumes. The subvolumes are called cells or blocks. Thus one is allowing some finite volume of overlap between subvolumes and also some holes provided that the offending volumes are small. Ideally the volume of overlap and of holes will be zero, but in complicated geometries and with the possible constraint to hexahedral cells this is not always practical.

For example, *the uniformly tessellated cube* or *logical grid* is the tessellation

$$\Omega = \bigcup_{i,j,k} \Omega_{i,j,k},$$

where

$$\Omega_{i,j,k} = \{\mathbf{x} \mid ih_x \leq x \leq (i+1)h_x, jh_y \leq y \leq (j+1)h_y, kh_z \leq z \leq (k+1)h_z\},$$

and where h_x, h_y, h_z are the grid sizes in the x, y, z directions and i, j, k are integers.

3.1 Structured Grid Generation

A structured grid is a cell-by-cell mapping of a given volume into a part of, or the whole of, the logical grid. When mapped into only part of the logical grid, it is said that the unmapped cells are *inactive*. An example is shown in Figure 1 where the inactive cells are shown with dotted lines.

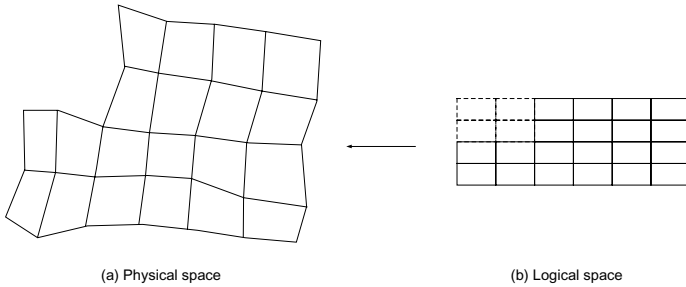


Fig. 1. Structured grids in 2D.

A line of constant i and j is called a coordinate line. A line of constant i and k or j and k is called a grid line. Roughly speaking coordinate lines are

vertical lines and grid lines are *horizontal* lines (in physical space, not on the page).

Strategies: Most literature on structured grid generation concerns boundary conforming grids. In many cases, such as flow in a pipe, the boundary is external, and in other cases such as flow around a vehicle, an internal boundary. In both cases the boundary is a closed surface.

Grid generation requirements in the geosciences are more demanding. Not only must the grid conform to an external boundary, but it must also honour the layers and the faults. Layers tend to divide the volume or area defined by the external boundary into well-defined segments, but the faults are not generally introduced in such a convenient form. In a geological system there may be many of these *internal* boundaries due to faults and layer boundaries. Many of the internal boundaries will not divide the system into pieces; for example they mark a region where rocks were fractured and then displaced that is quite local.

Standard structured grid generation methods position the grid nodes according to some criterion of smoothness. This can be expressed in the form of an energy functional to be minimised. Sometimes the method is presented as that of solving a partial differential equation, but this is normally equivalent to minimising an energy or smoothness function or functional. In traditional engineering grid generation the constraint on the minimisation is that the grid conforms to the external boundary, and this formulation naturally generalises to one in which the individual internal grid nodes associated with internal boundaries are constrained to particular values. Thus if one can identify which grid nodes are to be related to which geological surfaces one has solved most of the structured grid generation problem.

There are three main strategies for building structured grids which are as follows:

Zigzagging: The first approach is to build a structured grid of coordinate lines without reference to the internal boundaries. The coordinate lines, in some sense nearest to the internal boundaries, are then located and the internal boundary is displaced to the lines. That is, the geometric data is itself modified. This process is called *zigzagging*. This is the most robust technique and can generate a grid for any object if the initial grid has sufficient resolution.

Snapping: The second approach is to build a structured grid that conforms to the external boundary. An algorithm then identifies the coordinate lines nearest to the internal surfaces and displaces them to the surfaces. This process is called *snapping*. If the initial snapping only involves a small deformation, the subsequent grid may be of sufficient quality. However, the snapping might cause badly deformed cells or even cell-folding, where a grid cell is self-intersecting. Thus the snapped position of the nodes might be used as constraints and the grid generation algorithm is then executed again, but this

time applying the internal constraints. There is no theory behind this strategy that guarantees a good quality grid. Nevertheless, if the grid smoothness algorithm involves curvature terms, then the results can be good.

In practice each geological object is introduced in a sequence in which snapping is followed by smoothing. In other words, one does not introduce all of the internal boundaries in a single step. Success in grid generation may be sensitive to the order in which the internal boundaries are applied as constraints.

Block Splitting: The third approach is to divide the system into large pieces so that the internal boundaries are included in the boundaries of the large pieces. This requires that the internal surfaces are extended to the boundary in some way. This is quite difficult to do, but with some help from the user, algorithms for this can perform quite well. This particular strategy is reducing the problem of grid generation with internal components of the boundary to a set of problems equivalent to pure boundary grid generation problems. A good implementation would, however, only use the topological information arising from the splitting process, and in the grid generation it would minimise the smoothness functional subject to the constraint that the grid nodes associated with the internal boundaries are constrained to lie on the internal boundary surfaces.

The second and third approaches are usually combined with the first approach, so that the most distorted internal boundaries are zigzagged and the smoother internal boundaries, that align with parts of the external boundaries and amongst themselves, are modelled by splitting or snapping.

Some methods require the internal boundaries to be classified as lining up with the i - or the j -direction. This means that the external boundary has four main parts, corresponding to the four sides of the logical cube. Once the external boundary is deformed there are two families of internal coordinate lines that can be mapped onto the internal boundaries. Software needs help to make this classification. Users can help further, by cutting the more distorted internal boundaries into pieces, and mapping the pieces onto different families of coordinate lines.

Partial Differential Equation Methods: The classical, beautiful, paper of [158] is of particular significance to structured grid generation. The key idea, given by Winslow in an appendix to his paper, is to solve *heat conduction* problems - *in the physical space* - without sources or sinks and with boundary conditions chosen so that each isotherm divides the region into two pieces. Since the maximum principle applies, that the maximum and minimum temperatures must occur on the boundary, the isotherms cannot cross. In two-dimensions, by solving two problems with two sets of isotherms that intersect one another broadly at right angles, one can construct the required grid cells. Of course, to solve these problems one needs a grid. To escape from the obvious dilemma, Winslow transformed the equations into the logical space and solved for the coordinates of the cell corners, rather than the temperatures. This procedure

works very well, although by applying the boundary conditions in the logical space, rather than the physical space, the robustness of the method is compromised. (In unpublished numerical experiments of the author, where having first constructed an unstructured grid, and having solved the heat conduction problems on this grid with the physical boundary conditions of zero flux through the appropriate sides, it was possible to map essentially arbitrary shapes onto a rectangle. A similar technique, [57], is outlined a little later.)

The paper of Winslow has inspired much further work. An early contribution along the Winslow path was [147].

Variational Methods: Techniques that use an elliptic partial differential equation can also be derived from a variational principle. Thus for heat conduction analogies the functional

$$\int ((\nabla \xi)^2 + (\nabla \eta)^2) d^2x,$$

is minimised, where ξ and η are the two temperatures in the 2D case. With this variational principle it is possible to add extra terms, such as terms to encourage orthogonality, or equi-distributed areas. The ideas generalise easily to three dimensions. The paper of [25] develops this in some detail and shows how to cast the principles in the logical space so that numerical solutions can be found. The book [102] explores the variational approach and in particular Knupp's area-orthogonality technique. Reference [102] also contains valuable illustrations showing the features of the different structured grid generation methods enabling a comparison of their behavior to be made. It is the experience of the author that the area-orthogonality method is robust and generates pleasing grids.

Direct Discrete Methods: The related technique of solving Laplace's equation for the coordinates of the grid cell corners in the logical space, a technique introduced by [6] is simple to implement but not that robust. This method is equivalent to imagining that the *energy* of the grid is the sum of the squares of the length of the cell sides. Thus one minimises the grid function

$$\sum_{i,j} \{(\mathbf{x}_{i,j} - \mathbf{x}_{i-1,j})^2 + (\mathbf{x}_{i,j} - \mathbf{x}_{i,j-1})^2\}$$

prescribing and fixing the positions of the nodes on the boundary. Minimisation of this generates the same scheme as discretisation of a Laplace equation in the logical space. As shown in the pictures of [102] it is rather easy to generate folded grids when the boundary contains non-convex regions. To try to fix these inadequate methods, extra terms can be added, in a direct, discrete framework. The work of [32] and [105] is representative of this approach.

An important application and extension of the idea of discrete grid generation is found in the work of [113] and [114]. See Section 4.1 for further discussion of this *discrete smooth interpolation*.

Corner Point Grids: An interesting and practically important method of grid generation in the geosciences is that of the corner-point grid. An early example can be found in the reservoir simulator described by [101]. The idea, when first introduced, was a two-stage grid generation method. First an N_x by N_y by 1 structured grid is built that honours the boundary, probably using inactive cells, and, where possible the interior coordinate lines are aligned with fault surfaces. Where this alignment is impossible then the fault is zigzagged onto the grid. The surfaces that define layers are then introduced into the grid by finding the intersection points of the surfaces with the coordinate lines. In the absence of faults this is a simple procedure, and, as long as the coordinate lines are broadly orthogonal to the layers the resulting grids are of high quality and conform exactly to the layers. When there are faults, circumstances are more challenging. If the coordinate lines are aligned with the faults then the line can be temporarily displaced to one side of the fault by ϵ and the intersection computed, and then temporarily displaced by ϵ on the other side of the fault and again the intersection found. In this way *split nodes* are associated with the fault. If the coordinate lines are some distance from the fault then *zigzagging* is used where the idea is to move, as an approximation, the fault to the grid and repeat the procedure just described.

In the absence of faults, grid blocks conform, in the sense that the physical neighbours are also the logical neighbours. When faulting is present the logical and physical neighbours no longer coincide. Any physical connections that are not also logical connections are referred to as *non-neighbour connections* or *NNCs*.

When there are more complicated faults, such as intersecting faults in a y -shape, it is very hard to make the corner-point grid method work, at least without a lot of help from users. One promising technique, known as *ijk gridding* or *vertical zigzagging*, is to build an *adaptive raster* using extensions of the surfaces near faults and build a grid with some refinement around the fault. Software that used this method was first released in [136]. The grid blocks do not conform exactly to the geometry, but they are closer than if the grid was just an arbitrary set of cells, as in a rectangular Cartesian grid. Various candidate patterns of grid blocks are proposed (based on assigning grid blocks to either of the different sides of the fault). The choice of candidate patterns is then made on the basis of the best representation of volume and adjacency.

More material and illustrations relating to corner point grids can be found in Section 7.1 on structural modelling.

A Technique for Dividing a Region with Internal Components of the Boundary: As the complexity of the geometry increases, so unstructured grids are generally much easier to build than structured grids. One can exploit this fact in building structured grids. The idea of first building an unstructured grid and then converting to a structured grid was explored in [57]. In that

paper an unstructured triangulation was constructed using a *slicing approach* followed by building vector fields and then building the structured grid.

An initial triangulation is made by dividing the squares in a structured rectangular grid. Then the boundary polygons, for both the external and internal boundaries are processed, line-segment by line-segment. That is, each line segment is used to divide any triangles which they cut into three triangles (two in degenerate cases). At the ends of the internal boundaries, a line is drawn at right angles to its end-point. This extra line is first absorbed into the triangulation so that the end-point of the internal boundaries are included amongst the nodes of the triangulation in subsequent steps.

The lines from the boundaries are then used as boundary conditions for two vector fields, defined on the vertices of the triangulation so that they minimise a measure of smoothness of the fields. The smoothness condition enables an interpolation of the boundary vectors to be constructed.

Once the vector fields are constructed, they can be used to extrapolate the internal boundaries to the external boundary. This divides the volume inside the external boundary into large pieces whose boundaries can be used as the external boundary of a standard structured grid generation method such as the area-orthogonality method. See [57] for the details and some illustrations.

3.2 Unstructured Grid Generation

Conventional Unstructured Grid Methods: In general any grid that is not structured is an unstructured grid. Of particular importance are Voronoi tessellations and their dual the Delaunay tessellation. In three dimensions Voronoi cells are convex polyhedra and Delaunay cells are tetrahedra. In two dimensions Voronoi cells are convex polygons and Delaunay cells are triangles.

The Voronoi grid consists of points, called centres, that are scattered over the domain. The Voronoi cell, Ω_b , with centre x_b consists of the points

$$\Omega_b = \{x \mid \|x - x_b\| \leq \|x - x_{b'}\|, \forall b' \neq b\},$$

where the index b' ranges over all the other centres. In words, the cells correspond to those points that are closest to their respective centre. The faces of a Voronoi cell, that do not lie on the surface of the entire volume, Ω , are flat. The points on the interface between two grid cells are equidistant from the centres of each cell. The lines joining the centres of cells that share a common face, define the dual, Delaunay grid. The tetrahedra of the Delaunay grid possess the remarkable property that their circumsphere does not contain any of the centres other than the centre at the centre of the circumsphere. See [123] for a comprehensive review of Voronoi and Delaunay tessellation theory. See [145] for applications to unstructured grid generation.

A problem with unstructured grid techniques, particularly in 3D, is to build grids honouring the surface of a given volume, or internal surfaces such as faults and horizons. This can be achieved but not without considerable

difficulty in programming and in computation. In 2D the method is robust, but in 3D it can fail and require *user intervention* to help the algorithms achieve good results.

Unstructured grids have found widespread application in many areas of computational fluid dynamics and elasticity theory but have not been used very much in the geosciences. See [66] for a selective example in the geosciences. Unstructured grids have, however, found application in the context of 2.5D unstructured grid generation as explained next.

Corner Point Unstructured Grids: The idea of the corner-point unstructured grid is to first *verticalise* all of the faults in the model. The fault traces of the verticalised faults are then projected onto a plane, and a conforming Voronoi or Delaunay grid constructed. A coordinate line is then introduced at each vertex in the planar unstructured grid. These coordinate lines extend vertically until they cut an upper and a lower plane, both parallel to the projection plane. The coordinate lines that lie on the corners of each of the unstructured cells in the plane define a coordinate tube analogous to the tubes defined for the structured grid case. This is essentially an unstructured logical space. The task of building the final grid is now to deform these logical tubes to conform to the original (non-verticalised) fault surfaces and to impose the condition that, at least in the region of space occupied by the reservoir, none of the tubes are self-intersecting or inside-out.

The coordinate lines that lie on faults are then sloped until they lie optimally on the fault surface. The intersections of these coordinate lines are found with the upper and lower planes. The intersection points are then used as boundary conditions in two smoothing problems on the upper and lower planes. The coordinates of the other, non-fault, coordinate lines are determined by a condition that relates their coordinates to the average of their neighbours. This is essentially an unstructured version of the Laplace equation method in logical space. On the upper and lower planes the resulting unstructured grid can be very complicated, with many self-intersecting cells. Miraculously, in most cases anyway, the grid when examined in the region of the reservoir is perfectly satisfactory.

The layers and faults are finally sampled onto the coordinate lines in the same way as for the same task for the structured grid case. A detailed explanation can be found in [77].

Notes on the literature. In the oil reservoir simulation literature the papers of [82, 83, 141] are of note.

For reviews of the grid generation literature see [59, 102, 146, 148] for information concerning structured grids or [145] for reviews of both unstructured and structured approaches.

4 Spatial Statistics: Interpolating Scattered Data

Spatial statistics, often called *geostatistics* and sometimes *property modelling* is concerned with problems of *interpolation under conditions of uncertainty*.

Consider, for example, interpolating a scalar valued function $\varphi = \varphi(x)$, in some region of D -dimensional space, \mathcal{R}^D , where the values of φ , $\{\varphi_i\}$, at the points $\{x_i\}$ have been measured with only small errors. Further data is abstracted from some *prototype* or analogue that could be said to *look like* the property that φ is to model. To be specific; given detailed information about a rock outcrop or a densely sampled reservoir of the same depositional environment as the target reservoir, construct an interpolant of the actual measurements that is qualitatively the same as the prototype. Where there are manifest differences between the prototype and the system to be modelled it is necessary to devise methods of transforming the data relating to the prototype in response to expert judgement. The prototype is used to assign realistic estimates of statistical measures such as correlation functions (equivalent, essentially, to variograms). It is a mistake to only use the data available from the target reservoir to ascertain the correlation structure, unless the data are sampled on a scale smaller than the correlation length.

In general, other types of data will be available for many different properties and on several scales. However, this level of generality will not be considered until later sections.

There are obviously many possible interpolants of the data that look like the prototype. Uncertainty quantification is the characterisation of the variation between these different, but data consistent, interpolants. Sometimes only one of these interpolants is selected. For example, the one that is, in some sense, the *smoothest* or the *most probable*. Some methods, such as kriging, allow an estimate of uncertainty to be assigned to these single estimates. See Section 4.6 for an explanation of the dangers in using a single representative from the set of all possible interpolants.

There are several approaches to this interpolation problem; approaches that are not equivalent. It is, however, generally agreed that some probabilistic element is required. Having said that, it is also the case that deterministic interpolation procedures are in widespread use. Thus, before reviewing statistical and stochastic methods, a survey of deterministic methods is given. Later sections show that these methods are closely related to kriging. This is not a new result [89] but does not seem to be widely known.

Note that the problem of scattered data set interpolation is discussed in many other contexts: for example in weather forecasting [39] and in oceanography [160].

4.1 Deterministic Methods

Delaunay Triangulation: Assuming a mappable, continuous surface project the data points onto a datum plane. Applying Delaunay triangulation build

an unstructured grid in the plane with the data points located at the nodes. Then perform linear interpolation. If the data points are located at the points $\{\mathbf{x}_i \mid i \in [0, M-1]\}$ then introducing piecewise linear basis functions $\{b_i(x) \mid b_i(x_j) = \delta_{ij}\}$, where $\delta_{ij} = 1$ if $i = j$ or $\delta_{ij} = 0$ if $i \neq j$, the interpolant is of the form $z(x) = \sum_i z_i b_i(x)$. This method works well if the data points are uniformly distributed, uniformly or fully at random, in the region of interest. When the data points are clustered, and large triangles occur, then the method is insufficient. It is difficult to inject any interpretation or style into the method other than by manually inserting control points. This is only a local means of control and not based on any principle.

The method does not easily generalise to problems with overturned surfaces or discontinuities.

(Note that in Delaunay triangulation the data points form the vertices of the triangles in such a way that the circumcircles of the triangles do not contain any data points. Data points can only lie on the circumcircles of the triangles.)

Search Radius Methods: The search radius technique assumes a single valued surface, but accounts for discontinuities. A circle is specified by its radius and, centred on the sampling point at which the height (or other property) is required, all scattered data points inside the circle are located. A polynomial, of some specified degree, is then determined by a least-squares method. Many variants are possible, such as weighting data points by their distance from the sampling point. Discontinuous surfaces are accommodated by ignoring data points which are not on the same side of the discontinuity as the sampling point. A more sophisticated version might use a restored surface estimate from the other side of the discontinuity.

Search circle techniques, with user controls allowing increasing or decreasing circle radii and changes in the order of the polynomials in response to the number of scattered data within the circle, have been used for many years in commercial mapping packages. However, these methods do not have much support from theory, can be slow, and without extensive use of surface patches and help from the user, do not work for reverse faults. See [95] for an extended discussion of search circle techniques.

The Method of Minimum Curvature: Briggs, [27], introduced this method which has found widespread application in commercial mapping software (for example, see [84]). The method is known to be closely related to spline interpolation [90, Chapter 9]. As shown later, minimum curvature methods are a special case of the radial basis function approach and also of the kriging method.

The technique is based on the requirement that interpolating surfaces render the functional,

$$\int_{\Omega} (\nabla^2 z)^2 d^2x$$

stationary, subject to the constraints that $z(x_i) = z_i^*$, where the $\{x_i \mid i \in [0, M-1]\}$ are data points at which the height, or other, data is z_i^* .

Briggs studied the case where the surface was single valued and without discontinuities. Applying the calculus of variations one obtains the problem

$$\nabla^2(\nabla^2 z) = 0, \quad z(x_i) = z_i^*, \quad i = 1, \dots, N-1,$$

with the natural boundary conditions

$$\nabla^2 z = 0, \quad \nabla^2 \left(\frac{\partial z}{\partial n} \right) = 0, \quad x \in \partial\Omega.$$

On a rectangular grid, with scattered data points located on the grid vertices it is straightforward to solve this problem using a finite difference method. A slight modification, providing the user with some qualitative control on the character of the surface, is to use the functional

$$\alpha \int_{\Omega} (\nabla^2 z)^2 d^2x + (1 - \alpha) \int_{\Omega} (\nabla z)^2 d^2x$$

with $\alpha \in [0, 1]$, which implies the partial differential equation

$$\alpha \nabla^2(\nabla^2 z) - (1 - \alpha) \nabla^2 z = 0,$$

but with slightly more complicated boundary conditions. It is unnecessary to use the natural boundary conditions for this composite problem, and using the natural conditions for the pure biharmonic problem might be preferable, as long as α is greater than zero. This functional contains a single parameter that can be used to inject some interpretation or style. As α decreases to zero from unity, the peaks and troughs that occur at the data points become sharp, and the surface comes to resemble an elastic material suspended on a set of vertical poles. When α is near unity the peaks and troughs are rounded and it is often difficult to see where the data points were located.

The author has found that in applications of the minimum curvature method to surface modelling that a linear solver (a preconditioned conjugate gradient method) greatly increases the speed of solution, compared to a simple relaxation method such as the Gauss-Seidel iteration, particularly with a non-zero value of α . A similar method, but ignoring cross-derivatives, has been discussed at length by [10]. These authors use a fast alternating-direction-implicit solver. An interesting and, from a practical point of view, a very important generalisation of the Briggs method of minimum curvature is to perform a transformation of coordinates before the surface modelling. When the transformation is implemented via a set of, unstructured, or structured, coordinate lines all faults appear *vertical* in the new coordinate system, but without error. It must be emphasised that this particular *verticalisation* is very different from the *active* verticalisation that can be made (by default or as an option) in some modelling systems. Once the transform is applied

then a Briggs type method can be implemented. Care must be taken, however, now that a curvilinear coordinate system is in use. This idea is used, with great effect, in the application described in [64].

Discrete Smooth Interpolation: DSI is as much a philosophy of mathematical modelling as it is an interpolation method [113, 114]. A topological structure, in the form of a set of nodes with a pre-assigned neighbourhood structure, is assumed. A *local roughness function* is then defined for each node. An essential feature of the method is the assumption that each roughness function is a quadratic form in the values to be interpolated. Note that the interpolated function can be vector valued.

A *global roughness function* is then defined as the sum of the local roughness functions. The global function, too, is then a quadratic function of the unknowns. A simple node-by-node minimisation technique can be quite effective if the number of cells in the grid is not too large. Otherwise simultaneously setting all of the derivatives of the global function with respect to the unknowns, to zero defines a linear system. This system can then be solved efficiently by one of the many methods for solving large, sparse, symmetric linear systems.

[113] and [114] presents DSI as an essentially discrete approach although sometimes the choice of local roughness function is motivated by discretising a derivative. DSI is a variational method that restricts the roughness function to be quadratic in the unknowns.

There is a long history of using variational methods in structured grid generation - see Section 3 - in which quadratic and non-quadratic functionals are used. During the last few years (although interest has now diminished) there were many papers on direct discrete formulations of the grid generation problems [33]. In the case of structured grid generation, where the problem is to map a given shape onto a rectangular grid (in 3D and 2D) the quadratic method, introduced by [6] is known to perform badly unless the shape is close to rectangular. This is a very simple application of a method, equivalent to DSI, that is known to be of limited usefulness. The technique of [158], which solves Laplace type problems on the physical region, showed that *non-quadratic* functionals are required for robust interpolation to be possible. Thus it would seem preferable to focus on problem formulations using a continuum approach with subsequent discretisation in the implementation.

Another disadvantage of direct discrete methods is their requirement for the assignment of many weights. When the discrete variational form arises from a continuum variational principle most of the weights (except those controlling the global balance of the major terms of the functional such as total area or curvature) are deduced via the discretisation.

Radial Basis Functions: In these methods a continuously differentiable, *radial basis function*, ϕ , is introduced and interpolants of the form

$$z(x) = a + b \cdot x + \sum_{j=0}^{M-1} \lambda_j \phi(x - x_j)$$

are sought, where the $M + 1 + D$ unknowns, the λ_j 's, a and b , are coefficients to be determined using the conditions

$$\begin{aligned} z_i^* &= a + b \cdot x_i + \sum_{j=0}^{M-1} \lambda_j \phi(x_i - x_j), \quad i = 0, \dots, M-1, \\ \sum_{j=0}^{M-1} \lambda_j &= 0, \\ \sum_{j=0}^{M-1} \lambda_j x_j &= 0, \end{aligned}$$

noting that b and x are D -vectors. These conditions give $M + 1 + D$ conditions for the $M + 1 + D$ unknowns. Generalisation to higher dimensions (in the x -variable) and to generalisations which include higher order polynomials other than the affine terms $a + b \cdot x$ are sometimes used. Specialisation to one or two dimensions is straightforward, and often the affine term, a , is omitted. The function φ can be chosen from a large list [31], where r , c and α are real parameters, r satisfies $r > 0$, and $\|x\| = \sqrt{(\sum x_i^2)}$,

$\phi = r = \ x\ $	linear
$\phi = r^2 \log r$	thin-plate spline
$\phi = e^{-\alpha r^2}$	Gaussian
$\phi = (r^2 + c^2)^{\frac{1}{2}}$	Multiquadric.

See [31] and [117] for specific applications and interesting further details.

The classical *multiquadric* method of [79] has often been used in the geosciences. See [63] for a review of *classical* methods of scattered data set interpolation.

Radial basis function methods are elegant, do not need a grid, and possess excellent convergence and robustness properties. However when the number of scattered data points is large it requires sophisticated iteration methods to determine the coefficients which, though in itself not an obstacle, when coupled with a requirement to evaluate the interpolant - a sum of a large number of products - on a large number of points, such as on a grid, reduces the attractiveness of the method.

There is very little literature that accounts for discontinuities in radial basis function interpolation. However, a search radius method, in which a radial basis interpolant is used, rather than a polynomial, would be practical

and would generalise to discontinuous cases. The paper [78] considers the detection of vertical faults using a radial basis function technique.

Overtaken surfaces are a greater problem, although application of a search radius method in combination with sloping coordinate lines could lead to a practical solution.

It is of interest that $r = \|x\|$ is the Green's function for the biharmonic operator in 3D and $r^2 \log r$ the Green's function for the biharmonic operator in 2D. With these particular choices of ϕ , the radial basis function method is an exact solution of the pure Briggs minimum curvature method, or, depending on the implementation, a close approximation.

Thus for large sets of scattered data and with a need to evaluate the interpolant at a large number of points on a grid one might be better served, when D is small, by the numerical solution of a partial differential equation as in the Briggs technique. However, the recent research into radial basis functions with compact support [61] and application of the fast multipole method [29] do provide efficient methods.

Recent reviews of radial basis function methods can be found in [29] and [92].

4.2 Statistical Approaches

Two classes of probabilistic approach are possible. One class is the direct probability density functional (pdf) approach, often generalising the multivariate Gaussian (normal) distribution. The other class consists of assumptions and rules that define a stochastic process. In this second class of method it is not usually possible to state an explicit pdf for the interpolants; the process must be studied via its sample realisations and their properties. The derivation of standard geostatistical results often appears to be rule based but, as shown in the next few pages, can be derived from an explicit pdf. More research using explicit pdfs could lead to new results and insights into the methods of spatial statistics.

4.3 Random Functions

There is insufficient space here to give a full treatment of the theory of random functions. Thus the following specialises the treatment and proceeds formally. There are many texts on basic multivariate probability theory and statistics, and so a basic knowledge of these subjects is assumed on the part of the reader. Texts on the theory of turbulence, such as [65], present the theory in sufficient detail for applied geostatistics. Background in statistical field theory as reviewed by [18, 19, 73] is very relevant.

Review of Some Basic Theory: This subsection reviews some fundamental properties of *Gaussian random fields* in D -dimensions. The case $D = 2$ is needed for surface modelling, and the $D = 3$ case for property modelling.

The following needs the notion of the *functional derivative*,

$$\frac{\delta F}{\delta \varphi(x)}$$

of a functional $F[\varphi]$.

To define this, first introduce the *first functional differential*

$$DF[\varphi : \delta\varphi] = \frac{d}{d\epsilon} F[\varphi + \epsilon\delta\varphi]|_{\epsilon=0}$$

for arbitrary functions $\delta\varphi$. If the expression for the differential can be written as

$$DF[\varphi : \delta\varphi] = \int \xi(x)\delta\varphi(x)d^Dx,$$

then the function valued functional, $\xi(x)$, is called the *functional derivative* of F and the notation

$$\xi(x) = \frac{\delta F}{\delta \varphi(x)}$$

is used. Higher order functional derivatives are then defined by applying functional differentiation to the lower order functional derivatives, as all functional derivatives are themselves functionals. For more information concerning the functional differential calculus see [18, 19].

A later theorem needs the well known result that

$$\int_{-\infty}^{\infty} e^{-y^2/2} dy = \sqrt{2\pi} \quad (1)$$

and the further expression, obtained by completing the square that

$$\int_{-\infty}^{\infty} e^{-\frac{\lambda}{2}\gamma^2 + j\gamma} d\gamma = \sqrt{\frac{2\pi}{\lambda}} e^{\frac{j^2}{2\lambda}} \quad (2)$$

for real λ , γ and j . The functional probability density of a general Gaussian random field, $\gamma(x)$ with zero mean is of the form

$$\pi(\gamma) = C \exp(-H[\gamma]), \quad (3)$$

where

$$H[\gamma] = \frac{1}{2} \int \gamma(x) a(x-y) \gamma(y) d^Dx d^Dy \quad (4)$$

and the integral is over Ω , the volume, or area, of interest. C is a normalisation constant such that

$$\int_S \pi(\gamma) D[\gamma] = 1, \quad (5)$$

where $D[\gamma]$ denotes integration over some suitable space of functions, S . A general Gaussian random field with non-zero mean is written as $\varphi(x) = h(x) + \gamma(x)$, where $h(x)$ is the expectation value, or mean of φ and γ has an average of zero.

One way to make sense of functional integrals such as (5) is to discretise on a finite grid of N cells, with γ_i a uniform value in the i -th cell. Then, using the same symbol for the approximate γ function,

$$\pi(\gamma) = C_N \exp\left(-\frac{1}{2} \sum \gamma_i a_{i,j} \gamma_j\right), \quad (6)$$

and the summation is over i and j and $a_{i,j} = \int_{x \in \Omega_i, y \in \Omega_j} a(x-y) d^D x d^D y$ is an integral over the cells, Ω_i and Ω_j . (6) is just the usual expression for the multivariate Gaussian distribution. The coefficient C_N is chosen so that the integral of the distribution over all N variables is unity.

Introducing Green's function, $g(x-y)$, defined as the solution of the integral equation

$$\int a(x-y) g(y-z) d^D y = \delta(x-z), \quad (7)$$

where $\delta(x-z)$ is the usual Dirac δ -function, the following result holds:

$$\langle \gamma(x) \gamma(y) \rangle = g(x-y). \quad (8)$$

That is, the Green's function is the *correlation function*, where the angular brackets denote the average obtained by integrating over all functions in the space, S , with the probability measure, $\pi(\gamma)$.

To prove this result, first define the *moment generating functional*

$$Z[J] = \int_S \exp\left(-H[\gamma] + \int \gamma(x) J(x) d^D x\right) D[\gamma].$$

Before giving meaning to this last formal expression note that the correlation functions can be derived via functional derivatives of Z with respect to J evaluated at $J = 0$. Thus

$$\langle \gamma(x) \gamma(y) \rangle = \frac{1}{Z[0]} \frac{\delta^2 Z[J]}{\delta J(x) \delta J(y)}.$$

To define the functional integral and to prove the result (8), expand all functions as infinite superpositions of eigenfunctions $\psi_n(x)$ defined by the equations

$$\int a(x-y) \psi_n(y) d^D y = \lambda_n \psi_n(x).$$

Then set

$$\gamma(x) = \sum \gamma_n \psi_n(x), \quad J(x) = \sum J_n \psi_n(x),$$

assuming the eigenfunctions are normalised so that $\int \psi_n(y) \psi_m(y) d^D y = \delta_{nm}$.

By substitution into the integral equation (7), it follows that

$$g(x - y) = \sum_n \frac{\psi_n(x)\psi_n(y)}{\lambda_n} \quad (9)$$

is a representation of Green's function. Let us also note the standard result that

$$\delta(x - y) = \sum_n \psi_n(x)\psi_n(y),$$

(for arbitrary $f(x)$, $f(x) = \sum f_n \psi_n$, $\int f(x) \sum_n \psi_n(x)\psi_n(y) d^D x = \sum f_n \psi_n(y)$).

Substitution into the generating functional gives

$$Z[J] = \int_{-\infty}^{\infty} \prod_n d\gamma_n e^{-\frac{1}{2}\lambda_n \gamma_n^2 + J_n \gamma_n}.$$

Exchanging the order of the product and the integral leads to

$$Z[J] = \prod_n \int_{-\infty}^{\infty} d\gamma_n e^{-\frac{1}{2}\lambda_n \gamma_n^2 + J_n \gamma_n},$$

and using (1) and (2)

$$Z[J] = \prod_n \sqrt{\frac{2\pi}{\lambda_n}} e^{-\frac{J_n^2}{2\lambda_n}}.$$

Finally using the expression (9), gives

$$Z[J] = Z[0] \exp \left(\frac{1}{2} \int J(x) g(x - y) J(y) d^D x d^D y \right),$$

where

$$Z[0] = \prod_n \sqrt{\frac{2\pi}{\lambda_n}}.$$

It thus follows that

$$\frac{1}{Z[0]} \left(\frac{\delta^2 Z[J]}{\delta J(x) \delta J(y)} \right)_{J=0} = g(x - y).$$

4.4 Kriging

In this section the theory of kriging is reviewed along the lines of its usual presentation. See, for example, [85, 96].

In some cases the variance of a property is infinite, so geostatisticians use the *variogram*,

$$\nu(x - y) = \frac{1}{2} \langle [\varphi(x) - \varphi(y)]^2 \rangle,$$

which is an affine transformation of the correlation function. As the treatment in this chapter is formal the correlation will be used throughout.

Simple Kriging: Consider the problem of interpolating a *random* function. That is, given M sample values $\varphi_i, i = 1, \dots, M$, at each of M spatial points x_i , estimate the value of the function, φ at the point x .

In simple kriging it is *assumed* that the interpolant is a linear superposition of the data,

$$\varphi = v_0 + \sum_j v_j \varphi_j,$$

where the scalar parameters, v_i are to be found.

Conditions for the determination of the v_i 's are motivated by the arguments (i) the interpolant is correct on average and (ii) if the true value, φ_0 were known then for each realisation the interpolant should minimise the variance of the error. Note the v_i 's are *not* random, and have the same values in all realisations; they are, however, functions of x .

Thus it is asserted that

$$\bar{\varphi} = v_0 + \sum_j v_j \bar{\varphi}_j,$$

and that the *error*, $\langle (\varphi - \varphi_0)^2 \rangle$ is a minimum, considered as a function of the v_i 's. Where the overbar notation and the angular bracket notation both indicate the expectation of the expression within their scope.

If it is also assumed that the mean of the process is a known constant, m , say, then it follows that

$$v_0 = m - \sum_j v_j m.$$

Minimising the expression for the error gives the linear equations

$$\sum_j g_{ij} v_j = g_{0i}, \quad (10)$$

where $g_{ij} = \langle (\varphi_i - m)(\varphi_j - m) \rangle$ and $g_{0i} = \langle (\varphi_0 - m)(\varphi_i - m) \rangle$ are the assumed known covariances of the random function φ . In applications the covariances are determined from sample averages of an analogue system, possibly inferred from the data, or just guessed. The values of the covariances can also be adjusted as part of the process of integrating further data into the model.

By solving the system of equations, (10), to give $v_i = \sum_j [g_{ij}^{-1}] g_{0j}$ the interpolant

$$\varphi_0 = m + \sum_{ij} [g_{ij}^{-1}] g_{0j} (\varphi_i - m)$$

is obtained, where $[g_{ij}^{-1}]$ denotes the elements of the inverse of the $[g_{ij}]$ matrix.

Ordinary Kriging: In ordinary kriging the mean is an *unknown* constant. As before, an interpolant of the form $\varphi = v_0 + \sum_j v_j \varphi_j$ is sought. The conditions for the v_i 's are that (i) the mean error is zero and (ii) the mean square error is a minimum. Thus

$$m = v_0 + \sum_i v_i m$$

for *arbitrary* m . This can only hold if $v_0 = 0$ and if $\sum_i v_i = 1$. The minimum error variance is then sought, subject to the constraint that $\sum_i v_i = 1$. By introducing a Lagrange multiplier, τ say, and looking for the stationary point of $\langle (\varphi_0 - \varphi)^2 \rangle - 2\tau(1 - \sum_i v_i)$, the set of equations

$$\sum_j g_{ij} v_j + \tau = g_{0i},$$

$$\sum_i \lambda_i = 1,$$

is deduced. These can be solved for the v_i 's so that $\varphi = \sum_i v_i \varphi_i$. It is interesting that the mean, m , is not required in evaluating the interpolant.

Universal Kriging: In universal kriging the mean is unknown but a function of x in the form of a linear superposition of a small number of basis functions, $\psi^k(x)$ which are here assumed to be orthonormal. Thus $\int \psi^k(x) \psi^i(x) d^D x = \delta_{ki}$, and $h(x) = \sum_k b_k \psi^k(x)$, where the coefficients b_k are to be determined by the interpolation procedure. In this method, once again the interpolant is *assumed* to be a linear superposition, $\varphi = v_0 + \sum_j v_j \varphi_j$, of the values at the data points. The usual conditions (i) that the mean error should be zero and (ii) the mean square error should be a minimum are imposed.

The zero mean error condition implies that

$$\sum_k b_k \psi^k(x) = \sum_{k,j} v_j b_k \psi^k(x_j).$$

This can only be satisfied for arbitrary b_k , provided that

$$\psi^{k0} = \sum_i v_i \psi^{ki},$$

for $k = 1, \dots, K$, where $\psi^{ki} = \psi^k(x_i)$ and $\psi^{k0} = \psi^k(x_0)$. These conditions are known as the *universal kriging* constraints and to compute the v_i the expression $\langle (\varphi_0 - \varphi)^2 \rangle$ is minimised subject to the universal kriging constraints.

Introducing Lagrange multipliers τ_k , and setting the derivatives of

$$\langle (\varphi_0 - \varphi)^2 \rangle + 2 \sum_k \tau_k \left(\sum_i \psi^{ki} - \psi^{k0} \right)$$

to zero, the set of equations

$$\sum_j g_{ij} v_j + \sum_k \tau_k \psi^{ki} = g_{0i}, \quad (11)$$

$$\sum_j v_j \psi^{kj} = \psi^{k0}, \quad (12)$$

$$\varphi_0 = \sum_i v_i \varphi_i, \quad (13)$$

is deduced. These can be solved for the v_i and the interpolant evaluated. (11)-(13) are the *universal kriging equations* introduced by Matheron in 1969. See [34] for a sympathetic exposition.

Indicator Kriging: This technique transforms the observations into integer valued quantities with the transformation

$$\begin{aligned} I_\nu(\varphi) &= 1, & \varphi < \nu, \\ &= 0, & \varphi \geq \nu, \end{aligned}$$

for some cut-off value ν . One then performs simple kriging [42] on these transformed values for a sequence of ν values. The interpolants, f_ν , say, are not integers, but real numbers that are interpreted as the probability that the value is less than ν . This seems plausible, but unfortunately there is no guarantee [85] that this honours the necessarily true requirements that $f_\nu \geq f_{\nu'}$ if $\nu > \nu'$. Apparently the response [85] on failure to satisfy the conditions is to impose them as constraints. [42] provide a detailed discussion of corrections to indicator kriging so that the conditions are satisfied. The main application of indicator kriging is to the numerical simulation of stochastic processes. The ad hoc nature of this method implies the need for a better technique.

Disjunctive Kriging: The methods just described make an implicit assumption that the underlying random process is Gaussian (this is shown in detail in the next section). Often the data are manifestly non-Gaussian. The approach of disjunctive kriging or nonlinear geostatistics is a response to this in which (i) a *normal scores* transformation is performed on the original data before interpolation (that is, the single point probability density is transformed to that of the normal distribution) (ii) the correlation structure and mean values are assigned or estimated from the transformed data (iii) the interpolation is performed (iv) the results are back transformed using the inverse of the normal scores transform. There exists some elegant theory using Hermite polynomials to construct the forward and inverse normal scores transform [85]. There is more, however, to a Gaussian random function than just its single point probability distribution. The other key property is that the process is completely specified by the mean and the correlation function.

Failure of this property is not addressed in disjunctive kriging. For reasons of space, non-Gaussian spatial statistics are not discussed in this chapter. However see [56] or [97] for examples of non-Gaussian techniques.

4.5 Maximum Probability Interpolants

If one assumes that a given property is characterised by a general Gaussian pdf of the form (3) then a natural interpolation technique is obtained by posing the question: Given data $\{\varphi_i^*\}$ on a discrete set of points $\{x_i\}$, which function $\varphi(x)$, with the values $\{\varphi_i^*\}$ at the data points, maximises the probability functional (3)?

In general the mean will be unknown, and following the lead of universal kriging, it is assumed that the mean is given by $h(x) = \sum_k b_k \psi^k(x)$, where the basis functions ψ^k are orthonormal with $\int \psi^k \psi^l d^D x = \delta_{kl}$.

This formulation implies the task of minimising the functional argument

$$\sigma = \frac{1}{2} \int a(x-y) (\varphi(x) - h(x)) (\varphi(y) - h(y)) d^D x d^D y$$

subject to the constraints $\varphi(x_i) = \varphi_i^*$. Introducing Lagrange multipliers, λ_i one can write

$$\tilde{\sigma} = \sigma - \sum_i \lambda_i (\varphi(x_i) - \varphi_i^*)$$

or

$$\tilde{\sigma} = \sigma - \sum_i \lambda_i \int (\varphi(x) - \varphi_i^*) \delta(x - x_i) d^D x.$$

Taking variations with respect to φ the equations

$$\int a(x-y) \left(\varphi(y) - \sum_k b_k \psi^k(y) \right) d^D y = \sum_i \lambda_i \delta(x - x_i) \quad (14)$$

are deduced.

Differentiation with respect to λ_i gives $\varphi(x_i) = \varphi_i^*$ and differentiation with respect to b_k gives

$$\int a(x-y) \varphi(y) \psi^k(x) d^D x d^D y = \int a(x-y) \sum_j \psi^k(x) b_j \psi^j(y) d^D x d^D y. \quad (15)$$

Multiplying (14) by $\psi^k(x)$, integrating over x and using (15) together with the usual properties of the δ function, leads to the expression

$$\sum_i \lambda_i \psi^k(x_i) = 0,$$

which is the condition used in the general radial basis function method.

Introducing a Green's function, $g(x - y)$, satisfying

$$\int a(x - y)g(y - z)d^Dy = \delta(x - z)$$

reduces the calculation to solving

$$\sum_k b_k \psi^{kj} + \sum_i \lambda_i g_{ij} = \varphi_j^*, \quad (16)$$

$$\varphi(x_j) = \varphi_j^*, \quad (17)$$

$$\sum_i \lambda_i \psi^k(x_i) = 0, \quad (18)$$

where $\psi^{kj} = \psi^k(x_j)$. These equations determine the λ_i and the b_k and also provide the interpolant

$$\varphi(x) = \sum_k b_k \psi^k(x) + \sum_i \lambda_i g(x - x_i). \quad (19)$$

The following theorem can now be proved:

The radial basis function system (19) is the adjoint of the universal kriging system (11) and (12).

Before the proof is given the adjoint method will be explained. Here one has a linear system $A_{ij}x_j^u = r_i^u$ (using the usual convention regarding repeated indices) with a symmetric matrix, A_{ij} , and multiple right hand sides r_i^u thus generating multiple solutions, where x_i^u is the i -th component of the u -th solution. The aim is to compute scalar products of the form $s^u = \sum_j c_j x_j^u$. That is, the s^u rather than the solution are of primary interest. It is easy to prove that this problem is equivalent to solving the *adjoint problem* $A_{ij}^T \alpha_j = c_i$ and evaluating $s^u = \sum_j \alpha_j r_j^u$. This replaces many direct linear systems with one indirect adjoint system. Adjoint methods are thus vastly more efficient than the original formulation.

To prove the equivalence of radial basis functions and the universal kriging method, the universal kriging system will be now transformed into the radial basis function equations. Multiply (11) by λ_i and sum over i to give

$$\sum_{ij} \lambda_i g_{ij} v_j + \sum_{ik} \tau_k \psi^{ki} \lambda_i = \sum_i \lambda_i g_{0i}.$$

Then using (17) and substituting (16) obtain

$$\sum_j \varphi_j^* v_j - \sum_{kj} b_k \psi^{kj} v_j = \sum_i \lambda_i g_{0i}.$$

Finally substituting from (13) and (12), (18) is derived, which proves the equivalence.

A corollary of this result is that both the radial basis function method and the kriging method are maximum probability interpolants.

Further results can be obtained using the maximum probability formalism. For example, by discretising the functional and exploiting well-known properties of the multivariate Gaussian distribution [115] one can derive closed form expressions for the single point probability density.

4.6 Stochastic Sampling Techniques

The Reason for Stochastic Sampling ('Simulation' or 'Monte Carlo'): Attention now turns to using random function theory in geological modelling and reservoir simulation. For example, a fluid flow simulator will compute, say, the production of oil from a producing well over some time interval. This can be written formally as $q = Q[\varphi]$, where Q represents the simulator and any post-processing, and q is the numerical value obtained from the simulation results. If φ is a random function (such that porosity and permeability functions are specified functions of φ) then q is a random variable - or in general a random function. Functionals, such as Q , are called *diagnostic functionals*, or just *diagnostics*. The central task in applications of spatial statistics is to determine pdfs of diagnostics, or at least to provide a summary of the properties of such pdfs. The main quantity of interest might be just the average $\langle q \rangle$ or $\langle q^2 \rangle$. Thus it is necessary to evaluate integrals of the form

$$f = \int_S F[\varphi] \pi(\varphi) D[\varphi],$$

where F denotes a general diagnostic functional. F is often a very expensive functional to calculate - it might take several hours of computer time to make a single evaluation. So how is one to calculate a function space integral, essentially an infinite dimensional integral?

One case where the problem is simple to solve, is when the probability density functional is sharply peaked about its maximum value, φ^* . This is of course the value obtained from the maximum probability method. When π is sharply peaked it follows that $f = F[\varphi^*]$ is a good approximation to the exact value. Thus the equivalent methods of kriging, radial basis functions or minimum curvature are all valid approaches to providing input for simulation when the functional probability density of the geological properties is very sharply peaked about its maximum value.

Now, what is to be done when $\pi(\varphi)$ is *not* sharply peaked, as might be expected to happen in an actual reservoir simulation study? In such cases kriging or its equivalents should not be used, as the errors can be very large.

Monte Carlo Methods and the Metropolis Algorithm: If the diagnostic functional is discretised on a spatial grid the dimension of the integral is then of the order of N , the number of grid blocks. (It could be more as there may

be several random fields involved in a model.) N can be of the order of 100's of thousands or even millions. This is, in terms of integration, a large dimension. It would clearly be very difficult to perform a conventional numerical integration over so many variables, bearing in mind that the diagnostic is so difficult to evaluate. In such circumstances it is widely accepted that methods using *random numbers* - Monte Carlo methods - are a suitable approach.

The basic principle can be explained by discretising the values of φ into, say, G levels. There are then G^N possible arrangements of values on the grid. Most of these arrangements approximate very rough functions, with wildly varying values, a few will be smooth. Most of the arrangements have a very low probability as given by the value of π . Suppose now that M sample functions, $\varphi^r, r = 1, \dots, M$, have been generated by simply choosing a value independently at random in each cell uniformly from the possible discrete values.

It can be proved that as M increases, the estimate

$$\langle f \rangle \approx \frac{1}{M} \sum_r F[\varphi^r] \pi(\varphi^r) \quad (20)$$

will converge to the average of the diagnostic. Although the above method will work *in principle*, it is very inefficient because most of the realisations have negligible probability density of occurring. Thus methods which take into account the structure of the pdf, π , and weight the selection of the realisations according to π will be a vast improvement.

At least three subject areas make use of stochastic sampling: statistical physics, statistics and geostatistics. Each area has its own favourite methods, partly a result of the different application areas, but, one suspects, largely due to cultural reasons. There are many texts in these areas, so the following only gives an outline and some selected references. A relevant review may be found in [55].

The statistical physicists were the first to use Monte Carlo methods in the celebrated paper of [118]. The Metropolis algorithm has the following ingredients. First there is a starting state, perhaps a random state with each cell value chosen at random. Then there is an update method which is stochastic, in that (i) the probability of choosing φ' from φ is the same as choosing φ from φ' (ii) all states, φ' , are accessible from any other state φ . The algorithm, where $\pi' = \pi(\varphi')$, then visits each cell of the discrete grid and performs the operations:

- Generate a new field φ' from the current state φ ;
- Evaluate the *energy* difference $\Delta E = \ln \pi' - \ln \pi$;
- Calculate $P = \min(1, e^{-\Delta E})$;
- Generate a uniform random number r on $[0, 1]$;
- Accept the update, φ' , if $r < P$.

Note that if $P = 1$, i.e., $\Delta E < 0$, evaluation of r is not required as the condition, $r < P$, is automatically satisfied.

To use this algorithm it is necessary to calculate the energy difference, and the new energy very efficiently. In physics applications the energy is a *local* function. That is, the energy is a sum over cells, where the energy associated with any cell only depends on the state of the cell and its immediate neighbours. Thus only a few arithmetic operations are needed to update each cell. Nevertheless, many Monte Carlo iterations are needed. Each cell must be visited thousands of times before equilibrium is achieved. After that there must be many Monte Carlo iterations between samples if the selected realisations are to be statistically independent. Careful monitoring of convergence is required. See [121] for a detailed evaluation of the method. There is scope for simultaneous updating of multiple sites and this too, is discussed in [121]. Parallelism is easy to achieve if the model is local. Once equilibrium is achieved and multiple independent realisations are obtained the diagnostic functional is calculated from

$$\langle f \rangle \approx \frac{1}{M} \sum_r F[\varphi^r],$$

noting that the factor $\pi(\varphi^r)$ is no longer needed as in (20). An important property of the Metropolis algorithm is that it is unnecessary to compute the normalisation factor in the pdf.

The Gibbs Sampler: This technique was introduced to the image processing literature by [71] and is a stochastic simulation method of key interest in mathematical statistics, particularly Bayesian Statistics. [67] and [122] review the statistics literature with sections on the *Gibbs sampler*, the next algorithm to be described.

The Gibbs sampler, after r iterations, updates to the $(r+1)$ -th iteration by visiting each cell and setting

$$\begin{aligned} \varphi_1^{r+1} & \text{ by sampling from } \pi(\varphi_1 | \varphi_2^r, \varphi_3^r, \dots, \varphi_N^r) \\ \varphi_2^{r+1} & \text{ by sampling from } \pi(\varphi_2 | \varphi_1^{r+1}, \varphi_3^r, \dots, \varphi_N^r) \\ & \dots \\ \varphi_i^{r+1} & \text{ by sampling from } \pi(\varphi_i | \varphi_1^{r+1}, \varphi_2^{r+1}, \dots, \varphi_{i-1}^{r+1}, \varphi_{i+1}^r, \dots, \varphi_N^r) \\ & \dots \\ \varphi_N^{r+1} & \text{ by sampling from } \pi(\varphi_N | \varphi_1^{r+1}, \varphi_2^{r+1}, \dots, \varphi_{N-1}^{r+1}), \end{aligned}$$

where $\pi(\varphi_i | \varphi_1^{r+1}, \varphi_2^{r+1}, \dots, \varphi_{i-1}^{r+1}, \varphi_{i+1}^r, \dots, \varphi_N^r)$ is the conditional probability density of observing φ_i given $\varphi_1^{r+1}, \varphi_2^{r+1}, \dots, \varphi_{i-1}^{r+1}, \varphi_{i+1}^r, \dots, \varphi_N^r$. It is defined by the expression

$$\pi(\varphi_i | \varphi_1^{r+1}, \varphi_2^{r+1}, \dots, \varphi_{i-1}^{r+1}, \varphi_{i+1}^r, \dots, \varphi_N^r) = \frac{\pi(\varphi)}{\int \pi(\varphi) d\varphi_i}.$$

As with the Metropolis method, it is necessary to make many iterations before the realisations are suitable for use in (20). [122] shows that the Gibbs sampler does produce realisations with π as their pdf.

Using pdf functionals with local energy functions enables very efficient algorithms to be constructed. The single site conditional pdfs used in the Gibbs sampler can be derived by integrating out just the i -th variable. This is straightforward for the Gaussian distributions, but also feasible for more general, non-Gaussian probability density functionals. As with the Metropolis method it is not necessary for us to compute the normalisation factor in the functional pdf.

Sequential Simulation Methods: In applications of geostatistics the method of *sequential simulation* has achieved great popularity. Geostatisticians do not usually exploit locality. The pdfs are non-local as they are correlation function based models rather than models using local coupling constants.

The sequential method is based on the following exact result that can be proved by induction [34].

Suppose that the site labels, $1, \dots, N$ are ordered so that the observations are labelled by $1, \dots, M$. Then the joint conditional probability of the unknown values, conditioned on the M observed values is a product of single point conditional probabilities as follows.

$$\pi(\varphi_{M+1}, \varphi_{M+2}, \dots, \varphi_N | \varphi_1, \dots, \varphi_M) = \prod_{i=M+1}^N \pi(\varphi_i | \varphi_1, \dots, \varphi_{i-1}). \quad (21)$$

This is proved by starting with the equation

$$\begin{aligned} \pi(\varphi_{M+1}, \varphi_{M+2}, \dots, \varphi_N | \varphi_1, \dots, \varphi_M) = \\ \pi(\varphi_N | \varphi_1, \dots, \varphi_{N-1}) \pi(\varphi_{M+1}, \varphi_{M+2}, \dots, \varphi_{N-1} | \varphi_1, \dots, \varphi_M), \end{aligned}$$

and repeatedly using the definition of conditional probability. The final expression is then written in reverse order to give (21).

A sequential simulation proceeds by performing the following operations:

- Randomly order the cells after the first M cells with conditioning data.
- Visit the first cell and draw a random value from $\pi(\varphi_{M+1} | \varphi_1, \dots, \varphi_M)$.
- Visit the second cell and draw a random value from $\pi(\varphi_{M+2} | \varphi_1, \dots, \varphi_{M+1})$
- ...
- At the i -th cell, draw a random number from $\pi(\varphi_{M+i} | \varphi_1, \dots, \varphi_{M+i-1})$
- ...
- Finally draw a random number from $\pi(\varphi_N | \varphi_1, \dots, \varphi_{N-1})$.

In principle this will work, and will only require a single pass through the unconditioned cells. In practice the difficulty is in calculating the conditional probability densities. Modifications introducing approximate locality, so that conditional pdfs are only dependent on geometrically close points, are needed.

As soon as this is done the elegance of the exact statement just given is lost. The resulting methods are fast, the images that result from visualising the results are convincing - provided a random path is taken through the unconditioned cells - but the statistics of the results are unknown. The statistics of the results have to be determined by analysis of the numerical results. It is likely that further analysis will show that *sequential* simulation is a first pass of an approximate Gibbs sampler. Further passes are needed for the statistics to converge to the correct values.

There is thus a basic problem in geostatistics: find a method that is as fast as a sequential method but which has a sound theoretical basis as in the Metropolis or Gibbs sampling methods.

Note on the literature. For further information about functional methods see [19, 73, 164]. Reviews of geostatistics are to be found in [34] or [42].

5 Forward and Inverse Modelling

5.1 Introduction

Physical systems are modelled by postulating a relationship between three objects - the properties, φ , the state ψ and the auxiliary data, ψ_a . The auxiliary data and the properties together are referred to as *input*. The state is sometimes called the *output*. The properties characterise the unchanging aspects of the system; the state characterises the aspects of the system that respond to different selections of the auxiliary data. The auxiliary data corresponds to those aspects of the system that are under human, or other, control. An example is that of single phase fluid flow in a porous medium; the properties are the permeability, the state is the pressure and the flux. The auxiliary data are the boundary conditions imposed on the flow system. In a time dependent problem, the auxiliary data will also include the initial conditions.

In a *discrete system*, φ will be a vector of values, one for each cell in the system. The values themselves might be vectors, so that φ is a vector of vectors. In a continuum system φ will be a function of x and sometimes also of t . Sometimes φ will be a vector or tensor valued function and can be discontinuous. In computer simulation the continuum system is approximated by a discrete system. For the purposes of *deterministic* mathematical modelling, the properties are supposed given as specific vectors or functions. In *stochastic* modelling, properties are specified by probability density functions, or perhaps implicitly by some other stochastic model.

Similarly, the state and auxiliary data are also described by vectors or functions with the same possibilities of space or time dependence. The auxiliary data which models control parameters such as flow rates in wells, boundary and initial conditions, can be deterministic or stochastic. The state is deterministic if both the properties and the auxiliary data are deterministic.

If one or both of the properties and auxiliary data are stochastic, then the state is stochastic.

A *mathematical model* then takes the form of a postulated relationship between φ , ψ_a and ψ which is written formally as

$$\mathcal{N}(\varphi, \psi_a, \psi) = 0.$$

In many models of practical use, it is assumed, and can sometimes be proved, that for any particular choice of φ and ψ_a , the state exists and is a unique solution of the equation, $\mathcal{N} = 0$.

In most cases, the state is not itself the main item of interest. Various *diagnostic functionals* are needed. In the deterministic setting these will be quantities such as the oil in place in some volume, the total production of oil over some period of time, the rate of water production, and so on. In the stochastic setting the expectation values of such quantities and their associated variances will be required.

The problem of determining the output given the input is known as *forward modelling*. The task of determining an unknown input from the values (or expectation values) of one or more diagnostic functionals is called *inverse modelling*. This inverse problem has to be solved when the values of the diagnostics contain errors, thus rendering the values mutually inconsistent. In addition, there may be far too little data for the problem, as stated, to be able to determine the input even if the input is error-free.

Deterministic and stochastic approaches to such inverse problems are discussed in the following two subsections.

References of particular value, that go further than the following brief review, are [131], [142] and [151].

5.2 Deterministic Inverse Problems

Consider the problem of finding a function (or vector) φ given the values of the vector valued diagnostic,

$$f^* = F[\varphi, \psi, \psi_a],$$

such that

$$\mathcal{N}(\varphi, \psi_a, \psi) = 0. \tag{22}$$

Three possible situations are of interest; (i) there are no functions, φ (ii) there is exactly one function, φ (iii) there are many functions, φ , possibly an infinite number, that satisfy the equation $\mathcal{N} = 0$ and are approximately consistent with the values of the diagnostics.

Interest is only in functions that have a continuity property. That is, small changes in f^* should imply only small changes in φ . A problem is said to be *well-posed* if it has a unique solution that is continuously dependent upon the

data. A problem that is not well-posed is said to be *ill-posed*. Usually inverse problems are ill-posed. This arises from the existence of experimental errors in the data (thus making the f^* constraints mutually inconsistent) and too few measurements. There is usually far from sufficient data and what data there is, is inconsistent.

There are several possible responses to such a problem. A popular first step is to at least remove inconsistency by formulating a least-squares problem. When the problem is well-posed the least-squares reformulation does not change the answer, but when the data are inconsistent it forces one or more solutions into existence.

Thus the problem implied by (22) is written as:

Given the values f^* , find φ such that

$$\mathcal{J} = \frac{1}{2}(f^* - F[\varphi, \psi, \psi_a])^2 \quad (23)$$

is a minimum subject to the constraint $\mathcal{N}(\varphi, \psi_a, \psi) = 0$.

Let $S_{\mathcal{J}}$ denote the set of functions that minimises \mathcal{J} . $S_{\mathcal{J}}$ usually contains more than one function and often an infinite number of functions.

To obtain a unique solution, further information is required. One approach is to seek the function amongst $S_{\mathcal{J}}$ that minimises $\int \varphi^2 d^D x$. This is a possible procedure, but very difficult to implement when \mathcal{N} is a nonlinear functional. Thus a more common approach is to form the problem:

Given the values f^* find φ such that

$$\mathcal{J} = \frac{1}{2}(f^* - F[\varphi, \psi, \psi_a])^2 + \epsilon \int \varphi^2 d^D x \quad (24)$$

is a minimum subject to the constraint $\mathcal{N}(\varphi, \psi_a, \psi) = 0$ and where ϵ is a positive real parameter.

This is known as zeroth-order *Tikhonov regularisation*. See [129] for an excellent overview of deterministic inverse problem solving. The book [49] is a treatment of inverse problems from the point of view of the applied mathematician.

This method removes inconsistency and looks for solutions biased towards *smallness*. As ϵ increases the value of 0 is gradually recovered everywhere.

A detailed discussion of how to interpolate scattered data has already been given. This interpolation problem can be considered an example of an inverse problem. Indeed the situation is very often that measurements of diagnostic functions are available and a few *direct* measurements of the properties φ are also available at a small number of points. Then it makes sense to combine interpolation techniques with the general inverse problem.

Thus consider the problem:

Given the values f^* , and the values φ_i^* at the M points x_i find φ such that

$$\mathcal{J} = \frac{1}{2}(f^* - F[\varphi, \psi, \psi_a])^2 + \epsilon\alpha \int (\nabla^2 \varphi)^2 d^D x + \epsilon(1 - \alpha) \int (\nabla \varphi)^2 d^D x \quad (25)$$

is a minimum subject to the constraints $\mathcal{N}(\varphi, \psi_a, \psi) = 0$ and $\varphi(x_i) = \varphi_i^*$.

When the point data values, φ_i^* , are not available then the method implied by the functional in (25) is called first-order Tikhonov regularisation for $\alpha = 0$ and second-order Tikhonov regularisation for $\alpha = 1$.

Given the background in deterministic interpolation this method of higher-order regularisation seems quite reasonable. However, it is rather arbitrary and difficult to justify. For this reason it is interesting to seek procedures that are well-founded upon statistical concepts.

5.3 Stochastic Inverse Problems

In the sections on stochastic interpolation the theory of random functions was introduced. To apply the theory to inverse problem solutions it will be assumed that the formalism of *Bayesian statistics* is a sound foundation. There is no space here to discuss this contention, and there is no need, as an extensive literature exists. A recommended overview of the subject is [122]. A practical and complete review of inverse problems, with a distinct Bayesian flavour is [131].

The main ingredients of a Bayesian formulation of the inverse problem are (i) the prior probability distribution (ii) the likelihood function (iii) the data (iv) Bayes' theorem formulated as Bayes' rule for producing the posterior probability distribution (v) a technique for sampling from the posterior distribution (vi) techniques for visualising the posterior distribution and (vii) a technique for summarising the posterior distribution. *Summarising the distribution* implies, for example, calculating the mean and correlation functions.

For the inverse problem a reasonable prior might be the functional pdf that would be used in a stochastic interpolation without the values of the diagnostic functionals. However this needs to be extended, as the parameters (which are also called *coupling constants* in the following) are also uncertain. As argued in more depth later on, uncertainty in the parameters is an important contributing uncertainty in practical multiscale modelling.

Care must be taken in developing the prior distributions. *Dogmatism* must be avoided if calculations are to be useful. That is, any region of parameter space that is assigned a probability measure of zero by the prior will remain with a measure of zero whatever data is available. Thus a zero measure must be applied only when complete certainty is appropriate. A similar consideration applies to the deterministic methods, where badly characterised prior information and solution algorithms can prevent convergence to realistic solutions.

The precise form of the prior is a matter of individual judgement, computational expedience, and familiarity with the circumstances of a particular modelling exercise.

A convenient prior for permeability is to use the log-normal form, where the permeability (assumed a scalar here) is given by an expression of the form

$k = b_0 e^{b_1 \varphi}$ with parameters b_0 and b_1 treated as known for convenience of exposition, and $\pi(\varphi, c)$ is

$$\pi(\varphi, c) = C \exp(-H[\varphi, c])\pi(c), \quad (26)$$

where

$$H[\varphi, c] = c_2 \int (\nabla^2 \varphi)^2 d^D x + c_1 \int (\nabla \varphi)^2 d^D x + c_0 \int \varphi^2 d^D x$$

and $\pi(c)$ is an appropriate characterisation of the state of knowledge of the coupling constants, $c = (c_0, c_1, c_2)$. In some applications there are local, or point, values of φ available. Other information, through the diagnostics, is more global. In such cases it may be appropriate to consider the diagnostics as providing information to improve $\pi(c)$ rather than $\pi(\varphi|c)$. However, it is not clear how to analyse this intuition in more depth. It is noted that in the statistical literature, the parameters, c , are called *hyperparameters*.

The likelihood function is derived from the probability distribution of the measurement errors relating to the diagnostic functionals. An appropriate distribution is a multivariate Gaussian with independent errors. Thus the joint probability density of the diagnostics and the input is

$$\pi(f, \varphi, c) = C g_\sigma(f, \varphi, \psi_a) \exp(-H[\varphi, c])\pi(c), \quad (27)$$

where, as an example, consider the case of a single scalar-valued diagnostic,

$$g_\sigma(f) = C' \exp(-(f - F[\varphi, \psi_a])^2 / 2\sigma^2).$$

The posterior pdf for the input is then,

$$\pi(\varphi, c|f^*) = C'' g_\sigma(f^*, \varphi, \psi_a) \exp(-H[\varphi, c])\pi(c),$$

for normalisation constants, C , C' and C'' . In cases where σ is small, and g_σ is close to a δ -function, great difficulties are experienced in sampling from the posterior distribution.

A convenient and popular summary of such a posterior distribution is the maximum probability interpolant (known as the MAP, *maximum a posteriori probability* estimate). If this is calculated using the calculus of variations, then a minimisation problem, similar to that of the Tikhonov methods is obtained. In the Bayesian formulation however, the free parameters need less ad hoc arguments for their assignment and have a clearer interpretation.

In oil field problems, the functionals $\pi(c)$ and $\pi(\varphi|c)$ have large variances. Thus MAP is not appropriate, and Monte Carlo sampling, direct from the posterior probability distribution, is perhaps the correct method. The Tikhonov methods are best regarded as asymptotic approximations in the limit of small variance.

Thus in general, one should not use summary values of φ , but instead use the pdf and compute the expectation values of the diagnostic functionals in a

predictive computation. Since the likelihood function is close to a δ -function this is expensive using existing techniques. More is said about such inverse problems in the section on history matching of production data. There is an urgent need for further extensive research into the sampling of posterior pdfs.

At present there is only a small literature applying the Bayesian philosophy of inverse problems in the oil field data integration problem. For a representative sample see [99, 100, 125]. The number of publications in this area is likely to grow rapidly over the next few years.

5.4 The Problem of Scale Dependence in Inverse Modelling

It is well known that the permeability of a one dimensional system, in which there is incompressible single phase flow, can be replaced by the harmonic mean. This ensures the same total flux for a given pressure drop. Now consider the inverse problem, where the flux and the pressure drop are given, and the problem is to determine the permeability distribution. In this case it is easy to see why the problem has a non-unique solution. All distributions with the same harmonic mean are candidates - all give complete agreement with observations and all leave the physics of the problem unchanged without error.

Systems defined on different scales (in the sense of the grid cell size) can have the same harmonic mean, and so flow measurements provide no information at all concerning the length scale of the heterogeneity in the one dimensional case.

In the general case, therefore, one must expect very little information regarding length scales to be available from flux and pressure measurements. After water breakthrough there may be information regarding length scales, but generally integration of cores, logs and outcrop studies is needed for the assignment of length scales. Early time data from well tests may be an exception to this general rule. Research is needed on this matter of length scale determination during data integration.

6 Sources of Data

Our main concern is combining, or *integrating*, all available (and relevant) data by building geological models to be used as input to forward models of fluid flow. Such models are used in reserves estimation and designing optimal recovery plans. The required data, at a minimum, consists of the porosity, the permeability tensor, the relative permeabilities and capillary pressures, fluid properties and the rock compressibility. All of these items are functions of position in 3-dimensional space.

The available information is sparse, indirect and difficult to interpret. However, oil companies and oil service companies have been building models

for many years and there is a consensus on how to best build models, when the best possible model is the goal.

Data quantifies the response of rocks and fluid to the introduction of various forms of energy. All measurements require inversion, and, in principle are uncertain. However, some measurements are more uncertain than others. There is no neat classification of measurement processes (of which the author is aware) and so each type of measurement is discussed independently. All the methods share a dependence on geological knowledge that is essential in building the prior information needed in the inversion. Thus this section will start with a brief outline of basic geological concepts (those that are important in reservoir simulation and geological model building). After this, a brief outline of seismic acquisition, processing and inversion (often called *migration* in the seismic community - although there are subtle nuances of meaning involved). Well logging is discussed, and then an outline is given of the information available from flow tests in wells. The flow tests can be on a very small scale, in which case they are a form of logging, or the tests can be on a large scale, in which case they are closer to production data and are known as *well tests*. The final source of information is from production history.

6.1 Geology: Geological Processes from a Mathematical Viewpoint

Definition of Geology: Geology is the study of the structure and history of Earth and other astronomical bodies. The main branches of the subject are:

- Petrology, the study of rocks on the smallest scale.
- Mineralogy, the study of the chemical composition of rocks.
- Structural geology, the study of the geometric forms and the forces involved in the creation and existence of geological structures.
- Sedimentology, the study of the processes which form the rocks, before the large scale features are formed.

See reference [48] for a useful and fascinating overview of geology, Earth science and petroleum science.

A key principle of geology is that *the present is the key to the past*, also known as the *principle of uniformitarianism*. This states that most structures result from processes currently operating today. Thus, by observing and theorising about the geology on the surface today geologists can reconstruct the history beneath the surface, and are able to understand the geological features of our environment.

Another key principle is that *for any two layers of rock, the youngest layer is above the older* - the *law of superposition* [22]. Of course this is not a universal truth, as sometimes the forces of nature overturn the rocks to a startling degree, nevertheless it appears to be a useful guiding principle for understanding the layers in the ground.

The main physical processes that operate are:

- Sedimentation (forming of rocks by transport and deposition in the sea, in rivers, and in deserts).
- Diagenesis (fossilisation of sediments by pressurisation and chemical reactions, associated with fluids that flow through the rock long after the original deposition).
- Deformation (bending, elastic and plastic, of rocks resulting from large scale earth movements, and differential pressurisation).
- Intrusion (flow of material, such as salt, upward, causing bending, fracturing and faulting).
- Jointing (breaking of the rock within a thin volume, usually idealised as a surface) - when deformation follows jointing one speaks of faulting, otherwise of fracturing.
- Erosion (the opposite of sedimentation, when ice, water and air remove already deposited rock).

The combination of these processes causes the complexity observed in surface outcrops and subsurface observations in seismic surveys, cores and well logging.

Sedimentology: Rocks are classified into types determined by colour, texture, fossils and electrical and other physical properties such as seismic response. The internal structure of the layers is largely determined by the depositional environment. In sandstone reservoirs, for example, sands may have been deposited in a river delta, in a desert or on the seabed. After deposition, large scale movements - turbidites (great landslides under the sea) or earthquakes - might occur, which mix up the sands. Other oil reservoirs are found in carbonate rocks, which have their own characteristic patterns, being much more affected by diagenesis than sandstones. The geologist determines the depositional environment from the spatial association of rock types, as a single rock type can be found in different environments. A large body of rock from a single environment is known as a *formation*. Formations are divided into *members*, members into *beds*. Beds are informally referred to as *layers* - but layers can be much thinner than beds. Formations, if there are some common factors, are combined into *groups* which can be further combined into *super-groups* [22]. The International and the North American Stratigraphic Codes bring order and consistency to the terminology [22].

There is a large literature involving literal modelling of the sedimentation process, [4, 5]. There is a newer and growing literature, in which a more abstract, schematic, view is taken [144].

At the far end of the abstraction spectrum, is the geostatistical school of modelling, in which the pattern of rock properties is modelled without any input from physical principles [34].

The simplest oil reservoir is a collection of broadly horizontal layers, with varying thicknesses. Such models are frequently called *layer cakes*. The sur-

faces defining the boundary between two layers are called *horizons*. Next in complexity is the case where layers are (i) discontinuous or (ii) *pinchout* where there was a change in the mode of deposition. A further increase in complexity is when a geological event leads to erosion of part of a layer cake before recommencement of deposition. With just non-uniform deposition and erosion, complex patterns of rock can evolve. An example of this is the Grand Canyon [110]. When the horizons are relatively smooth and continuous, it is easy to model them with parameterised *maps*. These can consist of an array of depth values on a regular rectangular grid. At points away from the grid points, values can be interpolated. The various methods described in the section on spatial statistics are employed in the making of computer maps.

Structural Geology: Structural geology studies rock deformation during and after deposition. Faulting greatly complicates matters. When faults are vertical, horizons are torn along the fault lines and this leads to displacement of the maps. When faults are *normal*, meaning the fault surface slopes such that any vertical line intersects a particular horizon once or not at all, description is fairly straightforward. In more general situations, such as intersecting faults, or reverse faults (where a vertical line may intersect the same horizon twice) it is not possible to describe the geometry in a simple way.

Another complication occurs when horizons are folded, as in the case of salt domes, so that again vertical lines exist that intersect horizons more than once. These are also difficult to model.

Operational Geology: The standard approaches to geological modelling attempt to build the model as directly as possible. That is, the sequence of operations involved in the model building does not attempt to mimic actual geological processes (although horizons and unconformities may be ordered in a time sequence, so as to specify the erosion rules). In operational geology a sequence of the basic geological processes (sedimentation, deformation, jointing, diagenesis and erosion) that is a feasible sequence is postulated. One might even conjecture a sequence of operations as the actual history of a particular formation.

Reconstructive Geology: In reconstructive geology, the attempt is made to provide a model of the actual sequence of events that caused a particular rock pattern, in as realistic a manner as is useful. Reconstructive geology is a special case of operational geology, in that operational geology may not suggest that the sequence of events is the actual sequence. An introduction can be found in [76].

Basin Modelling: In basin modelling, an operational approach is applied to a very large volume of space, in which there may be many oil reservoirs. By looking at this larger scale it is possible to postulate the source of the sediment that has been deposited, and to model the actual formation of the oil - an example of a diagenetic process, [5].

Notes on the literature. Books that introduce geology, aimed at people involved in petroleum studies, are [43, 108, 110, 138].

6.2 Seismic Acquisition, Processing and Interpretation

Seismic acquisition involves sending acoustic energy into the subsurface and analysing the echoes. This is an inverse problem on the wave equation. Data are gathered from many independent experiments, as a sound source is moved over the land or sea surface. The results are preprocessed using a wide range of techniques designed to correct for topographical features and noise. A complete review of these techniques can be found in [139]. Clear explanations of the older techniques can be found in [3].

After preprocessing, the main inversion step is known as *migration*. The amount of data, and the size of the system under investigation are both very large. This precludes the use of simple numerical techniques for solving the forward model, as described for the fluid flow forward problem. Instead a range of semi-analytical approximations are used. The approximations vary in accuracy, complexity and applicability. The simplest methods are known as *time migration*, using Fourier processing on wave equations, linearised about a simple background spatial distribution of properties.

The more sophisticated and more accurate methods known as *depth migration* are based on high-frequency ray-tracing methods. Occasionally, in very complicated situations, full finite difference or pseudo-spectral approximations are used, but the resolution requirements are very demanding. A major decision, relating to the amount of spatial variation in the acoustic properties, is to migrate pre- or post-stack. This refers to one of the major preprocessing steps where an averaging technique is applied to the raw measurements that combines the observations from different sources and receivers. This indicates the complexity of the seismic processing activities. The mathematics is explained in detail in [21].

The results are usually presented in the *time domain* which, to a first approximation, removes the effects of any layer cake background model. Users of the inverted results are able to apply their own *time-to-depth* conversions as more data becomes available, or as the seismic data is integrated with other data. The time-to-depth conversion is performed using alternative layer cake models of the sound speed and rock density. Note that depth processed seismic results using depth migration are often displayed in the time domain by applying a depth-to-time conversion.

After migration, and display in the time domain, the observations are equivalent to a numerical experiment that measures the response that would be observed in an ideal experiment where the sound waves are assumed to propagate in vertical, straight lines, and that any reflectors that are encountered are locally horizontal. The resulting calculations are then displayed as seismograms of the virtual experiment.

It should be noted that even though the results may be very realistic, they are not unique. There will be many different spatial distributions of acoustic properties that will explain the observations.

The final step in the use of seismic observations is the *interpretation*. Even at this stage further modelling, involving ray tracing or analytical wave equation approximations are tried in efforts to devise models that give the same reflection behaviour as that observed in the seismic measurements. Reviews of this can be found in [12] and [51]. The aims of interpretation are to locate the major structural features, perhaps by hand picking or autopicking. Seismic attributes, functions of the seismic amplitudes and locations, are sometimes selected as input to property modelling algorithms where, for example, porosity might be interpolated using a stochastic realisation conditional on the seismic attributes.

6.3 Core Data

Core data is recovered using special hollow drill bits. The rock is very valuable, and provides prior information for inversion of indirect measurements such as seismic and well logs. Samples can be taken from the cores, and measurements made in the laboratory. Such laboratory measurements do not generally require complicated inversion procedures, but as the measurements are on the scale of centimeters care is needed when applying this information to inversion of properties that are on a larger scale.

One of the most important uses of core is to help geologists identify the particular depositional environment as a function of distance along the wells. Petrologists examine the cores through a microscope. Microscopic features can be important in developing hypotheses about the origin of the rocks, and the diagenetic processes that have occurred. Such interpretation is important as it improves the reliability of conjectures concerning the larger scale texture of the reservoir.

With an identification of depositional environment, it is then possible to use observations from surface outcrops or well-studied reservoirs to specify larger scale geometric features and their associated length scales.

6.4 Well Logs

Aims of well logging. Well logging is used to determine the type and properties of any fluids in the rocks and to determine the geometric and physical properties of the rock. The results of interpreted well log measurements are used to determine the boundaries between layers and the occurrence of fracturing. Interpreted results from well logging are used as input to mapping and geological modelling models. The points along the well log that mark the boundaries between layers are called *picks* or *well picks*. A major aim of well logging is to tie horizons observed in wells to horizons seen in seismic data. Such integration improves the reliability of both types of measurement.

Recent reviews are those of [112] and of [138]. Useful, but older references, are [45] and [149].

Passive/active measurement. Most measurements involve the introduction of energy into the formation in a controlled way. The response from the rock is recorded and used as input to interpretation. Sometimes there is natural energy, already present as the result of processes in the rock, or as a result of the disturbances of drilling. In particular the presence of water or mud with a relatively low salt concentration causes a spontaneous flow of electric current. Measurement of the associated potential difference is the earliest form of well logging as performed by the Schlumberger brothers in the 1920's [112].

The procedure of well logging involves sending a package of instruments - called a sonde - suspended from a cable or *wire*, into the formation. The well is usually drilled using a special mud, that (i) controls the pressure to prevent blow-outs and kicks (ii) is a lubricant (iii) is a means of transporting drill cuttings to the surface, and (iv) sometimes as a medium for transmitting electrical signals. The mud will penetrate the reservoir rock: more where it is permeable, less where it is not. Sometimes the drill stem will disturb the mud cake that builds up on the walls of the well, allowing yet further mud to flow into the formation. Thus the mud will affect the response of the instruments and the interpretation of the results. Corrections for different mud geometries will be required.

The different zones around the well are divided into the mudcake, the invaded zone, the transition zone and the true zone.

Forward modelling. The design of the instruments to be lowered into the well and the interpretation of the results depends on the use of a forward model. This is an application of a theory such as Maxwell's for electromagnetics or Darcy's for fluid flow. An initial-boundary value problem can be constructed of the formation-measurement interaction and the processes in the measuring instrument. The theory requires a specification of geometry and properties. Such a theory can sometimes be solved exactly, more often approximately using an asymptotic technique exploiting any small parameters in the problem. Asymptotic theories, involving approximations such as the Born approximation, can be rearranged to show that the properties of the rock are a convolution of the measured response. In linear response theory this linear relationship is simply postulated and a laboratory procedure, involving actual physical mock-ups of a well, are used to calibrate the response function of the instrument. This avoids the need for a theoretical analysis. In practice, as usual, a combination of theoretical analysis, laboratory measurement and field results yield the best interpretation.

Increasing use is being made of numerical solutions. In some ways this is simple, but tables of numbers can be harder to understand than an analytical result. The theory can be used to optimise the response of the instrument,

maximising the information recovered, minimising the size and weight of the apparatus and the energy requirements [7].

Parameter inference. The forward model or theory relates the input properties and geometry to the instrument response. In the simplest case the theory will predict the response as a simple function of the input, such that the inverse formula, stating the input parameter as a function of the response can be obtained analytically. An example is calculating the resistance of a conductor as the ratio of potential gradient to electric current, or permeability as the ratio of fluid flux to pressure gradient. In a more complicated case there may be several parameters such as the radii of the different zones of mud invasion. When there are just a few parameters it may be possible to infer the parameters from one or more instrument responses using a least squares procedure. This is an application of the usual methods of the theory of measurement as reviewed in Section 5.

In general there are naturally occurring heterogeneities that may require hundreds or thousands of parameters for a realistic model. Such inversions are computationally demanding, but using the adjoint method, which is reviewed in the later section on history matching, it might be possible to make further progress in improving the realism of inverse modelling.

Transforming the results. The end result of a well logging measurement will be values of parameters such as electrical resistivity. This is not the information that is actually required. Instead, porosity, permeability, elastic constants and so on are needed. Some of these can be inferred by combining the results of several different logs and using a law, such as Archie's law (see [45, 138] for an explanation) to infer the property of direct interest.

Some Notes on the Different Types of Log: Temperature log. Many other measurements are sensitive to temperature, so this is always recorded in a suite of logging measurements.

Spontaneous potential (SP). The low resistance water or mud used in drilling evokes a spontaneous potential difference between a point on the well surface and a reference point at the well head. This potential varies along the well bore. High values correspond to high hydrocarbon saturations or high shale density. The SP log was the first type of well log (see [112] for the history and historical references). The method can only be used in uncased holes.

Resistivity logs. The introduction of a source of electrical energy leads to reliable and controllable measurements. There are many types of electrical resistivity log. They differ by their depth of penetration and their vertical resolution. The electrical resistivity of the different invasion zones can be inferred from these measurements. For a review of inversion procedures see the review of [7]. Resistivity logs measure the effective resistivity on scales of meters down to centimeters, depending on the characteristics of the instruments.

Dielectric logs. The dielectric *constant* of a material is a measure of its ability to store electric charge in an imposed electric field. The dielectric properties are fairly insensitive to the water salinity, unlike the resistivity. The dielectric constant for the vacuum is unity and that for gases only marginally greater. However, water has a dielectric constant of around 50 when fresh and 80 when saline. Oil has a value of about 2.2 and sedimentary rocks range from 4 to 10 [138]. Thus the dielectric measurement can be used to determine the porosity and the water saturation. The log does not distinguish between connate water, mud filtrate or the water content of shales. (Connate water is the original formation water, and a shale is a rock made of mud particles smaller than 0.06mm [22].) By altering the frequency of electromagnetic waves, different depths of investigation are possible.

Passive Gamma-ray logs. Radioactive elements are naturally present in the rocks. The most commonly occurring radioactive elements are potassium, uranium and thorium [43]. Potassium is prevalent in clays, and present to some extent in some other minerals, and so measurement of the gamma-ray emissions can be used to identify the chemical or mineralogical composition, estimate the concentration of shale and, like other logs, has an important role in well picking. More detailed measurement uses the energy wavelength spectrum and can identify minerals with more precision.

Active gamma logs. By emitting gamma radiation from a source in the sonde, and measuring the backscattered gamma radiation reflected from electrons in the formation, it is possible to determine the total or bulk density of the medium. This includes the rock and fluid in the pore space. The device, often called the gamma-gamma tool [138] can be used to estimate the bulk rock density and provide an upper bound on the flow related porosity. The gamma-gamma log works close to the well, in the invaded zone.

Neutron logs. A radioactive source is transported within the sonde, and the neutron bombardment causes emission of gamma radiation in proportion to the hydrogen content of the formation. As nearly all the hydrogen is present in the fluids, but not in the minerals, the neutron log determines the porosity of the rock. Since not all the pore space is open to flow (some pores contain fluid sealed in by diagenesis) the neutron derived porosity is an upper bound on the flow-related porosity. Neutron logs can be used in cased holes.

NMR logs. Nuclear magnetic resonance logs are another way of measuring the hydrogen content of the formation. They work by first applying a steady and strong magnetic field, about 1000 times stronger than the Earth's magnetic field. The nuclei of the hydrogen atoms carry a small magnetic moment and so there is an induced field of slightly larger magnitude than the strong static field. A second magnetic field, in the form of short high bursts of high frequency magnetic fields disturbs the induced magnetisation. By observing the decay of these responses it is possible to determine the hydrogen content. Remarkably there is sufficient information to enable estimates of the environments experienced by the hydrogen atoms. Thus the fluid saturations of

different fluids can be determined as can the size distribution of the pores of the rock. The histogram of pore sizes enables estimates of permeability to be made. It would appear that the scale of these measurements is of the order of 10 cms. Only in recent years has the NMR method become available in well logging. It would seem to be a measurement of particular power and usefulness in reservoir characterisation.

[112] gives a quite detailed review of NMR logging and [138] provides a short introduction, though longer than that just given. The book of [87] contains background about NMR in general.

Sonic logs. The sonic log provides in situ measurement of the speed of sound in the formation over the scale of the sonde. It can only be used in open, uncased holes. The measurement is useful in seismic processing, it can be used to infer porosity but not that accurately and can be used to identify the rock type since the sound speed is a definite characteristic of each type of rock. Further detail can be found in [45, 138].

Dipmeter log. The dipmeter, introduced in the 1940's, uses small electrodes to measure the resistivity along three or more parallel tracks along the well bore surface. Analysis of correlations of the resistivity between the tracks and fitting of a plane through the correlated points determines the tangent plane to the layers passing through the well. The geologists characterise this plane by the angle made to the horizontal by the line of steepest descent on the plane (the dip angle) and the angle made to true north of the projection of this steepest descent line when projected onto the horizontal plane (the azimuth). Assuming that layers of resistivity correspond to lithological layers, this is thus a very useful measurement. [45] and [112], amongst others, are enthusiastic about applying dip meter measurements. Both these authors give examples of interpretations of dipmeter data best done, as usual, in concert with other data. According to [112] the modern dipmeter, with a vertical sampling rate of 0.25 cm, and an electrode size of 0.5 cm has a resolution of 1cm. That is, the measurements can be used to distinguish features separated by a distance of 1cm. It would appear that careful geological consideration needs to be given as to the scale of the layers whose dip is measured. That is other data is needed along with interpretation (i.e., choosing one of many models that fit the data) to decide if the layers are cross bedding, or small scale laminations.

Borehole Imaging. The dipmeter has evolved into the borehole imager. Here there are 100-200 electrodes measuring the resistivity around the well bore. These are processed into convincing images which look like photographs of rocks. In principle such data can replace the dipmeter but, at present, according to [112] the dipmeter is still widely used. The borehole image can be used to determine dip, much as with the dipmeter log. However, via a borehole image it is also possible to determine the presence of fractures, faults, unconformities and sedimentary structures [138].

Rock-type analysis. Rock samples, from cores or drilling cuttings, of known depositional environment can be correlated with a suite of well logs. Then in other wells, the logs can be used without reference to rock samples to infer the depositional environments along the well. The processed logs (that is those with ascertained depositional environment) are used to make well picks. Then the geologist can build maps or 3D models of the spatial variation of rock type. The rock type variation can then be used in more complicated interpolations of properties such as permeability.

Notes on the literature. An extensive and modern review, that concentrates on reservoir model building is [112]. This also has useful references to the more general well logging literature. There is also an interesting history of well logging.

A general background, at a very accessible level may be found in [108]. A similar, but slightly more detailed review can be found in [43]. The modern review of petroleum geology by [138] is a mine of interesting and useful information. The book [72] gives case studies on how well logs are used in building geological models.

Articles, frequently on logging topics, appearing in the *Oilfield Review* are of general interest.

6.5 Well Testing, Production Logs and History Data

Observation of processes that directly involve fluid flow are of particular importance in building a model aimed at simulating fluid flow. Well tests provide data on pressure and flow in individual wells when such wells are disturbed from their normal state. For example, in a shut-in test, a well is closed to flow, and the transients in pressure and flow are used to infer permeability in the vicinity of the well. Tests in which the well is shut and then a very high pressure is induced in the well and allowed to decay, serve a similar purpose. The integration, into geological and simulation models, of production and other flow data is discussed in more detail in Section 9.

7 Geological Modelling

The aim in geological modelling is often to integrate all available data into a single representation for subsequent decision making. Increasing use is being made of multiple representations, in the process of quantifying uncertainty. The historical method for model building was to use maps; maps of the surfaces and maps of the properties in the regions close to the surfaces. Of course, the subsurface is a volume, and not a surface and so, in tandem with developments in computer technology, particularly in 3D graphics technology, geologists have turned to the use of the available 3D modelling packages. Until recently 3D models, too, were built using maps as input. This is still the most common method for modelling, and so it will be reviewed in some detail.

All interpolation schemes specify that the value of some property at a point is a weighted, generally nonlinear, average of neighbouring or nearby values. The weighting depends on direction and distance from the point to its neighbours. Properties generally depend more strongly upon neighbours within the same layer than in a layer above or below.

Geology shows this is not an arbitrary interpolation problem. Geological systems show marked patterns of layering, deformation, faulting and diagenesis. The aim of *structural modelling* is to provide a geometric framework incorporating the major discontinuities. Such discontinuities are boundaries or *horizons* between layers or fault discontinuities within layers. This geometric, structural, framework guides and constrains the development of a geocellular grid that, in turn, defines the neighbourhood structure used in property interpolation.

7.1 Structural Modelling

All software packages for geological modelling currently take the step of building a large scale structural framework.

Historically the first step in structural modelling was to focus on the horizons (the boundaries between adjacent layers). The faults were modelled via some indication of the fault-horizon intersections. Usually the assumption of *mappability* - that the horizon surfaces are single valued height fields above a flat datum - was made and the fault-horizon intersections were defined by the projections onto the datum plane. The projections of the fault-horizon intersection lines are known as *fault traces*.

More recently it has become the custom to model fault *surfaces* (not just their fault traces) before any attempt to model horizons. This approach (see [84]) helps ensure consistency between all horizons in a particular structural model.

Types of Structure to Model. In this section, illustrations with explanatory text are used to specify the main types of geological structure. The illustrations are all drawn as cross-sections. In three dimensions the geometry is much more complicated than shown, but the pictures that are shown are sufficient to indicate the difficulty of geometric modelling and subsequent or associated grid generation problems.

Simple Layered Systems: The simplest case is a system of layers, not necessarily flat, but mappable and continuous. This particular system is often called a *layer cake* and is illustrated in Figure 2.

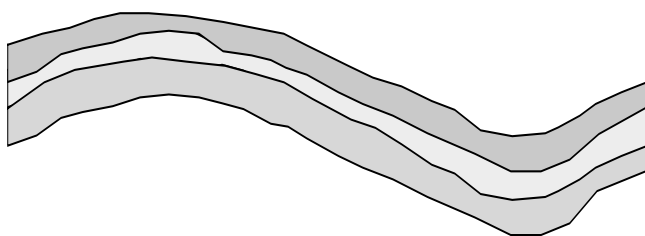


Fig. 2. Layer cake geological model.

Layered Systems with Overturned Surfaces: Overturned surfaces, or folds, which cannot be represented as single valued height fields relative to any flat reference surface, may be caused by, for example, (i) compressive deformation of sufficiently plastic layers from the boundaries or (ii) deformation from below by the upward movement of subterranean salt bodies under the influence of buoyancy forces. See Figure 3.

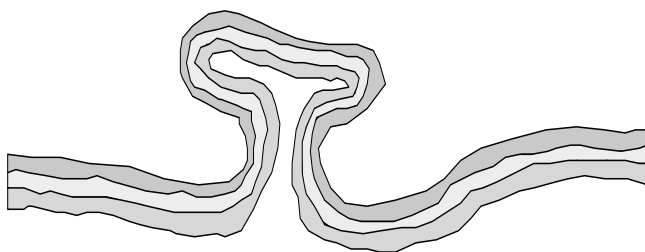


Fig. 3. Geological model with overturned surfaces.

Normally Faulted Layered Systems: Normal faulting, in which a gap opens up in the layers, may be caused by extensional forces. Each horizon, starting as a single mappable height field, remains as such but with holes appearing where the fault surface intervenes. Figure 4 also contains a vertical fault which may be considered a limiting case of a normal fault.

Reverse Faulted Layered Systems: A compressional force can cause a layer to fracture and then ride over itself. The resulting surface is not mappable, in any simple sense, as the height field is overturned. See Figure 5.

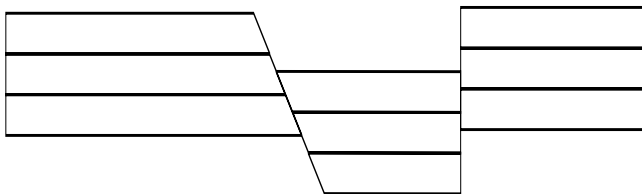


Fig. 4. Normal fault geological model.

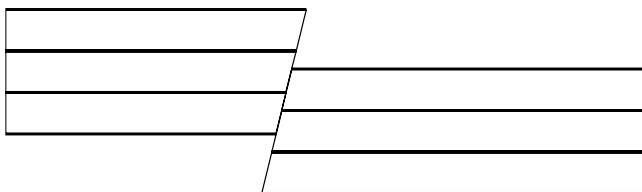


Fig. 5. Reverse fault geological model.

Overtured Surfaces in the Presence of Faulting: The situation shown in Figure 6 indicates a geometry in which oil may become trapped in layers that have been faulted by a salt dome intrusion. Although the structural geology of the reservoir itself may not involve overturned surfaces, the seismic inversion requirement to describe the sound speed model in a process of optimised migration means it is necessary to model such complicated geometric features.

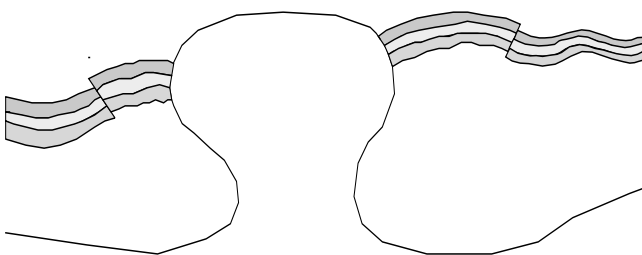


Fig. 6. Salt dome with faulted layers.

An important example, involving both overturned surfaces and reverse faulting, is the thrust fault where layers are pushed over themselves with considerable deformation as indicated in Figure 7.

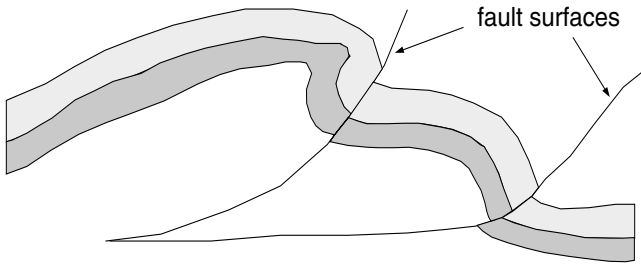


Fig. 7. Thrust fault.

Complex Faulting: Complex faulting involves the interaction of two or more faults. The example of two intersecting faults is illustrated in Figure 8.

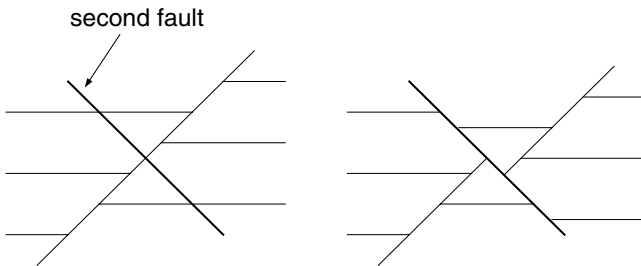


Fig. 8. An intersecting fault, showing the evolution.

Data Used in Structural Modelling. Data arrives from three main sources; seismic surveys, wells and geologists.

Seismic Data: Seismic data is voluminous in quantity and on a scale horizontally of 20m or more and vertically 15m or more, depending upon the circumstances. The interpretation of seismic data is subject to non-uniqueness in the inversion and migration process. Anyone can see horizons and faults in a seismic cross-section but it needs an expert geologist to identify such structural features with a useful chance of being correct. In a large, often

three-dimensional seismic data set, it is impossible to extract all of the surfaces of discontinuity in a purely manual fashion. *Autotracking* or *autopicking* techniques [81], implemented as part of seismic interpretation packages extract large sets of three dimensional points conjectured to lie on a particular horizon. Autotracking works by starting from a manually digitised line of points thought to lie on a common surface. The algorithm then seeks points on neighbouring seismic traces that have a similar pattern of seismic amplitudes. Points that lie on fault surfaces can also be identified by autotracking.

Identifying seed points for the autotracking algorithm, and assigning values for the autotracking parameters are ways of injecting geological expertise into model construction.

Well Data: Examination of cores or borehole image logs makes the position of some horizons obvious in a particular well. In the absence of cores or images petrophysicists and geologists must rely on a set of logs. Software exists to help segment the logs into layers [112]. The expert can identify the depositional environment from the patterns in selected well logs. When combined with core data or drill cuttings, the pattern of layers or *zonation* can be assigned with high confidence.

When there are several, or many wells the geologists and petrophysicists can correlate the picks in different wells by grouping them to belong to a particular surface. Combining this data with data on a seismic picked surface increases confidence in the well-to-well correlations and uses the seismic data to help interpolate the horizon surfaces between the wells.

Decisions made in correlating the layers in wells calls for considerable geological expertise. It would seem that the people called upon to make such judgements must imagine what the reservoir and surrounding geology must look like, in advance.

At this stage in the model building process, the model is a list of sets of scattered 3D points. Each set of points represents a geological horizon or fault surface. Since horizon surfaces are conventionally regarded as continuous, away from faults, (although horizons may touch other horizons at *pinchouts*) a natural requirement is to construct a surface interpolating these points. Techniques for doing this were reviewed in Section 4.

The Classical Map Based Methods: One structural model building approach is to first make contour maps or mesh maps (height fields on a grid). Recent reviews by [76] and [143] discuss such approaches in detail.

The simplest technique is to guess the projections of the fault-horizon intersections and to treat these as discontinuities. The surface data can thus be interpolated treating the fault traces as internal barriers. Although simple, such a technique can lead to a strange fault surface when traces are used to define a fault surface. A better method, but requiring more work, is to first build a surface model for each of the fault surfaces. When working by hand

([76, 143]) an iterative approach is adopted whereby fault traces are explicitly calculated by intersecting map contours with the fault surface contours.

Fault Framework Modelling: It is now generally agreed that the best approach for modelling a faulted geological structure is to first focus upon the fault surfaces. Explicit interpolations of the fault surface are needed. This approach is now used in the most commercially successful geological modelling software packages ([64, 84]). A particular difficulty is presented by fault-fault intersections - should they be an input or an output?

Manual Approach for Fault Framework Modelling: One approach, a manual technique, is a possibility [64] where the intersections and the fault surfaces are built together, interactively in a 3D visualisation environment, with visual cues provided by seismic data, interpolated horizons or both. In such an approach lines are digitized onto the observed intersections. Further lines are digitized that manually construct a ruled surface. These surfaces can be interpolated using bilinear patches or splines. Thus in this approach the fault-fault intersections are input to the modelling, provided by the user. A schematic is provided in Figure 9.

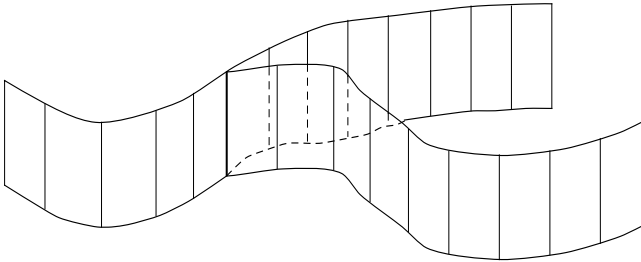


Fig. 9. Fault-fault intersection framework.

Automatic Approach for Fault Framework Modelling: The second approach is to interpolate the fault data for each fault separately and then to compute the fault-fault intersections. This may require some manual assistance to the algorithms to help extend surfaces so that the surfaces do intersect if there is insufficient data. In principle, surface-surface intersections are easy to compute. In practice, however, the intersections may have a very complicated topology largely arising from artefacts of the interpolation. The intersection calculations can be very delicate. At best a great deal of computer time is needed, and in the end a lot of user interaction may be required to *clean up* the results. Ironically it appears that in practice such an *automatic* approach is only suited to models with a small number of faults. The most practical

approach, that inserts the intersections directly - not needing any intersection calculations - is the easiest and fastest method. It is difficult to provide references to support these observations as the science of structural modelling is dominated by commercial companies who do not publish descriptions of their algorithms in the open literature.

Fault Block Splitting (FBS): One approach to the structural modelling problem imbeds the fault surfaces into an extended set of surfaces that divide the volume of interest (VOI) into a set of closed compartments. When there are only a few faults this is a simple extension of the fault framework modelling activity. Some extra surfaces need to be added, and parts of the fault surfaces on which there is a throw, and the parts on which there is not must be specified. There is however an extra burden on the user of the software; the order of the faults has to be chosen. The reason is that a convenient approach (for the software implementation) to fault block splitting is to build a *binary FBS tree*. Thus the volume of interest is defined, the first fault is extended so that it divides the VOI into two pieces. This operation is then repeated with each fault in turn. The extended faults must cut one or more fault blocks - the compartments in the binary FBS tree - into two pieces. In principle this is simple but in practice very difficult.

In two dimensions, with vertical faults, it is possible to automatically extend the faults and to carry out automatic subdivision [135]. This requires delicate programming but has been commercially available for some time. When the faults are sloping this automatic method can still be used. The approach is able to deal with very large numbers of faults.

When the faults have shallow dips, that is they are nearly horizontal surfaces, as in a thrust fault, then much user editing is required. When faulting is complex, the process of model building is essentially manual. As a general rule, software must allow user interaction to enable interpretation and assumptions of geological style to be imposed by a geologist. However, at the time of writing all software requires extensive user intervention. There is clearly much room for mathematical innovation in providing better algorithmic tools to assist the geological model builder.

The Corner Point Grid Method.

Geometry, Topology and Construction of Corner Point Grids: The main components of a corner point grid are:

- The bounding box.
- The boundary.
- The internal control surfaces (usually faults).
- The coordinate tubes.
- The tube dividing surfaces (usually horizons).
- The grid blocks.

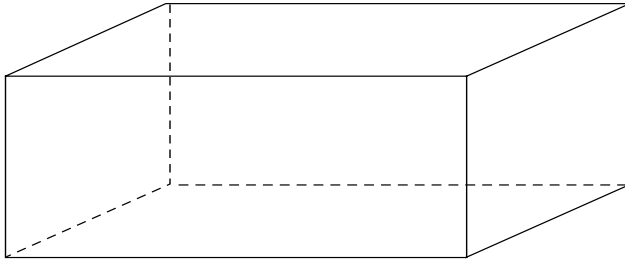


Fig. 10. The bounding box.

Imagine a finite, rectangular bounding box containing all relevant point, line and surface data, Figure 10.

Introduce the boundary; a surface that is broadly vertical or aligned with the sides of the bounding box. In practice the boundary is chosen to guide the slope of the final grid and plays an important role in guiding the general shape of the grid.

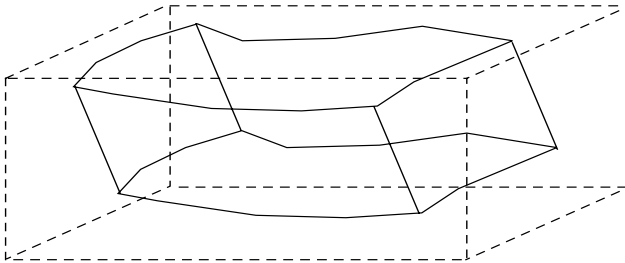


Fig. 11. The boundary inside the bounding box.

The internal control surfaces are surfaces that are again broadly vertical. These surfaces are divided into two sets: the *honoured surfaces* and the *zigzag surfaces*. Most of the time the control surfaces are fault surfaces. In some situations however, the control surfaces might be the flanks of a salt dome or other intrusion.

The structured coordinate tubes are the cells of an N_x by N_y by 1 grid that conforms to the boundary and the honoured surfaces. The edges of the coordinate tubes are called the coordinate lines. On a structured grid each tube has four coordinate lines, each one located at a corner of the tube.

In technical terms the tubes define a regular Cartesian N_x by N_y by 1 grid in a *logical cube* that deforms to fit the boundary and honoured surfaces. Often the grid will also be subjected, through the grid generation algorithms,

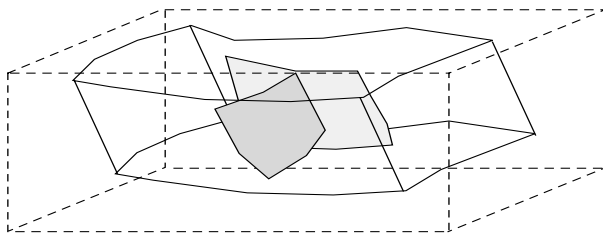


Fig. 12. Some honoured surfaces inside the boundary.

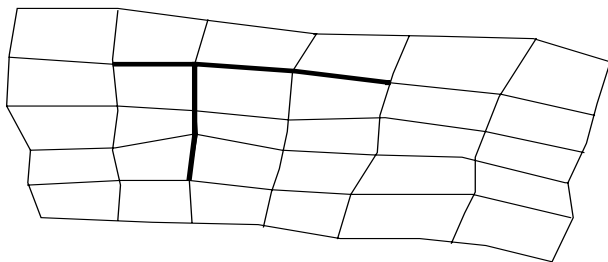


Fig. 13. Areal view of a structured corner point grid with honoured surfaces in bold.

to general trends in the zigzag surfaces. The construction difficulties concern the choice of coordinate lines to go with a particular honoured surface. Also the honoured surfaces need to be extended, automatically by an algorithm, so that the imbedding of the honoured surface in the grid of tubes is smooth and natural looking to the eye. Algorithms exist for the automatic assignment of coordinate lines to particular honoured surfaces [57].

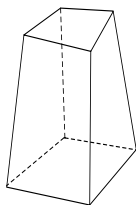


Fig. 14. A typical coordinate tube.

The sides of the coordinate tubes need not be flat. The only essential requirement is that the tube is a singly connected volume. In practice the

sides are often bilinear surface patches and the edges are straight lines. In such a case the tubes are hexahedra. The most advanced packages allow the edges to be piecewise linear or *segmented* lines [64]. The tubes are then stacks of hexahedra.

Surfaces that are not honoured by the tubes are the zigzag surfaces. In the case of zigzag surfaces the surfaces are moved to the nearest sequence of tube sides. This is analogous to the process of rasterisation that occurs on a digital display, but is in a 3D space. The geometric accuracy of the grid is proportional to the size of the tubes.

In the case of unstructured coordinate tubes an initial unstructured grid with vertical coordinate lines is built. This unstructured grid might be a Voronoi grid, a Delaunay grid or a grid made from aggregated cells of one of these types of grid. The control surfaces for the initial grid are obtained by essentially verticalising the original data. These vertical lines are then sloped to honour the actual control surfaces. Coordinate lines that do not lie on the control surfaces are positioned using an interpolation procedure.

The next stage in building a corner point grid introduces the *tube dividing surfaces*. In the simplest approach the tubes are collected into groups and a set of tube dividing surfaces is assigned to each group of tubes. It is assumed that each surface is continuous within the group and forms part of a consistent stack of surfaces. This is illustrated in Figure 15. Pinchouts are allowed but surfaces are not allowed to cross.

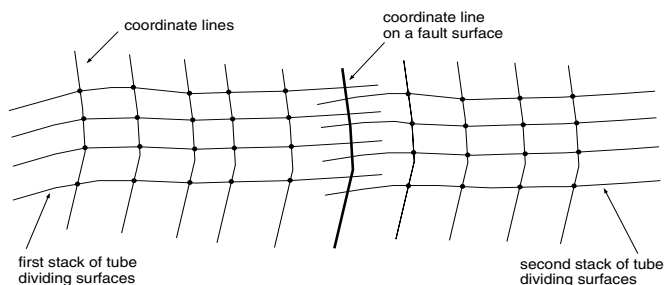


Fig. 15. Cross section of some tubes with two sets of tube dividing surfaces.

The simplest tube dividing method just samples the surfaces onto the coordinate lines at the intersection points of the coordinate lines with the surfaces. When coordinate lines are on the boundary of a tube dividing group there is a multiple intersection; one for each group. This leads to *split-nodes* on the coordinate lines. This is illustrated in Figure 16.

The corner point grid blocks are then defined by interpolating the cell corners with straight lines. On structured grids the blocks are generally hexahedra and on unstructured grids the blocks are general polyhedra. A cross section of a corner point grid is shown in Figure 17.

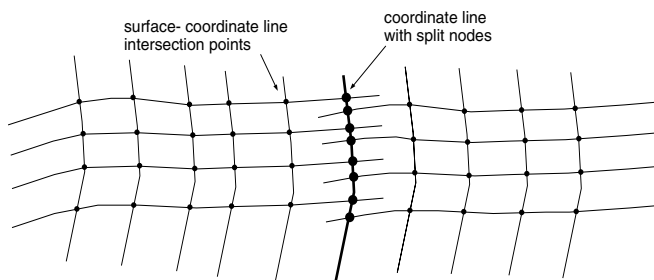


Fig. 16. Grid block corners at tube-dividing-surface/coordinate-line intersections.

The Slicing Method: An alternative approach for building corner point grids has been suggested by [107]. In this method the surfaces of the horizons and faults are assumed known and the coordinate tubes are simple vertical sided tubes with an orthogonal areal pattern. The simulation or geological grid cells are then defined as the intersection sets of the tubes with the layers. The cells can thus be constructed by slicing the tubes using the fault and horizon surfaces. In [107] the implementation is based on the assumption that the surfaces are height fields with respect to a flat reference plane. The method is promising and could be generalised to use overturned surfaces and any pattern of coordinate tubes. A disadvantage of this method is that the surfaces need to be constructed in an external application.

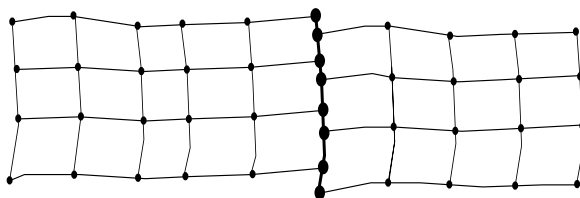


Fig. 17. Final stage of grid block construction.

Input Data for Corner Point Grids: In the earliest corner point grid building applications, the input data were in the form of *horizons* and *fault traces*. The fault traces were used to drive the construction of the tubes. The sides of a particular sequence of coordinate tubes then defined the fault surfaces. Horizons were used as the tube dividing surfaces. This workflow is still widely used, although it can involve a lot of work in editing fault traces so that they lie on their associated fault surface. An early case study is [74]. Often the horizon surfaces are inconsistent as they are constructed separately from one another, and the fault traces are assigned separately to each surface. If the

traces arrive from a mapping package that knows about fault surfaces then these difficulties can be avoided.

In the most recent corner point gridding applications there is a move toward building a framework of fault surfaces before any other model building operation. This is exemplified by the application described in [64], where it is even possible to perform scattered data interpolation of the tube dividing surfaces (most often horizons) directly onto the coordinate lines. One way to understand this step further is to regard a conventional mapping package as moving surface nodes up and down on vertical *coordinate* lines that are arranged in a regular Cartesian grid. In a mapping package the *tubes* have vertical, flat, sides. All faults are essentially zigzagged, although some packages perform local unstructured grid refinement, by slicing the tubes with the fault traces. Detail from a mapping package can be high, and use is convenient, provided all faults are normal and there are no intrusions such as salt domes.

When building surfaces directly inside the corner point grid application there are no problems with reverse faults, as the coordinate lines conform to the fault surfaces, and in the local coordinate system defined by the coordinate tubes there are no *reverse* faults. This is very convenient and powerful. The approach has only been partially exploited so far, and one looks forward to improvements in efficiency and quality. Much more remains to be done with regard to the proper evaluation of statistical uncertainty in structural modelling. Some discussion of this can be found in [152].

Problems with Corner Point Grid Modelling: For many situations the corner point grid approach is natural, accurate and fast. Problems occur when there are geometric or topologically complicated systems to model. One particular advantage of the corner point grid approach is that in simpler problems there are no performance limitations regarding the number of faults that can be included in the grid. Clearly, eventually memory becomes an issue, but this is much more of a difficulty in other approaches. A corner point grid can have 1000's of faults and yet be constructed on a relatively modest computer.

Geometric complexity often involves overturned surfaces such as found in an intrusion. If this is not too complicated then editing of the scattered data that lies on the surface, splitting it into groups that control the base surface, the sides, and the top can lead to a model. It is already possible for skilled users to build such a grid using the most sophisticated corner point grid applications. A schematic cross section of a salt dome grid is shown in Figure 18.

Another topological complication occurs when two or more faults intersect. An example of the geological nature of the problem is indicated in Figure 8.

These *y-faults* or *λ -faults* cause severe difficulties for current state-of-the-art geological modelling and grid generation systems. One promising approach, successfully implemented in [136], is able to build a grid as long as

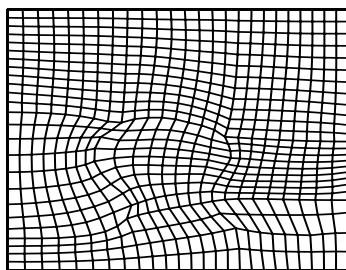


Fig. 18. Cross section of a grid that honours a salt dome.

the surfaces are provided as in the right hand side part of Figure 8. That is, the surfaces must be trimmed and related to one another so that all reasonable topological and geometric queries can be answered. [136] constructs an *ijk* or *vertically zigzagged* grid (see also Section 3.1). This means, essentially, that the geological model is digitised onto a grid, rather in the way that a 2D picture is rasterised onto a 2D raster of rectangular pixels. Here, a 3D *raster* is built, made of a 3D adaptive grid with general curvilinear hexahedral cells. The sophistication lies in the fact that the raster is adapted to the local surfaces. This increases the accuracy whilst reducing the number of grid blocks. A more natural and accurate solution can be constructed by exactly slicing the coordinate tubes with the tube dividing surfaces, a technique that has been commercialized by [107]. Another approach might use a vector field technique to build a system of coordinate lines that can then be used to sample the surfaces.

The final difficulty to be highlighted, regarding corner point grid generation methods, is the listric or thrust fault problem. A schematic of this geometry is shown in Figure 7. Again sophisticated use of curved coordinate lines, breaking up of scattered data into tube dividers and honoured surfaces could build adequate models, but this requires extensive work by a user of any software. The state-of-the-art for such structural modelling problems is to ask the users of software to construct the grid in a sequence of manual operations. Clearly, further research is needed for these difficult modelling problems.

7.2 Property Modelling

Spatial Statistics in Curved Spaces. Topics in spatial statistics have been reviewed in Section 4. There the coordinate system was assumed to be rectangular Cartesian. This assumption is often made in the geostatistical literature and in geostatistical software. See, for example, [42].

Geological systems are manifestly non-Euclidean. Layers are twisted, pinched-out, or faulted. At best there is a local Cartesian coordinate system.

The situation is reminiscent of continuum mechanics. There the requirement to describe the deformation of material objects has led to the development and application of differential geometric and tensor analysis techniques, that make it possible to describe systems without any particular assumption of a coordinate system until one has to actually perform a calculation. Indeed, if the calculation is performed numerically, by for example a finite volume method, global coordinate systems are unnecessary. One simply requires coordinates in the vicinity of various objects so that quantities such as areas and volumes can be computed.

This section outlines common approaches to statistical interpolation in curved layers. The last section indicates a solution along the lines of that used in continuum mechanics.

The usual approach assumes the geostatistical algorithms are satisfactory as they are, and that the problem is to find new coordinates (u, v, w) , given by a transformation, f ,

$$(x, y, z) = f(u, v, w)$$

with the property that for any two points, (x_1, y_1, z_1) and (x_2, y_2, z_2) in the same layer with,

$$w_1 = w_2$$

then the distance

$$((u_2 - u_1)^2 + (v_2 - v_1)^2)^{\frac{1}{2}}$$

is the *intrinsic* distance between the points in the layers. (The intrinsic distance is defined as the length of the shortest curve joining the two points where all the points on the curve lie on the surface.) These coordinates are a generalisation of isometric coordinates to a faulted surface. They are very difficult to construct and do not generally exist. However, one can treat them as an approximate goal; one tries to find a coordinate system as close to the isometric ideal as possible [114].

Stratigraphic Coordinate Interpretation.

Mapping Method: To introduce this method - the *straw man* of property modelling - let us remind ourselves about the geometric structure of a map of a faulted surface. Suppose that the faults are normal faults. In such a case each (x, y) point on a horizontal reference plane is mapped into the horizon, or into a fault surface. The boundaries of the fault surfaces are the fault traces which are polygons in the reference plane. The horizon is not itself a continuous surface. However, the union with the fault surfaces *repairs* the horizon surface to a continuous surface. That this can be done is the main reason for the historical success of mapping software and its main restriction - one cannot describe reverse faults without extensive extra mathematical (and thus software) objects.

However, having repaired a faulted horizon to a continuous surface it is possible to apply any 2D interpolation algorithm for any property such as the well values of, say, porosity. This completely ignores the effect of the faults. When the post faulting diagenesis has not markedly altered the continuity of the rock properties, this must be incorrect. The properties on either side of the fault, where corresponding points in the horizon were originally joined, should have the same value, but in this mapping method this is not generally the case. Although the approach is clearly defective, and is not used in any of the packages which have a stratigraphic 3D grid, it provides a useful example that contrasts in an interesting way with other, more sophisticated methods.

(i, j, k)-Method: Many geological modelling applications use a structured grid. Thus there is a natural mapping from (x, y, z) -space to a logical, rectangular (i, j, k) space. This mapping is a natural by-product of the grid generation process. The simplest technique for applying an algorithm that requires rectangular coordinates is to apply the algorithm in (i, j, k) -space. To do this, it is necessary to transform the scattered data into the (i, j, k) -space. Any correlation functions have to be defined in the (i, j, k) -space.

Advantages of this method are (i) it is fast (ii) it is qualitatively correct across faults when diagenetic effects, related to the fault are negligible and the pre-deformation properties of the rock are appropriate. The method does not properly account for the true distance between points, but does honour the connectivity across a fault surface.

(x, y, k)-Method: In some structural modelling approaches a 3D corner point grid is used to carry the properties. As part of model building, an intermediate 2D grid is built, assuming that the faults are verticalised. (This is done for purposes of analysing the topology.) This means that each grid cell, after the coordinate lines have been sloped or even bent into segmented lines, inherits an (x, y) coordinate from the intermediate areal grid. If the scattered data are transformed into this coordinate system and the properties interpolated in this space, then the true distance between the cell centres is more properly accounted for than in the (i, j, k) -method. In other words, because the faults are *verticalised* at this intermediate stage it is valid to use the mapping approach. Further, because the verticalisation is all through the model, it is possible to map the curvilinear grid into a 3D model space throughout the model. Three-dimensional property interpolation procedures can then be applied and posted back into the true geometric configuration [137].

The method is one of the best in current use but must be regarded as an interim solution, while research continues.

Mapping Methods. In the only book to have been published on 3D geological modelling [114], there is a section on building an isometric coordinate system such that given the coordinates of any two points they provide the distance using the Euclidean metric. It is possible to construct a best possible approximating set of isometric coordinates. This is the best one can do.

Coordinate Free Methods. The need to construct an approximately isometric coordinate system is an avoidable problem. All one needs to do is to use a functional probability density function that has a local form. That is of the form

$$\pi(\varphi) = Ce^{-H[\varphi]},$$

where $H[\varphi]$ is a functional that is an integral of a local function of φ and its derivatives of low order. (See Section 4.3 for an explanation of the symbols in the previous equation.) Such functionals are widely studied in the statistical physics literature. By discretising such a functional one can generate realisations or construct maximum probability interpolants that do not require any non-local coordinate system. Further research is urgently needed to fully explore such an approach.

8 Upscaling and Upgridding: Controlling Scale Dependence

8.1 Effective Medium Theories

Deterministic Version of Effective Medium Theory: Using the notation introduced in Section 5 consider the problem of: Find $\tilde{\varphi}$ belonging to the subspace \tilde{S} of S such that selected diagnostic functionals, $\tilde{f} = \tilde{F}[\tilde{\varphi}, \psi_a, \tilde{\psi}]$ of the problem

$$\tilde{N}(\tilde{\varphi}, \psi_a, \tilde{\psi}) = 0$$

approximate as closely as possible the diagnostic functionals $f = F[\varphi, \psi_a, \psi]$ of the problem

$$N(\varphi, \psi_a, \psi) = 0,$$

where φ belongs to the space S . In many situations it is assumed that the *effective medium* equations $\tilde{N} = 0$ and diagnostics \tilde{F} are of the same form as the original equations $N = 0$ and diagnostics F .

However, it is usually the case that the equations change form under the effective medium transformation. For example, in a layered system fine scale permeability scalars can become tensors, two-phase flow models become dual-porosity models, and so on. Further references and discussion may be found in the book [127] and the review [58].

Stochastic Version of Effective Medium Theory: Following the pattern of inverse problem theory, in the study of effective media there is a stochastic version where the problem is to find the best approximating functional probability density. Thus the problem is: find $\tilde{\pi}(\tilde{\varphi})$ over the subspace \tilde{S} of S such that

the expectation values of selected diagnostic functionals, $\langle \tilde{f} \rangle = \langle \tilde{F}[\tilde{\varphi}, \psi_a, \tilde{\psi}] \rangle$ of the problem

$$\tilde{\mathcal{N}}(\tilde{\varphi}, \psi_a, \tilde{\psi}) = 0$$

approximate as closely as possible the expectation values with respect to $\pi(\varphi)$ of the diagnostic functionals $\langle f \rangle = \langle F[\varphi, \psi_a, \psi] \rangle$ of the problem

$$\mathcal{N}(\varphi, \psi_a, \psi) = 0.$$

This formulation is close to that studied in the theory of the *renormalisation group* [19, 157, 164].

8.2 The Upscaling Approach

Full Upscaling Methods: In the deterministic effective medium problem it is assumed that a property model φ is available, in the stochastic problem the upscaling approach works on realisations of the stochastic process, π .

Upscaling methods have two aspects. First some *fine scale* experiments are performed. These can be *local*, in that they work on a very small part of the whole domain or *global* when the experiments are performed on a large part, or even all of the domain. Then the coarse model is defined by a coarse parameterisation - usually by introducing a coarse grid and assuming the properties to be piecewise constant on the coarse grid. Given the fine scale experiments and the coarse grid, a *coarse grid calibration* is performed. This too, can be local or global. Finding the coarse scale properties is an inverse problem with computationally generated data. The inverse problem requires solution of a subsidiary forward problem; when this is local, it is said to be a *local calibration*, and when the calibration inverse problem solves a forward problem on a large portion of the domain it is said to be a *global calibration*. A more detailed discussion can be found in [58]. The most common approach is the local-local method, where both experiment and calibration involve a single coarse grid block, perhaps including some influence from the nearest neighbours.

Generally speaking the more global is the calibration and experiment the more accurate will be the resulting upscaled model, but at increasing cost.

Upscaling is expected to work best when (i) the fluid process is stable (that is the displacing fluid has a lower mobility than the fluid that is displaced) (ii) the length scales of the heterogeneity are small compared to the averaging scale. In general averaging is performed by seeking the best approximation in the smoother space \tilde{S} . This idea is justified rigorously in the limit of infinite scale separation in the theory of homogenisation.

Preconditioning by Adaptive Coarse Grid Generation: It seems necessary for the fine grid properties within each coarse grid cell to be either constant or possess a very small length scale compared to a characteristic length scale

of the averaging process. Given a model with fine scale detail it might be possible, through a process of adaptive gridding, to build coarse grids with the desired properties.

[159] was the first to suggest a method. [106] continued to investigate the problem along the same lines as [159]. Methods in which a flow equation is solved on the fine grid and the equipotentials and streamlines are used to construct *optimal* coarse grids have been developed further by [2]. The heuristic approach, based on solving flow problems and then grouping layers according to the flux through the layers, introduced in [47], is of interest. The alternative of minimising the variance of some property in a coarse cell has received some attention in [13, 59, 60, 68, 133].

A moving finite element approach to variance minimisation was proposed by [13]. In [59] and [60], combinatorial aspects of the problem were tackled using a global optimisation algorithm. [133] made this method faster by restricting coarse grid cells to consist of strict subsets of fine grid cells.

There are many opportunities for further work in this area. By using unstructured grids, success might be easier. In two-dimensions progress in *image segmentation*, a very similar problem, could inspire a new attack on this *upgridding* problem. Deep results are available, which look as though they generalise to three-dimensions (see [120] for references).

Multiscale Simulation: Standard numerical methods, such as the finite volume method, seek approximate solutions in the form of piecewise constant or piecewise linear expansions. The basis functions are simple, and as the number of grid blocks is increased - known as *h-refinement* - so the error is reduced. Alternative methods, such as the spectral methods, seek expansions as finite superpositions of basis functions; for example a Fourier expansion in trigonometric functions. Spectral methods do not require a grid, although they are restricted to simpler geometries as a result. A compromise method is the finite element *p-refinement* method, where higher order polynomial expansion is used on a discretisation. In the interesting paper of [91] a numerical technique for constructing finite element basis functions that respond to local heterogeneity was described. This method is closer to the local-local upscaling method than one might at first think. Indeed a finite volume version of Hou's method was shown to be a form of local-local upscaling in [58].

The multiscale finite element and finite volume method is difficult to generalise to multiphase flow (however see [104] for a paper which discusses an approximate technique for modelling rate dependency effects). The novel, and very stimulating idea of using (i) an upscaling method for the average pressure, and (ii) a reconstruction stage to find mass-conserving approximate fine-scale fluxes was described in [94]. The reconstructed fluxes are used in an explicit method for the saturations. The method is very much faster than one solving the fine grid pressure equation with, apparently, little reduction in accuracy.

It will be interesting to observe research on multiscale simulation over the next few years. Will local upscaling methods be improved so that the two-scale method of [94] loses some of its apparent advantage?

8.3 The Homogenisation Approach

Homogenisation is a multiscale perturbation method in which the ratio of length scales is used as a small parameter. Consider a two-scale problem, with (i) a large-scale parameter, L , characterising, for example, the well spacing and (ii) a heterogeneity scale l , characterising the size of high permeability zones. In this case the expansion parameter is chosen to be $\epsilon = l/L$. Then the property model may be considered a function of the *slow* scale x and the fast scale $y = x/\epsilon$, that is $\varphi = \varphi(x, y)$. The gradient operator becomes

$$\nabla f = \nabla_x f + \frac{1}{\epsilon} \nabla_y f$$

for arbitrary functions, f .

The method then seeks expansions of the form $s = \sum_{i=0}^{\infty} \epsilon^i s_i(x, y)$ or even more general expansions with non-integer powers in ϵ or possibly general functions of ϵ . It seems that considerable skill is required to pre-scale the equations with ϵ 's inserted at various strategic places. For examples see, [44] and [127].

The procedure makes the expansion, gathers up terms of equal orders of ϵ and then a variety of arguments based on averaging are used to derive an equation for the order zero term. In the limit as ϵ goes to zero this lowest order term can, by more rigorous analysis (see [88]), be shown to be an exact model for the volume-averaged behaviour.

The method can be made rigorous, but as far as one can tell the degree of intuition required to find an appropriate expansion is similar to that required to set up an upscaling method. In many cases the homogenised equations are identical to those obtained by simpler and more intuitive upscaling arguments.

There are clearly opportunities for further research in this area, particularly in relating the homogenisation methods to the upscaling and multiscale methods. The results of [23] that show the need for dual permeability models as effective media for 2-phase flow are particularly interesting. Dual permeability behaviour has been observed in the field, [35], in apparently unfractured reservoirs.

8.4 The Method of Stochastic Equations

A method of considerable historical interest is the method of direct solution of stochastic equations. Thus for a stochastic problem of the form

$$\mathcal{N}(\varphi, \psi_a, \psi) = 0,$$

where the input, φ is a random function is studied using analytical perturbation techniques. Analytical methods for stochastic porous medium problems have been reviewed recently by [162]. Such methods appear to be limited to situations where a Green's function at zeroth-order can be found in closed form. Similar techniques have been reported in the turbulence literature for many years, where they have reached a higher level of sophistication (see [109]).

9 History Matching: Integrating the Production Data

9.1 The Problem of Integrating Production Data

Production data are defined to be any flow rates or pressures measured in the well bore other than measurements made on a scale of centimeters or less. Thus well testing and measurements made during field operation are included.

The problem of integrating production data involves either (i) constructing a deterministic property model that leads to flow diagnostics that broadly agree with the production data or (ii) modifying some prior probability model so that the posterior distribution is consistent with Bayes' rule and the data. The problem of integrating production data is often called *history matching*.

The general problems of forward and inverse modelling were discussed in Section 5 and the problem of integrating production data is, in principle, of the same type. However, in practice the large computer times needed to perform flow simulations and the strongly time dependent nature of the data to be processed makes the problem very difficult, compared to the inversion of small scale measurements.

Problems in other parts of the geosciences are very similar. In particular the problem of assimilating observations into weather forecasting [39] and ocean circulation models [160] are conceptually close to the oil reservoir forecasting problem. Indeed, there is probably much to be learned by cross-fertilisation between these different fields of geoscience.

Comparison studies of several different methods have been performed as reported in [15, 62, 111, 163].

Two key references in the petroleum simulation area are [124] and [116].

9.2 The Bayesian Formulation

The Bayesian formulation is not universally used in history matching, but there is a general trend toward thinking in this way. One advantage that the Bayesian formulation provides is that it places all methods in a common

framework. Within this framework many methods are viewed as approximations to other more *ideal* approaches or as summary methods of the posterior distribution.

As the Bayesian formulation was described in Section 5 it is sufficient to recall the main uses of the formulation in the *maximum a posteriori* (MAP) mode or in the *stochastic sampling* mode. The *maximum likelihood estimation* method is obtained by setting the prior to unity in the MAP method. The MLE method is essentially the least squares method. Without a suitable choice of prior it may be necessary to introduce further ad hoc regularisation in the case of MLE. A carefully chosen prior should regularise the problem in a satisfactory way.

9.3 Deterministic Algorithms

Deterministic algorithms are methods for solving the MLE or, preferably, the MAP equations. That is a unique, global minimum of the MLE or MAP functionals is to be computed.

Parameterisation Methods: If the objective functional is not suitably chosen, or the number of unknowns is considered too large, then it is necessary to *reparameterise* the unknowns.

The most common way of doing this is via *zonation*. That is, the domain of interest is divided into a relatively small number of subdomains, and either the values treated as piecewise constant by subdomain or a scalar multiplier is applied to the values in each subdomain.

Techniques for choosing the division into subdomains are assignment by (i) subjective decision (ii) regions of maximum sensitivity [20] and (iii) streamlines of the total flux as introduced by [155]. A clear example of the streamline method is [1]. Several papers [30, 40, 80, 103, 119, 161] have appeared recently using variants of streamline methods for history matching.

A generalisation of the subdomain method is to use a general basis, and represent the unknown parameters as a superposition of the basis functions. This method was used in an early and impressive paper by [70] in which all the ingredients for MAP are in place.

A special case of the basis function method works by choosing a subset of grid blocks - the *pilot points*, and setting the values in all other blocks using kriging. The pilot points might be chosen subjectively or using sensitivities. It was observed in [116] that the pilot point method is a version of a basis function method. The results in Section 4 are relevant to this observation.

A very interesting variant of the basis function method, introduced in [132], uses two or more realisations from the prior as basis functions.

Minimisation Algorithms: Production data integration must, in some way, involve forward simulation of the fluid flow model. In MLE or MAP, even with reparameterisation, an optimisation method must be used. There are two choices; to use a derivative-free method, or to use derivatives.

Derivative-Free Methods: Derivative-free methods can simply call the simulator and use the results. A simple technique is simulated annealing which was investigated in [126] and [41]. Using a fast simulator such as a streamline method (fast by virtue of the IMPES approximation and the one-dimensional approximation along the streamlines) or a coarse grid simulator, this might be practical.

The recent developments in streamline zonation use a simple iterative, derivative free, update of the permeability field along the streamlines.

Gradient Methods: If the aim is to find the MLE or MAP estimates then the method of choice must be a derivative method. Once the effort is made to modify the simulator so that derivatives can be calculated exactly (that is without using numerical differentiation) then the higher order convergence of a gradient method can easily outperform a derivative free method.

Gradient methods fall into two classes, depending on the number of derivatives to be calculated [124]. If the number is small, then direct calculation of the objective function gradient is best. The reason for this is that with knowledge of the gradient vector, the Gauss-Newton method (where the Hessian is approximated as the direct self product of the gradient) can be applied. This tends to be a second order convergent technique. Simulators with a fully implicit formulation calculate many derivatives as part of the Newton step at each time step. The extra derivatives needed for the gradient (when the number of unknowns is small) can be obtained with a small overhead.

When the number of unknowns is large, as for example in the case that all grid block property values are regarded as unknown parameters, then it is impractical to find the derivatives of the objective function. By treating the fluid flow model as a constraint, the adjoint method can be used. This is, conceptually, the same adjoint method as described in Section 4.5. The method exploits the fact that the dot product of the gradient with a small number of fixed vectors can be obtained at relatively low cost. However, this means that a lower order optimisation method, such as the conjugate gradient technique must be used. This is why for small numbers of unknowns the direct technique is best.

9.4 Stochastic Methods

As explained in Section 4, unless the prior pdf is very sharply peaked about the maximum, the MLE or MAP estimates are not actually all that useful. The real problem is to compute diagnostic functional integrals of functionals, using the posterior distribution as the probability measure.

With the ever increasing power of computers, this is now just feasible. Monte Carlo integration is likely to become increasingly important and, in the opinion of the author, should be regarded as the method of choice and the method in which to invest research and development. That is to say, current approaches to Monte Carlo need to be improved, but Monte Carlo is a fruitful line of investigation.

The simplest technique is to generate multiple realisations from the prior and reject those that do not agree with the production history. Some studies report success in this endeavour [15]. However, the study of [111] would imply the need for caution in the use of Monte Carlo.

10 Workflow Analysis

In recent years the notion of *workflow* has become popular, particularly with software vendors. The idea is that a distinctive sequence of activities involving different items of software or features in a particular application can be identified. User decisions are needed at many critical stages, making it impracticable to fully automate most workflows. In the next section the older style 2D workflow is described. This 2D workflow is still used in many, if not most, applications of geological and reservoir modelling. Many stages in this workflow are found in the contemporary 3D workflows as discussed in Section 10.2. Finally a first attempt is made to classify workflows with a view to identifying possible approaches that might help improve efficiency or accuracy in model building.

There are many case studies in the literature of the Society of Petroleum Engineers [140]. Three papers that give a reasonable overview are; for 2D modelling [154]; for 3D modelling [93, 156]. The books [52] and [72] are the only extended published discussions of workflow as a whole. The book [72] has detailed case studies that emphasise the geoscience aspects, whereas [52] contains more reservoir engineering detail.

10.1 The 2D Workflow

Seismic Data: Seismic data usually provides the starting point. The processed seismic cross-sections are displayed, in the time domain, on a computer screen. The user digitises the *seismic picks* that are points along an important horizon. In sophisticated programs the well logs will also be displayed so that identification of layer boundaries is made with all data in mind. *Autopicking* algorithms are available that will take a users initial pick, and then by pattern matching identifies other points on the horizon. The results can be good, or might - because of noise or poor signal strength - require extensive manual editing. See [36] and [12] for detailed descriptions of this process.

Each horizon is picked in this way. The resulting scattered data sets are then passed to a *mapping package*, an embodiment of one or more of the many scattered data interpolation algorithms reviewed in Section 4.

Well Logs: In some studies there may be no seismic data available, and so all of the scattered data, used for building surface models, is obtained from picking the layer boundaries on well log displays. Specialised software exists

for such purposes, that automates the traditional method of placing paper copies of logs on a large table or on meeting room walls.

It is now common for well logs and seismic cross-sections to be displayed in the same software package. Seismic has a large scale resolution - perhaps on the order of 20 meters but possibly 50 meters. Well logs clearly show the existence of much smaller scale features. In the 2D workflow, the positions of important layer boundaries, below seismic resolution but important to flow simulation or reserves estimation, are mapped by correlating the surface with other already mapped surfaces. Techniques for mapping are reviewed in [95]. Maps may have a resolution of 1000 by 1000 (or more) cells, and will explicitly store the fault polygons which define the intersections of faults with the horizons. In many 2D workflows the faults are just modelled as a set of such *fault traces*. In more rigorous workflows the fault surfaces are also interpolated from fault picks, where fault-horizon intersections are visible in the well logs or where the fault has been identified in the seismic.

At this stage a property map will also be made for each layer. Usually one map per layer. Sometimes a map showing the fraction of rock that is permeable and the fraction that is impermeable shale is made. The fractions are expressed as a *net-to-gross* ratio [52]. A disadvantage of this technique is that there is no obvious way of computing an effective permeability without some model of the spatial distribution of the heterogeneities. Indeed, avoiding the use of net-to-gross concepts is one of the main advantages of the newer, 3D, workflows [156].

The number of layers and thus maps might exceed the capacity of a flow simulator to model flow on a simulation grid of the same resolution as the maps. Therefore, even in a 2D workflow upscaling is required. In older simulation gridding packages this was done using algebraic averaging, and in the newer grid generation packages there are options for upscaling methods using flow solvers.

Well Tests: If available, a well test permeability could be used as conditioning data for the mapping interpolation, rather than a well log. In the absence of clear algorithms for scaling between the log and well test scale, subjective judgement is required in choosing the values to be used at the conditioning points.

Simulation Grid Building: Once the surface maps are available, a simulation grid can be built. A boundary for the simulation region is defined, and a corner point grid is constructed to honour chosen fault traces and the boundary. In older packages this was a very manual task, but is now largely automatic due to advances in grid generation algorithms that can handle internal components of the boundary as constraints.

History Matching: Once the simulation grid and properties have been built, and the simulation has been performed, the properties are modified, usu-

ally by manual editing, but more recently with assistance from optimisation methods [93] implemented in software.

10.2 The 3D Workflow

The 3D workflow is very similar to the 2D workflow. The differences are quantitative, rather than qualitative. More detail is captured, and there are growing efforts to quantify the uncertainty or non-uniqueness in the models that are consistent with available measurements. The attempt is made, subject to computer constraints, to map all of the *important* layers that can be seen at the wells. This, if successful, will capture the low and high permeability structures which influence the flow. The consequence is that the size of the model can be of the order of 20 million active cells. In the study of [93], there were 25 million cells, of which 19 million were active. The cells were of a size, 75m by 75m by 0.5m. These are actually very large objects. Nevertheless simulation is not practical on such a grid, and so upscaling is performed. The resulting simulation cells in [93] were 90m by 100m with thicknesses ranging from 2-4m in a 104-layer model to tens of meters in a 19-layer simulation grid. The areal upscaling factor is quite small in this instance, with the majority of the averaging taking place in the vertical direction.

In [93] it is stated that an advantage of this workflow is that multiple simulation models can be built from a single *shared earth* geological model. It was found that by including the extra detail in the model the initial model was a good starting point for history matching. In [93] five realisations were generated, and the structural framework was deterministic.

In practice it would seem that *fine models* are actually quite coarse, and that attempts to quantify uncertainty are still limited by inability to handle large numbers of realisations.

In [17] it is stated that oil companies often underestimate risk. Of the many possible causes of such underestimates (from the point of view of this chapter) clearly (i) insufficient numbers of realisations in Monte Carlo studies (ii) suppression of fluctuations caused by upscaling methods are contributors.

The question is: can one do better? One answer is to wait for improved hardware - and this will help in some ways. The next section speculates on possible ways in which different workflows and new algorithms could help.

10.3 Workflow Possibilities

There are six main classes of flow simulation model relevant to the question of scaling. The first distinction is between stable and unstable flow. Instability causes multiple length scale features to evolve in saturations and other state variables. Knowledge about modelling such unstable behaviour is rather scant. Stable flow is much better understood, although there are many unanswered questions.

An important characteristic is ϵ , the ratio of the smallest heterogeneity length scale to the flow modelling scale. The flow modelling scale is in practice set by the grid block size and for accuracy should be a few times the grid block size. The separation of length scales is then measured by the value of ϵ . Length scales can (i) be well separated (the $\epsilon \ll 1$ case) (ii) have large fluctuations on the averaging length scale (the $\epsilon \sim 1$ case) or (iii) have no small scale fluctuations on the averaging scale so that properties are essentially constant on the averaging scale (the $\epsilon \gg 1$ case).

Thus there are six cases in all and three cases to be discussed, as the unstable case is not considered in this chapter.

Stable and $\epsilon \ll 1$ Case: For stable flow and $\epsilon \ll 1$ there are no insuperable difficulties. The aim of upscaling is to transform a stable and $\epsilon \ll 1$ problem into a stable and $\epsilon \gg 1$ problem. If this works then it was not strictly necessary to build a finely gridded model for the whole reservoir in the first place. By building a detailed model, in the vicinity of the wells, for example, the large scale simulation model can be built directly. In fact, in this way one could build models that effectively contain billions of cells. One could go further and say that the attempt to build fine models, but with far from sufficient computer memory available, is a cause of error and unnecessary computation. Indeed in some cases *fine grids* are being used as an alternative to tensor modelling. A tensor requires three vectors, in addition to, if it is symmetric and second order, six numbers. The vectors are defining the bedding planes and they do not require explicit models of their geometry.

One factor preventing the increased use of tensors is the complete absence of geostatistical theory for interpolating vector and tensor properties. (The view expressed in [46] that “there are few areas where new algorithms need to be developed” is perhaps too optimistic. There are in fact many outstanding problems; for example, defining non-Gaussian geostatistics without explicit grids, interpolating vectors and tensors and constructing realisations that are reliable samples of the underlying distributions.)

Stable and $\epsilon \sim 1$ Case: When the problem is stable and $\epsilon \sim 1$ there are severe difficulties with upscaling. One possible improvement follows from the observation that the heterogeneity is *almost* resolved by the grid. Rather than upscale the realisations, an alternative is to resample the original pdf, but on the simulation grid. The change in workflow, although slight in implementation, is rather considerable in concept. That is, one realises that the geological model is the pdf, and not realisations of that pdf. It is in this case that shortcomings in geostatistical interpolation techniques are driving the design of the workflow. Interpolation methods that *rely* on a simple grid structure *must* be used in combination with an upscaling method. A grid-free geostatistical method could be used, on demand, *directly* on a corner point grid, for example.

Stable and $\epsilon \gg 1$ Case: In this case one need not upscale. Simple sampling is adequate. That is the geological value at the simulation cell centre is used for the whole simulation cell. Of course, in such a model there are always accuracy improvements to be obtained from grid refinement, as the pressure distribution and flow paths may be complicated as a result of the well pattern. One must not forget that the grid has to resolve the state variables as well as the input variables.

Unstable Flow: Unstable flow requires a review of its own. There are few results of substance, and many opportunities for useful and interesting research.

11 Concluding Discussion

11.1 Outstanding Problems in Mathematical Geoscience

As the various component disciplines have been discussed, with a focus on the mathematical structure, several problems have been highlighted. (The author must stress that the following remarks are expressions of personal opinion, and must be viewed as tentative and speculative. It is, however, useful to summarise such conclusions at the end of a review of mathematical geoscience.)

Flow through porous media and reservoir simulation: The method of streamline simulation is growing in importance. However, it has not received much attention from numerical analysts. Convergence analysis is needed, and insights gained could be valuable to streamline simulation and to more conventional finite volume methods.

Multiscale methods have started to appear, and show considerable promise. However, the link with upscaling approaches has not been clarified, and it may be the case that, as yet undiscovered upscaling workflows, are competitive. Multiscale methods are an area of growing academic interest, with substantial academic projects starting at several universities around the world.

Improved large scale models of the average behaviour of unstable flow are needed. The existing models have not been derived from fundamental theories at the small scale even in special cases. The phenomenological models do not themselves possess proven stability properties on the smaller length scales.

Grid Generation: Even when a model of the structural geometry of a reservoir is available, in three dimensions there are no universally applicable and robust grid generation methods - even in cases where the geometric input is perfect. (Perfection here means that all intersections are well-defined and there are no overlapping regions.) One might think that unstructured grid generation holds the key, with elegant Voronoi or Delaunay grids. However,

even for problems with just an external boundary this is a challenge. Geological problems, however, possess complicated internal boundaries and this is essentially uncharted territory. There is thus a real need for innovation in this area. But, as mentioned later, the problem is even harder than this: the geometry has to be built first.

Spatial Statistics: Interpolating Scattered Data: Many geostatisticians regard their subject as mature and the main task as being one of public education. From the point of view of general applications this is far from being the case. Spatial statistics, when stochastic realisations are required are overly dependent upon structured, and even regular grids with cells all the same size and shape. Ad hoc devices are needed to circumvent this problem. Grid-free methods may be possible and are a fruitful area for research.

The link between kriging, radial basis functions and maximum probability interpolants could be investigated in a much deeper way than in Section 4. The huge effort to analyse and develop radial basis function methods would be made more valuable if the participants in the growing radial basis function literature were more aware of the need for *statistical* considerations in the scattered data problem. Deterministic approaches to problems with sparse data are not applicable in most of the problems encountered in the geosciences.

The sequential sampling methods - popular with users because of their high speed - are suspect when compared with methods such as the Gibbs sampler which possess rigorous proofs of statistical convergence.

Methods that provide stochastic models of vector or tensor quantities are essentially absent.

Forward and Inverse Modelling: Many inverse problems in the geosciences involve sparse data used to constrain functions representing three-dimensional heterogeneous property fields, such as porosity or permeability. It is not that clear which parameters are to be determined in the inversion. Is it properties as functions of position, or is it the parameters in the correlation functions summarising the heterogeneity? It may be some mixture of the two, with the parameters in the correlation functions displaying the most sensitivity to the measurements. There is room for much research here: model problems should be studied so that our intuitions can be further developed.

The growing influence of the Bayesian viewpoint, is something to be welcomed, but with caution. The relationship between traditional *deterministic* solutions of inverse problems, maximum probability solutions and Monte Carlo approximation of output statistics needs further clarification and analysis. Studies of model problems, once again, would help us all to understand the issues better.

There seems to be no review of methods for inverse problems that compares and contrasts the various theoretical approaches in the way that was

outlined in earlier sections of this chapter. A substantial review, going into far more detail than provided here, would be of enormous value.

The role of length scales in the prior, as part of the inversion process, could be much clearer. This is related to the problems of upscaling, and clarification might require new insights into the general methodology of mathematical modelling.

The different inverse problems in the geosciences, particularly seismic inversion, resistivity inversion, and the history matching of production data are usually treated in quite different ways: is this an accident of history, or should there be changes in all areas, so that a unified approach is used?

Geological Modelling: The characterisation of uncertainty of geometric properties has not received the same level of attention as uncertainty in properties such as porosity. This needs to be rectified.

In general the subject of geological modelling is fraught with difficulty. Only relatively simple systems can be parameterised in a satisfactory way - using the corner point grid approach. Finding a way of building the geometric aspects of geological models, so they can be easily modified, by users and by software performing automated inversion algorithms is an open problem. A breakthrough is needed in this area if the dream of a *shared earth model* is ever to be achieved in a practical way. In situations involving complicated geometric features, such as intersecting faults, the problems are exceptionally difficult and interesting.

Upscaling and Upgridding: Controlling Scale Dependence: The upgridding problem is unsolved in the general case. Sometimes the problem could be avoided, but users are demanding better methods, as the workflow that builds fine grids and then upscales them, demands a solution to this problem.

The ideas involved in dual-porosity and dual-permeability models could be more widely applicable to upscaling than is generally realised. By using models that are designed to characterise behaviour involving two time scales, the need for fine scale models can be reduced.

History Matching: Integrating the Production Data: A solution of the history matching problem requires (i) a method of sampling that reduces the numbers of realisations needed for accurate Monte Carlo calculations (ii) better ways of generating realisations that are consistent with both the prior and the measured data.

Workflow Analysis: Deeper analysis of workflow possibilities is needed. Current methods are applied in an uncritical fashion, and are not examined with a view to establishing an optimum workflow for a particular engineering objective.

11.2 Concluding Remarks

The main mathematical techniques used in building geological models for input to fluid flow simulation have been reviewed. The subject matter concerns the entire geological and reservoir simulation modelling workflow in the subsurface. Seismic acquisition, processing and interpretation, well logging and geology have only been reviewed in outline. However, the topics of grid generation, geometric modelling and spatial statistics have been covered in considerable detail. A few new results in the area of geostatistics were proved. In particular the equivalence of radial basis functions, general forms of kriging and minimum curvature methods was shown. A Bayesian formulation of uncertainty assessment has been outlined. The discussion of upscaling was brief, consisting of a summary, as a recent, detailed review in this area, [58], is available.

The classical approach, using maps, is giving way to an approach that builds 3D geocellular models. Some of the methods for this are still map based - but some now work directly on the basic data - seismic picks, well logs and cores.

Accompanying this move to 3D is a strong tendency to build as detailed a model as computer memory allows. However computer memory is far too limited for properly detailed models of a whole reservoir to be built, and so geological detail is grossly under-resolved. Intuitive analysis of upscaling leads to the conclusion, when the fluid flow is stable and the length scales are well separated, that upscaling can be very accurate. By applying knowledge of the scales at which the length scales *are* well separated, one can design multiscale models that *do* upscale. When this is possible one can build fine scale - but now truly fine scale - models near the wells. Then a second application of geostatistics on the larger scale, conditioned on the upscaled near-well data, can suffice.

Acknowledgements

I would like to thank the Royal Society for the award of an Industry Fellowship at the University of Oxford. I would also like to thank Zhijie Cai (Fudan) and John Ockendon (Oxford) for stimulating discussions during the writing of this review. Discussion with many Schlumberger colleagues has been very helpful in understanding the various parts of the workflow. Particular thanks are due to Martyn Beardsell, Alberto Malinverno and Jonathan Morris. I am grateful to Michael Thambynayagam for support in initiating and completing the project of writing this review. Thanks are also due to Daniel Busby and the referees for their useful suggestions. Any errors or omissions are, of course, my full responsibility.

Notes on the References

Many papers listed in the bibliography are from the Society of Petroleum Engineers. Most of these, where they are not explicitly from an SPE journal, are available in electronic form from the SPE at <http://www.spe.org/>. *FloGrid* is a trademark of Schlumberger.

References

1. B. Agarwal and M. J. Blunt (2003) Streamline-based method with full-physics forward simulation for history-matching performance data of a North Sea field. *SPE Journal* **8**, 171–180.
2. R. Agut, M.G. Edwards, S. Verma, and K. Aziz (1998) Flexible streamline-potential grids with discretization on highly distorted cells. Proceedings of the 6th European Conference on the Mathematics of Oil Recovery (ECMOR VI). Peebles, Edinburgh, Scotland, 8–11 September, 1998.
3. H.N. Al-Sadi (1982) *Seismic Exploration*. Birkhäuser, Basel.
4. J.R.L. Allen (1982) *Sedimentary Structures: Their Character and Physical Basis*, v1–2. Elsevier, Amsterdam.
5. P.A. Allen and J.R. Allen (1990) *Basin Analysis - Principles and Applications*. Blackwell, Oxford.
6. A.A. Amsden and C.W. Hirt (1973) A simple scheme for generating general curvilinear grids. *J. Comput. Phys.* **11**, 348–359.
7. B. Anderson, V. Druskin, et al. (1997) New dimensions in modeling resistivity. *Oilfield Review* **9**, 40–56.
8. J.R. Appleyard and I.M. Cheshire (1983) Nested factorization. SPE 12264. Proceedings of the 7th SPE Symposium on Reservoir Simulation, San Francisco, 1983.
9. J.S. Archer and C.G. Wall (1986) *Petroleum Engineering: Principles and Practice*. Graham and Trotman, London.
10. E. Arge and A. Kunoth (1998) An efficient ADI-solver for scattered data problems with global smoothing. *J. Comput. Phys.* **139**, 343–358.
11. K. Aziz and A. Settari (1979) *Petroleum Reservoir Simulation*. Applied Science Publishers, London.
12. M. Bacon, R. Simm, and T. Redshaw (2003) *3-D Seismic Interpretation*. Cambridge University Press, Cambridge.
13. M.J. Baines (1994) *Moving Finite Elements*. Oxford University Press.
14. G.I. Barenblatt, I.P. Zheltov, and I.N. Kochina (1960) Basic concepts in the theory of seepage of homogeneous liquids in fissured rocks (strata). *J. Appl. Math. Mech.* **24**, 1286–1303.
15. J.W. Barker, M. Cuyppers, and L. Holden (2001) Quantifying uncertainty in production forecasts: Another look at the PUNQ-S3 problem. *SPE Journal* **6**, 433–441.
16. J. Bear (1988) *Dynamics of Fluids in Porous Media*. Dover Publications Incorporated, New York.
17. S. Begg, R. Bratvold, and J. Campbell (2002) The value of flexibility in managing uncertainty in oil and gas investments. SPE 77586. Proceedings of the SPE Annual Technical Conference and Exhibition, San Antonio, Texas, 2002.

18. M.J. Beran (1968) *Statistical Continuum Theories*. Interscience Publishers, New York.
19. J.J. Binney, N.J. Dowrick, A.J. Fisher, and M.E.J. Newman (1992) *The Theory of Critical Phenomena*. Oxford University Press, Oxford.
20. R. Bissell, Y. Sharma, and J.E. Killough (1994) History matching using the method of gradients: Two case studies. SPE 28590. Proceedings of the 69th SPE Annual Technical Conference and Exhibition, 1994, 275–289.
21. N. Bleistein, J.K. Cohen, and J.W. Stockwell (2001) *Mathematics of Multidimensional Seismic Imaging, Migration, and Inversion*. Springer, New York.
22. S. Boggs (1995) *Principles of Sedimentology and Stratigraphy*. Prentice Hall, Englewood Cliffs, New Jersey.
23. A. Bourgeat and M. Panfilov (1998) Effective two-phase flow through highly heterogeneous porous media: capillary nonequilibrium effects. *Computational Geosciences* **2**, 191–215.
24. J.P. Boyd (2001) *Chebyshev and Fourier Spectral Methods*. 2nd edition, Dover Publications Inc., Mineola, New York.
25. J.U. Brackbill and J.S. Saltzman (1982) Adaptive zoning for singular problems in two dimensions. *J. Comput. Phys.* **46**, 342–368.
26. F. Bratvedt, K. Bratvedt, C. Buchholz, H. Holden, L. Holden, and N.H. Risebro (1989) A new front-tracking method for reservoir simulation. SPE 19805. Proceedings of the 64th SPE Annual Technical Conference and Exhibition, San Antonio, 1989.
27. I.C. Briggs (1974) Machine contouring using minimum curvature. *Geophysics* **39**, 39–48.
28. S.E. Buckley and M.C. Leverett (1942) Mechanism of fluid displacement in sands. *Trans. of the A.I.M.E.* **146**, 107.
29. M.D. Buhmann (2000) Radial basis functions. *Acta Numerica* **9**, 1–38.
30. J. Caers, S. Krishnan, Y. Wang, and A.R. Kovscek (2002) A geostatistical approach to streamline-based history matching. *SPE Journal* **7**, 250–266.
31. J. Carr, W.R. Fright, and R.K. Beatson (1997) Surface interpolation with radial basis functions for medical imaging. *IEEE Transactions on Medical Imaging* **16**, 96–107.
32. J.E. Castillo (1991) Discrete variational grid generation. *Mathematical Aspects of Numerical Grid Generation*, J.E. Castillo (ed.), SIAM, Philadelphia, 33–58.
33. J.E. Castillo, ed. (1991) *Mathematical Aspects of Numerical Grid Generation*. SIAM, Philadelphia.
34. J.-P. Chilés and P. Delfiner (1999) *Geostatistics: Modeling Spatial Uncertainty*. John Wiley, New York.
35. B. Choudhuri and S.K. Khataniar (1997) Characterisation of a complex high permeability reservoir through transient analysis: A case study of the lower Eocene reservoirs of Upper Assam basin, India. Paper no. 145. Proceedings of the *National Seminar on Reservoir Management and Exhibition*, Baroda, India, Oct. 6–7, 1997.
36. J.A. Coffeen (1990) *Seismic on Screen*. Pennwell Books, Tulsa.
37. R.E. Collins (1961) *Flow of Fluids through Porous Materials*. Reinhold Publishing Corporation, New York.

38. P.S. Craig, M. Goldstein, A.H. Seheult, and J.A. Smith (1997) Pressure matching for hydrocarbon reservoirs: a case study in the use of Bayes linear strategies for large computer experiments. *Case Studies in Bayesian Statistics III*, Springer, New York.
39. R. Daley (1991) *Atmospheric Data Analysis*. Cambridge University Press, Cambridge.
40. A. Datta-Gupta, K.N. Kulkarni, S. Yoon, and D.W. Vasco (2001) Streamlines, ray tracing and production tomography: generalization to compressible flow. *Petroleum Geoscience* **7**, S75–S86.
41. A. Datta-Gupta, L.W. Lake, and G.A. Pope (1995) Characterizing heterogeneous permeable media with spatial statistics and tracer data using sequential simulated annealing. *Mathematical Geology* **27**, 763–787.
42. C.V. Deutsch and A.G. Journel (1992) *GSLIB: Geostatistical Software Library and User's Guide*. Oxford University Press, New York.
43. P.A. Dickey (1986) *Petroleum Development Geology*. PennWell Publishing Company, Tulsa.
44. J. Douglas, Jr., M. Kischinhevsky, P.J. Paes-Leme, and A. Spagnuolo (1998) A multiple-porosity model for a single-phase flow through naturally-fractured porous media. *Computational and Applied Mathematics* **17**, 19–48.
45. J.H. Doveton (1986) *Log Analysis of Subsurface Geology: Concepts and Computer Methods*. John Wiley Sons, New York.
46. O. Dubrule and E. Damsleth (2001) Achievements and challenges in petroleum geostatistics. *Petroleum Geoscience* **7**, S1–S7.
47. L.J. Durlofsky, R.C. Jones, and W.J. Milliken (1994) A new method for the scale up of displacement processes in heterogeneous reservoirs. *Proceedings of the 4th European Conference on the Mathematics of Oil Recovery*, Røros, Norway, 1994.
48. Encyclopædia Britannica (2003): <http://www.britannica.com/>.
49. H.W. Engl, M. Hanke, and A. Neubauer (1996) *Regularization of Inverse Problems*. Kluwer, Dordrecht, 1996.
50. R. Ewing, ed. (1983) *The Mathematics of Reservoir Simulation*. SIAM, Philadelphia.
51. S.W. Fagin, ed. (1991) *Seismic Modeling of Geologic Structures: Applications to Exploration Problems*. Society of Exploration Geophysicists, Tulsa.
52. J.R. Fanchi (2002) *Shared Earth Modeling*. Butterworth-Heinemann, Amsterdam.
53. C.L. Farmer (1985) A moving point method for arbitrary Peclet number multi-dimensional convection-diffusion equations. *IMA Journal of Numerical Analysis* **5**, 465–480.
54. C.L. Farmer (1987) Moving point methods. *Advances in Transport Phenomena in Porous Media*, J. Bear and M.Y. Corapcioglu (eds.), NATO ASI Series E: Applied Sciences no. 128, Martinus Nijhoff, Dordrecht, 953–1004.
55. C.L. Farmer (1988) The generation of stochastic fields of reservoir parameters with specified geostatistical distributions. *Proceedings of the 1987 IMA Conference on Mathematics in Oil Production*, Sir Sam Edwards and P.R. King (eds.), Oxford University Press, Oxford, 235–252.
56. C.L. Farmer (1992) Numerical rocks. *Mathematics of Oil Recovery*, P.R. King (ed.), Oxford University Press, Oxford, 437–447.

57. C.L. Farmer (1998) An application of triangulations to the building of structured grids. Proceedings of the 6th European Conference on the Mathematics of Oil Recovery (ECMOR VI). Peebles, Edinburgh, Scotland, 8-11 September, 1998.
58. C.L. Farmer (2002) Upscaling: a review. *International Journal for Numerical Methods in Fluids* **40**, 63-78.
59. C.L. Farmer and D.E. Heath (1990) Curvilinear grid generation techniques. Proceedings of the 2nd European Conference on the Mathematics of Oil Recovery (ECMOR II). Arles, France, 11-14 September, 1990.
60. C.L. Farmer, D.E. Heath, and R.O. Moody (1991) A global optimisation approach to grid generation. SPE 21236. Proceedings of the 11th SPE Symposium on Reservoir Simulation, Anaheim, USA, 1991.
61. M.S. Floater and A. Iske (1996) Multistep scattered data interpolation using compactly supported radial basis functions. *Journal of Computational and Applied Mathematics* **73**, 65-78.
62. F.J.T. Floris, M.D. Bush, M. Cuypers, F. Roggero, and A.-R. Syversveen (2001) Methods for quantifying the uncertainty of production forecasts: a comparative study. *Petroleum Geoscience* **7**, S87-S96.
63. R. Franke (1982) Scattered data interpolation: tests of some methods. *Math. Comp.* **38**, 181-199.
64. N.P. Fremming (2002) 3D geological model construction using a 3D grid. Paper E01. Proceedings of the 8th European Conference on the Mathematics of Oil Recovery (ECMOR8), Freiberg, Germany, 3-6 September, 2002.
65. U. Frisch (1995) *Turbulence*. Cambridge University Press, Cambridge.
66. C.W. Gable, H.E. Trease, and T.A. Cherry (1996) Geological applications of automatic grid generation tools for finite elements applied to porous flow modeling. *Numerical Grid Generation in Computational Fluid Dynamics and Related Fields*, B.K. Soni, J.F. Thompson, H. Hauser, and P.R. Eiseman (eds.), Engineering Research Centre, Mississippi State University Press.
67. D. Gamerman (1997) *Markov Chain Monte Carlo: Stochastic Simulation for Bayesian Inference*. Chapman and Hall, London.
68. M.H. Garcia, A.G. Journel, and K. Aziz (1992) Automatic grid generation for modeling reservoir heterogeneities. SPE Reservoir Engineering, May 1992, 278-284.
69. A.O. Garder, D.W. Peaceman, and A.L. Pozzi (1964) Numerical calculation of multidimensional miscible displacement by the method of characteristics. *Society of Petroleum Engineers Journal* **4**, 26-36.
70. G.R. Gavalas, P.C. Shah, and J.H. Seinfeld (1976) Reservoir history matching by Bayesian estimation. *Society of Petroleum Engineers Journal* **16**, 337-350.
71. S. Geman and D. Geman (1984) Stochastic relaxation, Gibbs distributions and the Bayesian restoration of images. *IEEE Transactions on Pattern Analysis and Machine Intelligence* **6**, 721-741.
72. J. Gluyas and R. Swarbrick (2004) *Petroleum Geoscience*. Blackwell Publishing, Oxford.
73. N. Goldenfeld (1992) *Lectures on Phase Transitions and the Renormalization Group*. Perseus Books, Reading, Massachusetts.
74. W.H. Goldthorpe and Y.S. Chow (1985) Unconventional modeling of faulted reservoirs: A case study. SPE 13526. Proceedings of the SPE Reservoir Simulation Symposium, Dallas, 1985.

75. D. Gottlieb and S.A. Orszag (1977) *Numerical Analysis of Spectral Methods*. SIAM, Philadelphia.
76. R.H. Groshong Jr. (1999) *3D Structural Geology: A Practical Guide to Surface and Subsurface Map Interpretation*. Springer-Verlag, Berlin.
77. D. Gunasekera, J. Herring, and J. Cox (1998) Segmented coordinate line based unstructured gridding. Proceedings of the 6th European Conference on the Mathematics of Oil Recovery (ECMOR VI). Peebles, Edinburgh, Scotland, 8-11 September, 1998.
78. T. Gutzmer and A. Iske (1997) Detection of discontinuities in scattered data approximation. *Numerical Algorithms* **16**, 155–170.
79. R.L. Hardy (1971) Multiquadric equations of topography and other irregular surfaces. *J. Geophys. Res.* **76**, 1905–1915.
80. Z. He, S. Yoon, and A. Datta-Gupta (2002) Streamline-based production data integration with gravity and changing field conditions. *SPE Journal* **7**, 423–436.
81. D. A. Herron (2000) Horizon autopicking. *J. Geophys. Res.* **19**, 491–492.
82. R.V. Higgins and A.J. Leighton (1962) A computer method to calculate two-phase flow in any irregularly bounded porous medium. *J. Pet. Technology*, June 1962, 679–683.
83. G.J. Hirasaki and P.M. O'Dell (1970) Representation of reservoir geometry for numerical simulation. *Soc. Pet. Eng. J.*, December 1970, 393–404.
84. K.S. Hoffman and J.W. Neave (1996) Horizon modeling using a three-dimensional fault restoration technique. SPE 56445. Proceedings of the SPE Annual Technical Conference and Exhibition, Houston, Texas, 1996.
85. M.E. Hohn (1988) *Geostatistics and Petroleum Geology*. Van Nostrand Reinhold, New York.
86. G.M. Homsy (1987) Viscous fingering in porous media. *Annual Review of Fluid Mechanics* **19**, 271–311.
87. P.J. Hore (1995) *Nuclear Magnetic Resonance*. Oxford University Press, Oxford.
88. U. Hornung, ed. (1997) *Homogenization and Porous Media*. Springer, Berlin.
89. F.G. Horowitz, P. Hornby, D. Bone, and M. Craig (1996) Fast multidimensional interpolations. *26th Proceedings of the Application of Computers and Operations Research in the Mineral Industry (APCOM26)*, R.V. Ramani (ed.), Soc. Mining, Metall., and Explor. (SME), Littleton, Colorado, USA, 53–56.
90. J. Hoschek and D. Lasser (1993) *Fundamentals of Computer Aided Geometric Design*. A.K. Peters, Wellesley, Massachusetts.
91. T. Hou and X.H. Wu (1997) A multiscale finite element method for elliptic problems in composite materials and porous media. *J. Comput. Phys.* **134**, 169–189.
92. A. Iske (2002) Scattered data modelling using radial basis functions. *Tutorials on Multiresolution in Geometric Modelling*, A. Iske, E. Quak, and M.S. Floater (eds.), Springer, Heidelberg, 205–242.
93. T. Jacobsen, H. Agustsson, J. Alvestad, P. Digranes, I. Kaas, and S.T. Opdal (2000) Modelling and identification of remaining reserves in the Gullfaks field. SPE 65412. Proceedings of the SPE European Petroleum Conference, Paris, 2000.

94. P. Jenny, S.H. Lee, and H.A. Tchelepi (2003) Multi-scale finite-volume method for elliptic problems in subsurface flow simulation. *J. Comput. Phys.* **187**, 47–67.
95. T.A. Jones, D.E. Hamilton, and C.R. Johnson (1986) *Contouring Geologic Surfaces with the Computer*. Van Nostrand Reinhold, New York.
96. A.G. Journel (1989) *Fundamentals of Geostatistics in Five Lessons*. American Geophysical Union, Washington, USA.
97. A.G. Journel and F.G. Alabert (1989) Non-Gaussian data expansion in the Earth sciences. *Terra Nova*. **1**, 123–134.
98. P. Kaufman and P. Fjerstad (2002) Explicit simulation of conductive faults. Paper E64. Proceedings of the 8th European Conference on the Mathematics of Oil Recovery (ECMOR8), Freiberg, Germany, 3-6 September, 2002.
99. M.C. Kennedy and A. O'Hagan (2000) Predicting the output from a complex computer code when fast approximations are available. *Biometrika* **87**, 1–13.
100. M.C. Kennedy, A. O'Hagan, and N. Higgins (2002) Bayesian analysis of computer code outputs. *Quantitative Methods in Current Environmental Issues*, C.W. Anderson, V. Barnett, P.C. Chatwin, and A.H. El-Shaarawi (eds.), Springer, New York.
101. J.W. King, P.F. Naccache, O. Nichols, R.K. Pollard, D.K. Ponting, and J. Rae (1982) The use of non-neighbour connections in reservoir simulation. EUR 281. Proceedings of the European Petroleum Conference, London, October, 1982.
102. P. Knupp and S. Steinberg (1993) *Fundamentals of Grid Generation*. CRC Press, Boca Raton.
103. K.N. Kulkarni, A. Datta-Gupta, and D.W. Vasco (2001) A streamline approach for integrating transient pressure data into high-resolution reservoir models. *SPE Journal* **6**, 273–282.
104. A. Kumar, C.L. Farmer, G.R. Jerauld, and D. Li (1997) Efficient upscaling from cores to simulation models. SPE 38744. Proceedings of the Annual Technical Conference and Exhibition, San Antonio, Texas, 1997.
105. A. Kumar and N.S. Kumar (1988) A new approach to grid generation based on local optimisation. *Numerical Grid Generation in Computational Fluid Mechanics*, S. Sengupta, J. Häuser, P.R. Eiseman, and J.F. Thompson (eds.), Pineridge Press, Mumbles, Swansea, 177–184.
106. N. Lambeth and R.A. Dawe (1987) Boundary and crossflow behaviour during displacement in nodal systems. SPE 16972. Proceedings of the 62nd Annual Technical Conference of the SPE, Dallas, 1987.
107. T.J. Lasseter (2002) A new approach for the efficient construction of 3D geological models for reservoir applications. Paper E03. Proceedings of the 8th European Conference on the Mathematics of Oil Recovery (ECMOR8), Freiberg, Germany, 3-6 September, 2002.
108. R.C. Laudon (1996) *Principles of Petroleum Development Geology*. Prentice Hall, Upper Saddle River, New Jersey.
109. D.C. Leslie (1973) *Developments in the Theory of Turbulence*. Clarendon Press, Oxford.
110. P.K. Link (1987) *Basic Petroleum Geology*. Oil and Gas Consultants International, Inc., Tulsa.
111. N. Liu and D.S. Oliver (2003) Evaluation of Monte Carlo methods for assessing uncertainty. *SPE Journal* **8**, 188–195.
112. S.M. Luthi (2001) *Geological Well Logs: Their Use in Reservoir Modeling*. Springer, Berlin.

113. J.-L. Mallet (1989) Discrete smooth interpolation. *ACM Transactions on Graphics* **8**(2), 121–144.
114. J.-L. Mallet (2002) *Geomodeling*. Oxford University Press, Oxford.
115. K.V. Mardia, J.T. Kent, and J.M. Bibby (1979) *Multivariate Analysis*. Academic Press, London.
116. D. McLaughlin and L.R. Townley (1996) A reassessment of the groundwater inverse problem. *Water Resources Research* **32**, 1131–1161.
117. A.I. Mees, M.F. Jackson, and L.O. Chua (1992) Device modeling by radial basis functions. *IEEE Transactions on Circuits and Systems - I: Fundamental Theory and Applications* **39**, 19–27.
118. N. Metropolis, A.W. Rosenbluth, M.N. Rosenbluth, A.H. Teller, and E. Teller (1953) Equations of state calculations by fast computing machine. *Jour. Chem. Physics* **21**, 1087–1091.
119. W.J. Milliken, A.S. Emmanuel, and A. Chakravarty (2001) Applications of 3d streamline simulation to assist history matching. *SPE Reservoir Evaluation and Engineering* **4**, 502–508.
120. J.-M. Morel and S. Solimini (1995) *Variational Methods in Image Segmentation*. Birkhauser, Boston.
121. M.E.J. Newman and G.T. Barkema (1999) *Monte Carlo Methods in Statistical Physics*. Oxford University Press, Oxford.
122. A. O'Hagan (1994) *Kendall's Advanced Theory of Statistics, Volume 2B, Bayesian Inference*. Edward Arnold, London.
123. A. Okabe, B. Boots, K. Sugihara, and S.N. Chiu (2000) *Spatial tessellations: Concepts and Applications of Voronoi Diagrams*. J. Wiley and Sons. Ltd., Chichester.
124. D.S. Oliver, A.C. Reynolds, B. Zhuoxin, and Y. Abacioglu (2001) Integration of production data into reservoir models. *Petroleum Geoscience* **7**, S65–S73.
125. H. Omre (2003) www.math.ntnu.no/~omre/.
126. A. Ouenes, R.S. Doddi, Y. Lin, G. Cunningham, and N. Saad (1994) A new approach combining neural networks and simulated annealing for solving petroleum inverse problems. *Proceedings of the 4th European Conference on the Mathematics of Oil Recovery*, Røros, Norway, 1994.
127. M. Panfilov (2000) *Macroscale Models of Flow Through Highly Heterogeneous Porous Media*. Kluwer Academic.
128. D.W. Peaceman (1978) *Fundamentals of Numerical Reservoir Simulation*. Elsevier, Amsterdam.
129. W.H. Press, S.A. Teukolsky, W.T. Vetterling, and B.P. Flannery (1992) *Numerical Recipes in FORTRAN. The Art of Scientific Computing*. Cambridge University Press, Cambridge.
130. H.H. Rachford (1966) Numerical calculation of immiscible displacement by a moving reference point method. *Society of Petroleum Engineers Journal*, June 1966, 87–101.
131. C.D. Rodgers (2000) *Inverse Methods for Atmospheric Sounding: Theory and Practice*. World Scientific, Singapore.
132. F. Roggero and L.Y. Hu (1998) Gradual deformation of continuous geostatistical models for history matching. *SPE 49004. Proceedings of the SPE Annual Technical Conference and Exhibition*, New Orleans, 1998.
133. N. Saad, C.T. Kalkomey, and A. Ouenes (1994) Optimal gridding of stochastic models for scale-up. *Proceedings of the 4th European Conference on the Mathematics of Oil Recovery*, Røros, Norway, 1994.

134. Y. Saad (1996) *Iterative Methods for Sparse Linear Systems*. RWS Publishing Company, Boston.
135. Schlumberger (1997) *FloGridTM: A Simulation Grid Generation and Upscaling Software Application*. User Guide, Schlumberger, Abingdon.
136. Schlumberger (1998) *FloGridTM: A Simulation Grid Generation and Upscaling Software Application*. User Guide, Schlumberger, Abingdon.
137. Schlumberger (2002) *FloGridTM: A Simulation Grid Generation and Upscaling Software Application*. User Guide, Schlumberger, Abingdon.
138. R.C. Selley (1998) *Elements of Petroleum Geology*. Academic Press, San Diego.
139. R.E. Sheriff and L.P. Geldart (1995) *Exploration Seismology*. Cambridge University Press, Cambridge.
140. Society of Petroleum Engineers (2003) <http://www.spe.org/>.
141. F. Sonier and P. Chaumet (1974) A fully implicit three-dimensional model in curvilinear coordinates. Society of Petroleum Engineers Journal, August 1974, 361–370.
142. A. Tarantola (1987) *Inverse Problem Theory: Methods for Data Fitting and Model Parameter Estimation*. Elsevier, Amsterdam.
143. D. Tearpock and R. Bischke (2002) *Applied Subsurface Geological Mapping*. 2nd edition, Prentice Hall, New Jersey.
144. D.M. Tetzlaff and J.W. Harbaugh (1989) *Simulating Clastic Sedimentation*. Van Nostrand Reinhold, New York.
145. J.F. Thompson, B.K. Soni, and N.P. Weatherill (1999) *Handbook of Grid Generation*. CRC Press, Boca Raton.
146. J.F. Thompson and Z.U.A. Warsi (1982) Boundary-fitted coordinate systems for numerical solution of partial differential equations - a review. J. Comput. Phys. **47**, 1–108.
147. J.F. Thompson, Z.U.A. Warsi, and C.W. Mastin (1974) Automatic numerical generation of body-fitted curvilinear coordinate system for field containing any number of arbitrary two-dimensional bodies. J. Comput. Phys. **15**, 299–319.
148. J.F. Thompson, Z.U.A. Warsi, and C.W. Mastin (1985) *Numerical Grid Generation*. North-Holland, New York.
149. J. Tittman (1986) *Geophysical Well Logging*. Academic Press, London.
150. U. Trottenberg, C.W. Oosterlee, and A. Schüller (2001) *Multigrid*. Academic Press, San Diego.
151. S. Twomey (1996) *Introduction to the Mathematics of Inversion and Remote Sensing and Indirect Measurements*. Dover Publications Incorporated, New York.
152. G. Vincent, B. Corre, and P. Thore (1998) Managing structural uncertainty in a mature field for optimal well placement. SPE 48953. Proceedings of the SPE Annual Technical Conference and Exhibition, New Orleans, 1998.
153. P.L.W. Vinsome (1976) Orthomin, an iterative method for sparse banded sets of simultaneous linear equations. SPE 5729. Proceedings of the 4th SPE Symposium on Reservoir Simulation, Los Angeles, 1976.
154. D.T. Vo, M.I. Sukerri, et al. (2000) Reservoir modelling assists operations to optimize field development: Serang field, East Kalimantan. SPE 59441. Proceedings of the SPE Asia Pacific Conference, Yokohama, 2000.
155. Y. Wang and A.R. Kovscek (2000) Streamline approach for history-matching production data. SPE Journal **5**, 353–362.

156. S. Waryan, D.T. Vo, J. Stites, and M. Swanson (2001) Integrated 3D geological data into fluid flow model improves reservoir management plan: Serang field case study. SPE 68646. Proceedings of the SPE Asia Pacific Conference, Jakarta, 2001.
157. K.G. Wilson (1983) The renormalization group and critical phenomena. *Reviews of Modern Physics* **55**, 583–600.
158. A. Winslow (1967) Numerical solution of the quasi-linear Poisson equation in a nonuniform triangle mesh. *J. Comput. Phys.* **2**, 149–172.
159. A.M. Winslow (1981) Adaptive-mesh zoning by the equipotential method. Technical Report UCID-19062, Texas Institute for Computational and Applied Mathematics, Lawrence Livermore National Lab., USA, April 1981.
160. C. Wunsch (1996) *The Ocean Circulation Inverse Problem*. Cambridge University Press, Cambridge.
161. S. Yoon, A.H. Malallah, A. Datta-Gupta, D.W. Vasco, and R.A. Behrens (2001) A multiscale approach to production data integration using streamline models. *SPE Journal* **6**, 182–199.
162. D. Zhang (2001) *Stochastic Methods for Flow in Porous Media: Coping with Uncertainties*. Academic Press, San Diego.
163. D.A. Zimmerman, G. de Marsily, et al. (1998) A comparison of seven geostatistically based inverse approaches to estimate transmissivities for modeling advective transport by groundwater flow. *Water Resources Research* **34**, 1373–1413.
164. J. Zinn-Justin (2001) *Quantum Field Theory and Critical Phenomena*. Oxford University Press, Oxford.